HHS Public Access

Author manuscript

J Med Chem. Author manuscript; available in PMC 2022 February 21.

Published in final edited form as:

J Med Chem. 2018 June 28; 61(12): 5162–5186. doi:10.1021/acs.jmedchem.7b01862.

Design, Synthesis, and Biological Evaluation of 4-Quinoline Carboxylic Acids as Inhibitors of Dihydroorotate Dehydrogenase

Joseph T. Madak[†], **Christine R. Cuthbertson**[†], **Yoshinari Miyata**[†], **Shuzo Tamura**[†], **Elyse M. Petrunak**[§], **Jeanne A Stuckey**[§], **Yanyan Han**[‡], **Miao He**[‡], **Duxin Sun**[‡], **Hollis D. Showalter**[*,†], **Nouri Neamati**[*,†]

[†] Department of Medicinal Chemistry, University of Michigan, 1600 Huron Parkway, Ann Arbor, Michigan 48109, United States

[‡] Department of Pharmaceutical Sciences, College of Pharmacy, North Campus Research Complex, University of Michigan, 1600 Huron Parkway, Ann Arbor, Michigan 48109, United States

[§] Life Sciences Institute and Department of Biological Chemistry, University of Michigan, Ann Arbor, Michigan 48109, United States

Abstract

We pursued a structure-guided approach toward the development of improved dihydroorotate dehydrogenase (DHODH) inhibitors with the goal of forming new interactions between DHODH and the brequinar class of inhibitors. Two potential residues, T63 and Y356, suitable for novel H-bonding interactions, were identified in the brequinar-binding pocket. Analogues were designed to maintain the essential pharmacophore and form new electrostatic interactions through strategically positioned H-bond accepting groups. This effort led to the discovery of potent quinoline-based analogues **41** (DHODH IC50 = 9.71 ± 1.4 nM) and **43** (DHODH IC_{50} = 26.2 ± 1.8 nM). A cocrystal structure between **43** and DHODH depicts a novel water mediated H-bond interaction with T63. Additional optimization led to the 1,7-naphthyridine **46** (DHODH IC_{50} = 28.3 ± 3.3 nM) that forms a novel H-bond with Y356. Importantly, compound **41** possesses significant oral bioavailability (***F*** = 56%) and an elimination $\boldsymbol{t}_{1/2}$ = 2.78 h (PO dosing). In conclusion, the data supports further preclinical studies of our lead compounds toward selection of a candidate for early-stage clinical development.

Graphical Abstract

[*]Corresponding Authors: For N.N.: phone, (734)647-2732; neamati@med.umich.edu. Address: North Campus Research Complex, Building 520, 1600 Huron Parkway, Ann Arbor, Michigan 48109, United States., For H.D.S.: Showalh@med.umich.edu. Address: College of Pharmacy, CC Little, 428 Church Street, Ann Arbor, Michigan 48109, United States.

Notes

The authors declare no competing financial interest.

ASSOCIATED CONTENT

Supporting Information

The Supporting Information is available free of charge on the ACS Publications website at DOI: 10.1021/acs.jmedchem.7b01862.

Supplemental figures, copies of NMR spectra, and X-ray diffraction data (PDF)

Molecular formula strings and associated biochemical and biological data (CSV)

Accession Codes

Authors will release the atomic coordinates and experimental data for 6CJF and 6CJG upon article publication.

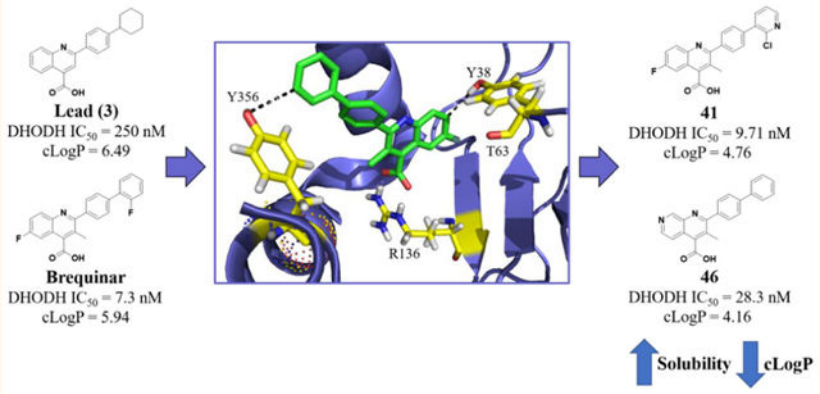

INTRODUCTION

Dihydroorotate dehydrogenase (DHODH) catalyzes the oxidation of dihydroorotate to orotate, which represents a committed step in the de novo pyrimidine biosynthesis pathway.[1,2] Inhibitors of DHODH induce pyrimidine depletion and halt cell cycle progression at S-phase, where a sufficient concentration of nucleotides is required for continued growth.[3] Pyrimidine depletion, through DHODH inhibition, has been exploited to develop therapies for many diseases including bacterial and viral infections, parasitic diseases (i.e., malaria), autoimmune disorders, and cancer.[4,5] Beyond directly halting cell growth, DHODH inhibitors sensitize cells to doxorubicin, fludarabine,[7,8] and TRAIL therapy.[9] Additionally, PTEN-deficient cancer cells are significantly more sensitive to DHODH inhibition.[10] DHODH inhibitors have also been shown to thwart self-renewal capacity of neural crest and melanoma cells.[11] Excitingly, DHODH inhibitors were found to induce differentiation in vivo, leading to the promise of DHODH-targeted therapy for acute myelogenous leukemia.[12] Collectively, these studies bolster interest for DHODH as an anticancer target.

Previous DHODH inhibitors have failed in clinical trials as single agents and in selected drug combinations for the treatment of various cancers. These include the well-known DHODH inhibitors, brequinar (**1**) and leflunomide (**2**, Figure 1), which have not demonstrated widespread success in cancer clinical trials. Despite promising preclinical data, brequinar failed to generate an objective response in multiple phase II clinical trials for breast,[13] colon,[14] head and neck,[1] gastrointestinal,[16] lung,[17] and skin[18] cancers. Brequinar sodium has poor water solubility (<0.10 mg/mL in room temperature water at pH 7.4), and molecular aggregation occurs at high concentrations.[19] In addition, common serum electrolytes, such as sodium chloride, have been demonstrated to reduce aqueous solubility by over 200-fold.[19] With a cLogP of 5.94, there is much room for improvement to increase water solubility and reduce formation of molecular aggregates. As such, a previous attempt to utilize brequinar in combination with cyclosporine A changed brequinar's pharmacokinetic profile in which its terminal half-life was extended and oral clearance rate was lowered.[20] Altered pharmacokinetic properties such as this present a significant liability for safe dosing, thus limiting the selection of potential patient populations for combination therapy. Leflunomide, an FDA approved drug for rheumatoid and psoriatic arthritis,[21]

is currently being evaluated as a single agent in clinical trials for multiple myeloma (ClinicalTrials.gov, NCT02509052)[22] but is no longer being evaluated in combination with vemurafenib for melanoma (ClinicalTrials.gov, NCT01611675).[23] Leflunomide is a reported agonist for the aryl-hydrocarbon receptor, which controls expression of drug metabolizing enzymes.[24,25] Despite the disappointing results of both of these agents in clinical trials, we feel that DHODH remains a promising anticancer target awaiting the discovery of small molecule inhibitors with better drug-like properties. As such, many drug discovery campaigns have been carried out for DHODH.[1,2,6] In this paper, we report the design and synthesis of a novel class of brequinar-like inhibitors toward the discovery of agents with improved physicochemical properties, principally better aqueous solubility, which we hypothesized would translate into improved enzyme and cellular potency.

RESULTS AND DISCUSSION

Analogue Design.

Our approach was guided by the basic pharmacophore interactions between brequinar and DHODH. Initially, we began with an unbiased cell-based screening approach to identify new small molecule hits possessing antiproliferative properties. This led to lead compound (**3**), which showed potent DHODH activity (IC_{50} = 0.250 ± 0.11 μM) (Figure 1). We postulated that **3** occupies a similar binding site as brequinar based on its structural similarity. The brequinar binding pocket of DHODH is primarily filled with nonpolar residues, therefore requiring lipophilic moieties. A high-resolution cocrystal structure of DHODH with a brequinar analogue (PDB 1D3G) provided insight into the essential pharmacophore.[27] The carboxylate of brequinar forms a salt bridge with R136 and a potential hydrogen bond interaction with Q47, exemplifying the importance of the carboxylic acid.[27,28] The remaining interactions between brequinar and DHODH occur in a hydrophobic channel with the biphenyl group or the quinoline core with residues such as M43, L58, A59, and P364.[28,29] To develop a DHODH inhibitor with a lower cLogP, we identified sites where ring heteroatom replacements could be tolerated toward enhancing binding without disrupting the essential pharmacophore.

Two regions were explored to potentially form electrostatic interactions. These regions were previously identified and are of interest because of their polar nature in a primarily lipophilic pocket.[30] The first region, located within a hydrophobic channel, has two hydroxyls, one on Y38 and another on T63. Each hydroxyl is in close proximity (Y38, 3.7 Å, and T63, 3.9 Å) to form an interaction with the *meta* position of the distal phenyl of a brequinar analogue (Figure 2).[27] The distance is suitable for an H-bonding interaction and, if achieved, may provide an inhibitor with improved enthalpy-driven potency and a lower cLogP.[31] Additionally, the hydroxyl of Y356 is nearly 2.5 Å away from C7 on the quinoline ring (Figure 2) and presents another opportunity to form a H-bond or other electrostatic interaction. With these residues in mind, we postulated that strategically positioned H-bond acceptors on the brequinar pharmacophore would improve potency while lowering the cLogP. The overall decrease in cLogP should significantly improve the aqueous solubility, leading to inhibitors with better drug-like properties.

To optimize our screening lead **3**, designed analogues were evaluated in the DHODH enzyme assay and MTT assay. We sought to develop analogues with a lower cLogP that may interact with T63 and Y356. Obviously, reducing the cLogP with analogues containing an ionizable acid could significantly reduce cellular permeability. However, we rationalized that, if necessary, an improved DHODH inhibitor could utilize a prodrug strategy to address this issue.[32] Therefore, our optimization process was primarily informed by the DHODH enzyme assay. Cellular activity was evaluated in HCT-116, a colon cancer cell line, and MIA PaCa-2, a pancreatic cancer cell line. Colon cancer has a high expression of DHODH and HCT-116 is sensitive to DHODH inhibition (Supporting Information, Figure l). DHODH is not overexpressed in pancreatic cancer and therefore should be less sensitive to DHODH inhibitors. Collectively, these two cell lines may help distinguish between DHODH-induced growth inhibition and potential off-target effects. Additionally, cLogP and LipE calculators were utilized to approximate aqueous solubility.[33] Using the cLogP, calculations of LipE should provide a statement of the lipophilicity associated with potency and approximate a compound's drug-like properties.

Synthesis.

The synthesis of analogues containing the quinoline core utilized the classic Pfitzinger condensation reaction.[34] 2,4-Disubstituted quinoline analogues were generated using synthetic routes **A–C** (Scheme 1). Route **A** generates analogues in one step. However, this approach was limited primarily to commercially available 4′-substituted acetophenones. To expand our SAR beyond these limitations, we developed routes **B** and **C**, which introduce diversity through carbon–carbon bond coupling via the Suzuki reaction on suitable precursors. These routes differ principally when such couplings take place with a phenyl-R_1 moiety generated at a late and early stage, respectively. The advantage of route **B** (Scheme 1) is that R_1 moieties sensitive to the harsh Pfitizinger reaction conditions can be successfully installed, whereas route **C** (Scheme 1) is less tolerant to such moieties.

Analogues containing a C3 methyl group were made by Pfitzinger reaction of 5-substituted isatins with 4′-bromopro-piophenone to give intermediates **54–57** (Scheme 2). Surprisingly, Fischer–Speier esterification conditions were low yielding on carboxylic acid analogues containing the C3 methyl. Alternatively, methyl ester analogues (**59–62**) were obtained through generation of the cesium salt of the carboxylic acid followed by exposure to iodomethane. Subsequent Suzuki coupling was used for installation of the terminal aromatic R_1 substituents (**79–90**). However, the C3 methyl thwarted mild ester hydrolysis, therefore harsher conditions with strong base (>60 °C with NaOH) were required for the reaction to occur. Unfortunately, this favored side product formation with little to no generation of acid, thus alternative deprotection methods were evaluated. Gratifyingly, the carboxylic acid could be unveiled upon exposure to BBr_3 in dichloromethane at room temperature with minimal side product formation (**34–44**, Scheme 2).

Additional analogues were generated to evaluate a scaffold hop from the quinoline series to the synthetically challenging naphthyridine congeners. As previously noted, we postulated that Y356 is close enough to potentially form an H-bond interaction with the N7 nitrogen of a 1,7-naphthyridine core (Figure 2 and Scheme 3). Initial attempts to generate this focused

on oxidation of aza-indoles to yield the corresponding aza-isatin for subsequent Pfitzinger condensation. However, reactions involving PCC oxidation[35] or a reusable poly aniline catalyst[36] on 1,6-aza-indoles did not provide the desired 1,6-aza-isatin. Inspired by the work of Stockmann et al.[37] and Zong et al.,[38] we sought to generate our naphthyridine series by installing an α-keto ester on an aminopyridine amide precursor,[38] which would provide an intermediate for a subsequent Pfitzinger condensation. Drawing on the work of Turner et al.,[39] Meanwell et al.,[40] and Zong et al.,[38] we generated our desired intermediate through directed metalation to control regioselectivity as shown in Scheme 3. A pivaloyl amide (**92–95**) was utilized to direct ortho-lithiation. Exposure of this intermediate to *n*-BuLi/TMEDA under strict temperature control provided the dianion, which was then quenched with diethyl oxalate to give the key α-keto-ester (**97–100**). This was then transformed to the naphthyridine (**45–50**) through base-catalyzed cyclization under Pfitzinger reaction conditions.

The synthesis of C6-substituted 1,7-naphthyridines presented an obstacle for SAR evaluation. Attempts to generate the C6-fluoro substituted 1,7-naphthyridine were foiled by the harsh reaction conditions necessary for the Pfitzinger cyclization (Scheme 3, box i). The high temperatures and basic conditions favor fluorine displacement through an SN_{Ar} mechanism, which likely proceed at a faster rate than cyclization. LCMS studies indicated that when the reaction temperature was above 50 °C, the fluorine was displaced under basic conditions within a few hours. Attempts to generate the C6-substituted methyl analogue were foiled using the ortho-lithiation protocol as the excess of *n*-BuLi favored kinetic deprotonation of the methyl group, leading to a variety of side products (Scheme 3, box ii). To overcome this, we opted to make the C6-trifluoromethyl analogue and were gratified to secure it despite low yields.

The overall low yield of our route to 1,7-naphthyridines presented an obstacle to expanding the SAR around this core. Efforts to improve the ortho-lithiation/acylation step initially focused on improving the electrophile's reactivity. Diethyl oxalate was replaced with asymmetric electrophiles such as ethyl chlorooxoacetate or ethyl 2-(methoxy(methyl)amino)-2-oxoacetate (Weinreb amide derivative) but without any yield enhancement. We then shifted our efforts to improving the Pfitzinger cyclization reaction (Scheme 3, reaction c). LCMS traces indicated that ester hydrolysis was followed by decarboxylation, which occurred at a faster rate than hydrolysis of the pivaloyl amide, resulting in low yields of product. To avoid the unwanted decarboxylation, we decided to swap the ortho-lithiating pivaloyl amide group with a Boc carbamate. Formation of the oxalate ester followed by mild Boc acid hydrolysis could then unmask the amine needed for intramolecular cyclization onto an α-keto acid. The reduction of this to practice is shown in Scheme 4. With α-keto ester intermediate **101** in hand, acid hydrolysis unveiled the amine followed by its condensation with 4′-bromopropionone and cyclization to provide the key 1,7-naphthyridine intermediate. Methyl esterification via cesium salt/methyl iodide failed, but was successful using TMS-diazomethane to give **102**. Suzuki coupling resulting in installation of the terminal 2-fluorophenyl substituent was followed by methyl ester hydrolysis to yield the final product (**52**). Alternatively, initial ester hydrolysis followed by Suzuki coupling on the resultant carboxylic acid successfully yielded final product **51**.

With the improved reaction conditions, we were able to incorporate the C6 CF_3 substituent into the 1,7-naphthyridine scaffold. This methodology should be readily amenable to the synthesis of additional naphthyridine analogues.

Structure–Activity Relationships.

Our initial goal was to validate that our synthesized analogues followed the same SAR trends (Table 1) as observed previously for the brequinar series.[28] With screen lead **3** and subsequent analogues, we noted an immediate decrease in potency for analogues containing a methyl ester substituent (e.g., compare **3** to **4**, Table 1). Attempts to lower cLogP by incorporating piperidine (**5**) or morpholine (**7**) substituents were not well tolerated and resulted in a marked potency decrease in comparison to **3**. Replacement of the cydohexyl group with branched aliphatic groups (**8, 9**) maintained modest potency in the DHODH assay but were far less potent than **3**. As expected, replacement of the cyclohexyl ring with a phenyl ring (**11**) resulted in a potency enhancement. This analogue has a lower cLogP than **3**, but substitution of the conformationally flexible cydohexyl with the planar phenyl allows for the formation of stacking interactions at high concentrations in aqueous solutions. Overall, these initial SAR trends are consistent with those observed for established DHODH inhibitors and suggest that our inhibitors bind in a similar pocket as brequinar.[28] To further confirm that DHODH is the primary target for cell growth inhibition, we evaluated screen lead **3** in the presence and absence of excess uridine, a nucleoside which, when entering the pyrimidine salvage pathway, ablates DHODH inhibition.[41,42] In the absence of uridine, cells are susceptible to growth inhibition by **3** and brequinar (Supporting Information, Figure 2). Uridine supplementation (5 μM) significantly decreased cell growth inhibition (below 50%), suggesting **3** inhibits an enzyme upstream of uridine nucleotide production. This data strengthened our initial postulate that **3** has a similar mechanism of action as brequinar, which shifted our attention toward incorporation of H-bond acceptors into our next set of analogues.

R_1 pyridine substituents were incorporated to probe for potential interactions with Y38 and T63. Our first goal was to evaluate positional pyridine isomers (Table 2). In the DHODH assay, the pyridine analogue **14** is 25- and 19-fold more potent than isomeric pyridine analogues **13** and **16**, respectively. This potency difference suggests a potential interaction between the pyridine nitrogen of **14** and DHODH. When docked into DHODH, **13**, **14**, and **16** all showed similar molecular docking energies (Supporting Information, Table 1), and all placements of the nitrogen were too far away to form an H-bond with either T63 or Y38 (≥4.0 Å). The pyridine nitrogen of **14** points toward the hydroxyl group of T63 at a distance of 4.6 Å and is therefore too far to form a direct H-bond. While we were not able to rationalize the difference in potency experimentally between the pyridine isomers, we observed that the *meta*-isomer (**14**) retained nanomolar activity against DHODH and had the highest LipE of any analogue at that juncture of our SAR campaign. In cells, **14** has a modest effect on cell growth in the HCT-116 line. In contrast, the methyl ester analogue **15** is inactive in the DHODH assay but possesses improved cytotoxicity in cells, which may be a result of improved permeability followed by intracellular hydrolysis to generate **14**. However, this has not been confirmed experimentally. The addition of the methoxy substituent at the 2′ position of the pyridine ring to increase its electron density (**17**)

improves potency in both the DHODH assay and cell-based viability assays. However, this enhancement is greater for phenyl analogue **18**, suggesting that enhancements from **14** to **17** are not due to electronic effects alone. In both cell lines, 18 is more potent than **17**, which may be a result of decreased permeability for **17** considering the relative cLogP values and modest DHODH potency differences.

Replacement of the pyridine ring with pyrimidine (**19**) resulted in a marked decrease in potency. Incorporation of the additional nitrogen increases tPSA, which may result in a repulsive interaction in a lipophilic pocket as this potency decrease is also observed with pyridazine (**20**) and reverse pyrimidine (**21**) analogues. The electron withdrawing CF_3 substituent was incorporated at the 2′- (22) and 4′- (**23**) positions (pyridine ring numbering; Table 3). Analogue **22** is more potent than **23** in the DHODH assay but shows no significant difference in cells. The same is observed for methyl substituents (**25, 26**) installed at various positions. Installation of a strongly electron-withdrawing fluoro substituent at the 2′- (**28**) and 6′- (**27**) positions of the pyridine ring resulted in a marked loss of potency. In fact, compound **28** is 64-fold less potent than **26** and 9-fold less potent than **22**, suggesting that steric effects also play an important role. Docking of these three analogues did not offer any insights as to why **28** is much less potent as it had the same predicted binding energy as **26**. Both **26** and **28** were predicted to bind about 2-fold weaker than **22** (Supporting Information, Table 1). On the basis of the steric effect hypothesis, we incorporated a chlorine at the 2′ position to provide **29**. Chlorine has a similar van der Waals radius as a methyl group but different inductive effects. Compound **29** is among the most potent analogues synthesized with predicted metabolic stability better than **26**. In cells, **29** is more potent in the HCT-116 and MIA PaCa-2 lines than **26**. Further installation of a methyl group at the 6′ position (**30**) of the pyridine ring was completed to increase binding in a lipophilic pocket. However, this does not improve potency. Neither does replacement of the pyridine with an imidazole (**31**).

Altogether, 2′-substutited pyridine analogues (e.g., **26, 29**) are among the most potent of the core quinoline series. Potency differences between 2′-position substituents may be a reflection of lipophilicity, inductive, or entropic effects that lower the total number of conformations the pyridine ring can adopt. A comparison between **17** and **22** suggests that inductive effects may not have a significant effect on potency. However, a comparison of analogues **17, 22, 26, 28**, and **29** suggests that substituent size may be a contributing factor. The size of the substituent may factor into undesirable clashes or limit the degrees of conformational freedom. Nonetheless, because analogues **26** and **29** were the most potent analogues synthesized at this stage of our campaign, the SAR was extended around **29**.

On the basis of SAR developed around the pendant R_1 position (Tables 1–3), we focused on further incorporating a C3 methyl substituent as is found in brequinar (Figure 1). We postulated that this added substituent would further limit conformational freedom around the C2 biaryl bond and hence minimize entropic penalties required for interaction with the nitrogen on the pendant pyridine ring for analogues shown in Tables 2 and 3. Additionally, the C3 methyl substituent should minimize potential stacking interactions between molecules in solution, leading to better aqueous solubility.[43] Synthesized analogues with the C3 methyl were generally more potent in the DHODH assay than the corresponding

C3 desmethyl congeners with the notable exceptions of **32** and **35** (Table 4). Analogue **32** is less potent than **11** in the DHODH enzyme and cell-based assays, whereas **35** is moderately less potent than **29** in both assays.

The next iteration of our optimization campaign was to evaluate core modifications of the C6 position of the quinoline ring. In general, the crystal structure (PDB 1D3G) depicts a small pocket that could be occupied by a suitable C6 substituent (Figure 3). Additionally, SMARTCyp, a software for predicting cytochrome P450-mediated metabolism, identified the C6 position of a nonsubstituted analogue as a site of metabolic liability.[44] Thus, incorporation of a C6 substituent might improve potency and decrease metabolic liabilities. The SAR around this position was limited to substituents that could be easily incorporated by our synthetic methodology. The data in Table 5 show that C6 substitutions improve the potency of the analogue series in the DHODH assay. In fact, analogues **39** (IC_{50} = 0.0542 ± 0.012 μM), **41** (IC_{50} = 0.00971 ± 0.0014 μM), and **42** (IC_{50} = 0.0360 ± 0.0058 μM) were all more potent than their corresponding C6 proton congener **35** (IC_{50} = 0.0543 ± 0.037 μM). Furthermore, the data in Table 5 show that C6 fluorine analogues are more potent than corresponding chloro or methyl congeners. This trend suggests that the size of the substituent is important with smaller lipophilic functional groups better tolerated at this position. For these analogues, **41** (IC_{50} = 0.00971 ± 0.0014 μM) possesses an IC_{50} on par with brequinar (IC_{50} = 0.00730 ± 0.0031 μM) but with a lower cLogP (4.76 vs 5.94, respectively). The lowered cLogP may explain the potency differences in the HCT-116 cell line. Despite similar potency in the DHODH assay, **41** is less potent than brequinar in HCT-116 (IC_{50} = 3.02 ± 0.35 μM vs IC_{50} = 0.679 ± 0.19 μM, respectively). This may be due to analogue **41** being less cell permeable than brequinar. Nonetheless, compound **41** is our most potent analogue in the DHODH assay within the quinoline series.

To form potential interactions with Y356, a scaffold hop was made from the quinoline to naphthyridine core (Table 6). The SAR highlights that 1,7-naphthyridines are the most potent within the broad series synthesized and supports our hypothesis of the importance of H-bonding interactions with Y356. Both the 1,6- and 1,8-naphthyridines (**47** and **45**) are less potent than the quinoline (**32**) and suggest that these positional nitrogen placements generate unfavorable interactions. In contrast, the 1,7-naphthyridine (**46**) displays greater potency than the quinoline congener (IC_{50} = 0.0283 ± 0.0033 μM vs IC_{50} = 0.0754 ± 0.017 μM, respectively). Molecular docking of these four compounds also supports these findings. Looking at the predicted binding energies alone was not informative with respect to potency differences, but when the optimal poses for **45, 46,** and **47** were overlaid in the binding site, it was clear that the 1,7-napthyridine (**46**) is in a favorable position to form a hydrogen bond with Y356 (Supporting Information, Table 1 and Figure 3). While **46** did not possess potent cell activity in both HCT-1116 and MIA PaCa-2 compared to brequinar, we were confident that incorporation of a substitution at the C6 position, as found in brequinar, would improve activity.

Our focus subsequently shifted to C6 substituted 1,7-naphthyridines. For the quinoline series, analogues possessing C6 substitution are far more potent than their nonsubstituted analogues (**35** vs **41, 36** vs **43**). We postulated that C6 substituted 1,7-naphthyridines would be more potent than corresponding C6 substituted quinolines and possess a lower cLogP.

While there was not much difference in DHODH potency between **46** and **48**, there was a significant increase in cell activity with the C6-substituted 1,7-napthyridine (**48**). The next obvious step was to incorporate the terminal 2-chloro-3-pyridyl moiety onto the core 1,7-naphthyridine scaffold.

Unfortunately, 1,7-naphthyridine analogues with a pyridine terminal attachment (**49–51**) (Table 7) are not as potent as naphthyridines with a terminal phenyl group (**46, 48**) or corresponding analogues within the quinoline series (**41, 43**). This result was unexpected and may be the result of the terminal aromatic ring adopting different conformations when binding to H-bond donors. If binding with the new residues modifies the binding conformation, it may increase the distance between small molecule H-bond acceptor and donor residues, leading to more unfavorable interactions (e.g., clashing with hydrophobic residues). However, this has not been confirmed experimentally and is being evaluated as part of another study. Furthermore, while terminal pyridyl analogues of Table 7 possess modest activity in the DHODH assay, they are not active in HCT-116 cells. In fact, analogues with a cLogP < 4 (**49, 50**) do not adversely affect cell growth below 100 μM. In contrast, analogue **52**, containing the terminal 2-fluorophenyl substituent found in brequinar, is potent in the DHODH assay and is the most potent analogue in the MTT assay against both cell lines by at least 2-fold over brequinar. Collectively, the potency of the 1,7-naphthyridines in the DHODH assay suggests potential interactions are being formed with DHODH, possibly via Y356. As DHODH inhibitors were recently discovered to have activity in acute myeloid leukemia,[12] we evaluated our optimized analogues for antiproliferative activity against HL-60 (Figure 5). Our inhibitors exhibited similar antiproliferative effects as were seen in HCT-116 and MIA PaCa-2. Inhibitors with a lower DHODH IC_{50} were generally more potent in HCT-116 than in MIA PaCa-2 cells. Additionally, the antiproliferative effects of our potent inhibitors of DHODH were rescued by uridine supplementation, validating their mechanism of action (Figure 5 and Supporting Information, Figure 4). In agreement with previously published DHODH inhibitors,[26,45] we observed that our inhibitors exerted their antiproliferative effects through a cytostatic rather than cytotoxic mechanism (Supporting Information, Figure 5).

Crystallography.

The structures of DHODH cocrystallized with **43** and **46** were solved to 1.63 and 2.85 Å resolution, respectively. DHODH:**43** (PDB 6CJF) was solved with two molecules in the asymmetric unit, while DHODH:**46** (PDB 6CJG) contained only one. Their overall structures are similar in that the single chain of DHODH:**46** aligns with RMSD values of 0.741 and 0.739 Å to the A and B chains of DHODH:**43**, respectively. The structures also adopt the same fold as other brequinar analogues bound to DHODH reported in the literature.[27,46,47]

Consistent with previous structures of DHODH bound to brequinar analogues,[27,46,47] inhibitors **43** and **46** occupy the proposed ubiquinone binding site, a hydrophobic channel formed by α1 and α2 helices directed toward the proximal redox site with the 4-carboxylic acid quinoline ring system oriented toward the active site. Both compounds are stabilized by a substantial number of hydrophobic interactions with the side chains of DHODH residues

lining the pocket (L42, M43, L46, P52, A55, A59, F62, and T63) (Figure 4A,B). The more deeply buried quinoline ring of **43** and naphthyridine ring of **46** form van der Waals contacts with a series of hydrophobic residues near the redox site, including F96, V134, V143, T360, Y356, L359, and P364 (Figure 4A,B). The C7-fluorine substituent of **43** is directed toward the FMN cofactor as in previous structures with other brequinar analogues,[27,47] and the C4 carboxylate of both inhibitors form salt bridges with R136 and participate in H-bonding with Q47 and T360 through a water molecule (Figure 4C,D).

In contrast to previous structures, the additional nitrogen incorporated into the 1,7-naphthyridine ring of **46** is within 3.3 Å of the Y356 hydroxyl group, allowing this inhibitor to participate in an additional H-bonding interaction within the binding site (Figure 4C).

In place of the unsubstituted phenyl ring of **46** and the 2-fluorophenyl ring of brequinar, **43** features a 2-chloro-6-methyl pyridine ring that can adopt two different orientations. On the basis of the ligand omit map density (Supporting Information, Figure 6), the chlorine substituent can be directed toward the α1 helix, but this orientation has low occupancy, likely in part due to steric clashes with the hydrophobic residues lining the binding pocket. The higher occupancy orientation of the pyridine ring directs the chlorine toward F98. In this orientation, the pyridine nitrogen is directed toward space usually occupied by the disordered 68–72 loop. In one molecule of the asymmetric unit, density corresponding to a water lies within 3.4 Å of the pyridine nitrogen and mediates a H-bond with the side chain of T63 (Figure 4D). The 6-methyl substituent is also directed toward space usually occupied by the loop connecting the two domains; steric clashes with this highly flexible loop might contribute to the intrinsic disorder of this loop and explain why density corresponding to residues 68–70 is absent in the structure with **43** in contrast to the DHODH:**46** structure in which these residues were able to be modeled.

There is additional density near the solvent-exposed entrance to the channel occupied by the inhibitor. The extra electron density in this site has been reported in previous structures of DHODH with brequinar analogues.[27,47] Liu and colleagues modeled a detergent, DDAO, in this site.[27] In our structures of DHODH:**43** and DHODH:**46**, we modeled the aliphatic chain in common to the two detergents, Anzergent 3–10 and HEGA-8, used for crystallization (Supporting Information, Figure 4). The aliphatic chain forms van der Waals interactions with the side chains of F62 and P69 as well as the backbone of residues 67–69. Additionally, the detergent makes contact with the phenyl group of **46**. In the DHODH:**43** structure, the aliphatic chain does not interact with the loop, but forms van der Waals interactions with the side chains of F62, L46, L42, and F37 along with the terminal substituted pyridine of **43**. Although the detergent is not physiologically relevant, it is likely that this face of the protein and the bound inhibitor make contacts with aliphatic chains of phospholipids comprising the membrane.[27]

Pharmacokinetic Evaluation and Thermodynamic Solubility.

We deemed compound **41** to possess an overall profile that merited pharmacokinetic evaluation in mice (Table 8). When **41** was administered either orally or intravenously, a similar elimination half-life of 2.73–2.78 h was observed. Oral bioavailability for **41** is

56%, which is suitable for DHODH inhibition considering its potency. For PO dosing, the C_{max} was 5313 ng/mL and was reached in 0.25 h. The clearance rate and volume of distribution are favorable for continuous inhibition, suggesting that **41** is well suited for further investigation.

Analogue **46** is more soluble in aqueous solutions than compounds of the quinoline series. In comparison to brequinar, compound **46** is 2.5–3× more soluble in PBS at pH 7.4 (Table 9). The nitrogen of the naphthyridine core significantly increases the aqueous solubility in comparison to the quinoline core. However, a comparison between 41 and brequinar highlights that despite a lower cLogP, **41**'s aqueous solubility is not significantly different from that of brequinar. The large chlorine group may limit the total solvent exposure of **41**'s pyridine moiety, which minimizes its effect on aqueous solubility. Nonetheless, compound **46** is endowed with better drug-like properties compared to brequinar, with potent DHODH inhibition and improved aqueous solubility.

CONCLUSION

This study reports on our drug discovery campaign to develop a novel DHODH inhibitor with improved potency and aqueous solubility. Our efforts toward designing molecular interactions with T63 led to the potent inhibitors **41** (DHODH IC_{50} = 0.00971 ± 0.0014 μM) and **43** (DHODH IC_{50} = 0.0262 ± 0.018 μM), each possessing a lower cLogP than brequinar (4.76, 5.27 vs 5.94, respectively). A cocrystal structure of **43** and DHODH depicts a water-mediated H-bonding interaction with the terminal pyridine and T63 (Figure 4D). Efforts to form an interaction with Y356 led to the synthesis of 1,7-naphthyridine inhibitors: **46** (DHODH IC_{50} = 0.0283 ± 0.0033 μM), **48** (DHODH IC_{50} = 0.0212 ± 0.0039 μM), and **52** (DHODH IC_{50} = 0.0118 ± 0.00090 μM). In a cocrystal structure with DHODH, the 7′-nitrogen of **46**'s core forms an H-bond with the hydroxyl of Y356 (Figure 4C). Furthermore, analogue **46** is significantly more soluble in aqueous solution than brequinar. Additionally, **52** exhibited improved cellular activity compared to brequinar. Moreover, optimized analogues displayed considerable antiproliferative activity in an acute myeloid leukemia cell line. Pharmacokinetic evaluation of **41** highlights suitable oral bioavailability (F = 56%) and half-life ($t_{1/2}$ = 2.78 h), suitable for further investigation. Collectively, these inhibitors demonstrate the potential to enhance binding with DHODH through novel H-bonding interactions. The results of our study highlight the possibility to simultaneously improve potency against DHODH while lowering the cLogP for inhibitors that occupy a lipophilic binding pocket. The disclosed inhibitors offer suitable leads for further inhibitor design and early-stage development. Future studies will seek to improve cell activity through prodrug design strategies. Additionally, we plan to evaluate the capability of these inhibitors to induce differentiation in acute myeloid leukemia in cell lines and in in vivo efficacy studies.

EXPERIMENTAL SECTION

General Methods.

Reagents and anhydrous solvents were used without further purification and purchased from commercial sources. Cinchophen and brequinar were purchased from commercial

sources and utilized without further purification. A Biotage Initiator+ was used to perform microwave catalyzed reactions in sealed vials. Reaction progress was monitored by UV absorbance using thin-layer chromatography (TLC) on aluminum-backed precoated silica plates from Silicycle (SiliaPlate, 200 ***μ*M** thickness, F_{254}). Purifications using flash chromatography were performed using Silicycle silica gel (SiliaFlash F60, 40–63 ***μ*M**, 230–400 mesh, PN R10030B), and a small percentage of compounds were purified using a Biotage Isolera chromatography system equipped with 10 and 25 g Ultra-SNAP Cartridge columns (25 ***μ***M spherical silica). Glassware for reactions were oven-dried in preparation, and reactions were performed using nitrogen or argon atmosphere using standard inert conditions. ^{1}H NMR spectra were obtained using a Bruker (300 or 400 MHz) or a Varian (400 or 500 MHz) instrument. Spectral data are reported using the following abbreviations: s = singlet, d = doublet, t = triplet, q = quartet, m = multiplet, dd = doublet of doublets, and coupling constants are reported in Hz, followed by integration. ^{13}C NMR spectra were obtained at 126 MHz on a Varian 500 MHz instrument with a proton decoupled probe. A Shimadzu LCMS 20–20 system was utilized for generating HPLC traces, obtaining mass spectrometry data, and evaluating purity. The system is equipped with a PDA UV detector and Kinetex 2.6 ***μ*M,** XB-C18 100 Å, 75 mm × 4.6 mm column, which was used at room temperature. HPLC gradient method utilized a 1% to 90% MeCN in H_2O with 0.01% formic acid over 20 min with a 0.50 mL/min flow rate. Purity of final compounds (≥95%) was assessed at 254 nm using the described column and method. Reverse-phase preparatory purifications were performed on a Shimadzu LC-20 modular HPLC system. This system utilized a PDA detector and a Kinetex 5 ***μ*M** XB-C18 100 Å, 150 mm × 21.2 mm column. Purification methods used a 27 min gradient from 10% to 90% MeCN in H_2O with 0.02% trifluoroacetic acid. The chemicals ***n***-BuLi and TMS-diazomethane present hazards. The chemical ***n***-BuLi is pyrophoric and must be utilized under an inert atmosphere. The chemical TMS-diazomethane is toxic and potentially explosive. Caution should be utilized when working with these chemicals.

General Protocol A, Pfitzinger Synthesis.—Isatin (1.0–1.2 eq) was added to a room temperature solution of KOH (4.0 equiv) in an EtOH/H_2O solution and mixed with various ***para***-substituted derivatives of acetophenone (1.0 equiv). The solution was heated to reflux for 24–48 h, concentrated in vacuo, and redissolved in 1 M NaOH/EtOAc. The aqueous layer was washed with EtOAc (3×) and acidified using HCl or glacial acetic acid until precipitant was observed (pH 2–3). The precipitant was filtered over a fritted funnel, washed with 1 M HC1, and washed again with 2-propanol, diethyl ether, or ethanol to yield final compounds (2–81%).

General Protocol B, Acid Catalyzed Esterification.—The corresponding carboxylic acid (1.0 equiv) was dissolved in solution containing anhydrous MeOH and a catalytic amount of H_2SQ_4 The reaction mixture was refluxed overnight before concentrating MeOH. Residue was redissolved in H_2O and neutralized before extracting product with EtOAc (3×). The organic layer was dried with $MgSO_4$, Altered, concentrated, and purified via flash chromatography using a gradient method from 5 to 60% EtOAc in hexane (63–88%).

General Protocol C, Base-Catalyzed Esterification.—The corresponding carboxylic acid (1.0 equiv), Cs_2CO_3 (1.2 equiv), and MeI (2.0 equiv) were dissolved in anhydrous DMF. The mixture was stirred at room temperature overnight. Upon completion, the mixture was diluted in EtOAc and washed with brine (**8**×). The organic layer was dried with $MgSO_4$ filtered, concentrated, and purified via flash chromatography using a gradient method from 5 to 60% EtOAc in hexane (43–93%).

General Procedure D, Suzuki Coupling. Nonmicrowave Protocol.—To a degassed round-bottom flask containing brominated starting material (l equiv), boronic acid (1.2–1.5 equiv), K_2CO_3 (3–4 equiv), and $Pd(PPh_3)_4$ (5–10% mol) was dissolved in dioxane or toluene. The reaction was heated at reflux until loss of starting material was observed via TLC (12–48 h). The reaction mixture was concentrated, partitioned between EtOAc/H_2O, and washed with EtOAc (3×). The organic layer was dried with $MgSO_4$ and concentrated to a residue, which was then purified by flash silica chromatography using a gradient of 10–60% EtOAc in hexane.

Microwave Protocol.—Brominated starting material (1 equiv), the corresponding boronic acid (1.5 equiv), base (Na_2CO_3 or K_2HPO_4 3–4 equiv), and $Pd(PPh_3)_4$ (≈ 5% equiv) were dissolved in 2:1 dioxane/H_2O or toluene/H_2O in a microwave vial. The vial was capped, purged with argon, and used in a microwave synthesizer. The reaction was heated at 125–130 °C for 1.5–2 h and followed the same purification as the nonmicrowave protocol. Yields for both protocols ranged from 7–97%.

General Procedure E, Basic Hydrolysis.—Ester derivatives were combined with 1–2 pellets of NaOH (large excess), LiOH, or KOH and dissolved in a 1:1 mixture of THF/H_2O or dioxane/H_2O. The solution was heated to 40 °C until starting material was no longer observed (2–6 h). Upon completion, solvent was concentrated; residue was redissolved in 1 M KOH and washed with EtOAc (3×). The aqueous layer was acidified with HCl until pH 2–3 was reached, chilled overnight at 2–8 °C, then poured over a fritted funnel to collect precipitated product. Product cake was washed with chilled deionized H_2O and product was dried under vacuum (15–100%).

General Procedure F, Acidic Hydrolysis.—Ester derivatives were dissolved in anhydrous DCM and 1 M BBr_3 in DCM was added to the solution. The solution was stirred at room temperature overnight. Upon completion, the solvent was concentrated; residue was redissolved in 1 M KOH and washed with EtOAc (3×). The aqueous layer was acidified with HC1 until pH 2–3 was reached, chilled overnight at 2–8 °C, then poured over a fritted funnel to collect precipitated product. Product cake was washed with chilled deionized H_2O, and product was dried under vacuum.

General Procedure G, Pivaloyl Protecting Group.—The corresponding aminopyridine (1 equiv) was added to a round-bottom flask containing anhydrous DCM and TEA/DIPEA (1.25 equiv). The solution was stirred on an ice bath for **20** min before trimethylacetyl chloride (1.1 equiv) was added dropwise. The solution was allowed to warm to room temperature and quenched with $H_2O/NaHCO_3$. The product was extracted in DCM

(3×), dried with $MgSO_4$, and concentrated in vacuo. The solid was recrystallized in hexanes to afford pivaloyl-aminopyridines (53–98%).

General Protocol H, ortho-Lithiation.—This procedure was adapted from Estel et **al.**[48] and Zong et **al.**[38] The corresponding pivaloylamino pyridine (1.0 eq) was added to a vacuum purged round-bottom flask under argon atmosphere. The solid was dissolved in Et_2O and TMEDA (2.5 equiv) then chilled to −78 °C. After 15 min, ***n***-BuLi (1.6 M in hexanes, 2.5 equiv) was added dropwise and the reaction mixture was stirred at −78 °C for 15 min and then stirred at −10 °C for 2.5 h. Afterward, the temperature was lowered to −78 °C for the addition of diethyl oxalate (3.0 equiv) and warmed to room temperature over 1.5 h. The reaction mixture was quenched with 1.0 M solution of HQ in ice water and extracted with Et_2O (3×). The organic layer was dried, concentrated, and purified via silica chromatography in a gradient from 1% to 10% MeOH in DCM gradient (1–51%).

General Protocol I, Generation of Naphthyridine Core.—Corresponding ketone (1.0 equiv), ***α***-keto-ester (1.0 equiv), and base (KOH or KOtBu, 3–6 equiv) were combined in anhydrous EtOH in a sealed vial. The mixture was heated to 100 °C overnight, concentrated to a residue, extracted with 1 M KOH, and washed with EtOAc. The basic layer was acidified by addition of HCl (pH 2–3), and the product was collected via filtration. Product was further purified by reverse-phase preparatory chromatography (3–21%).

2-(4-Cyclohexylphenyl)quinoline-4-carboxylic Acid (3).—Isatin (987 mg, 6.71 mmol), 1-(4-cyclohexylphenyl)ethan-1-one (1.00 g, 4.95 mmol), and KOH (1.55 g, 27.6 mmol) were dissolved in 30 mL of EtOH and 10 mL of H_2O. Following general protocol A, 2-(4-cyclohexylphenyl)quinoline-4-carboxylic acid was recovered as a white powder (374 mg, 1.13 mmol, 23%). ^{1}H NMR (500 MHz, DMSO-d_6) δ 8.64 (d, ***J*** = **8.6** Hz, 1H), 8.41 (d, ***J*** = 1.8 Hz, 1H), 8.21–8.15 (m, 2H), 8.14–8.08 (m, 1H), 7.85–7.79 (m, 1H), 7.71–7.61 (m, 1H), 7.40–7.34 (m, 2H), 2.59–2.50 (m, 1H), 1.83–1.73 (m, 4H), 1.72 1.65 (m, 1H), 1.49–1.27 (m, 4H), 1.27–1.10 (m, 1H). ^{13}C NMR (126 MHz, DMSO-d_6)) δ 168.1, 156.2, 150.1, 148.9, 138.0, 136.0, 130.6, 130.1, 128.0, 127.7 (2H), 127.6 (2H), 125.9, 123.8, 119.4, 44.0, 34.2 (2H), 26.7 (2H), 26.0. LCMS (ESI) 332.20 $[M + H]^+$, 330.20 $[M - H]^-$. HPLC purity at 254 nm, 98.6%.

Methyl 2-(4-Cyclohexylphenyl)quinoline-4-carboxylate (4).—Compound **3** (25 mg, 0.08 mmol) was dissolved in 2 mL of MeOH H_2SO_4 (16 drops, catalyst) was added to the reaction mixture, and the mixture was heated to reflux overnight. Following general protocol B, methyl 2-(4-cyclohexylphenyl)quinoline-4-carboxylate was recovered as an off-white solid (25 mg, 0.07 mmol, **88**%) ^{1}H NMR (300 MHz, $CDCl_3$-***d***) δ 8.76 (d, ***J*** = 8.5 Hz, 1H), 8.41 (s, 1H), 8.24 (d, ***J*** = 8.4 Hz, 1H), 8.15 (d, ***J*** = 8.0 Hz, 2H), 7.86–7.71 (m, 1H), 7.69–7.59 (m, 1H), 7.41 (d, ***J*** = 8.0 Hz, 2H), 4.09 (s, 3H), 2.70–2.57 (m, 1H), 2.03–1.85 (m, 4H), 1.84–1.67 (m, 1H), 1.61–1.21 (m, 5H). LCMS (ESI) 346.2 $[M + H]^+$. HPLC purity at 254 nm, 98.7%.

2-(4-(Piperidin-1-yl)phenyl)quinoline-4-carboxylic Acid (5).—Isatin (247 mg, 1.68 mmol), 1-(4-(piperidin-1-yl)phenyl)ethan-1-one (200 mg, 0.99 mmol), and KOH (336 mg,

6.00 mmol) were dissolved in 7 mL of EtOH and 2 mL of H_2O. Following general protocol A, 2-(4-(piperidin-1-yl)phenyl)quinoline-4-carboxylic acid was recovered as a red solid **(88** mg, 0.27 mmol, 27%). ^{1}H NMR (400 MHz, DMSO-d_6) δ 8.59 (d, J = 8.4 Hz, 1H), 8.37 (s, 1H), 8.18 (d, J = **8.6** Hz, 2H), 8.09 (d, J = 8.4 Hz, 1H), 7.80 (t, J = 8.4, 6.9 Hz, 1H), 7.68–7.58 (m, 1H), 7.16–7.04 (m, 2H), 3.34–3.27 (m, 4H), 1.71–1.54 (m, **6**H). LCMS (ESI) 333.25 $[M + H]^+$, 331.15 $[M - H]^-$. HPLC purity at 254 nm, 99.7%.

Methyl 2-(4-(Piperidin-1-yl)phenyl)quinoline-4-carboxylate (6).—Compound **5** (30 mg, 0.09 mmol) was dissolved in 2 mL of MeOH. H_2SO_4 (16 drops, catalyst) was added to the reaction mixture, and the mixture was heated to reflux for 12 h. Following general protocol B, methyl 2-(4-(piperidin-1-yl)phenyl)quinoline-4-carboxylate was recovered as a yellow solid (29 mg, 0.08 mmol, **88**%). ^{1}H NMR (400 MHz, $CDCl_3$-d) δ 8.71 (dd, J = 8.5, 1.4 Hz, 1H), 8.38 (s, 1H), 8.21–8.12 (m, 3H), 7.80–7.70 (m, 1H), 7.63–7.53 (m, 1H), 7.13–7.00 (m, 2H), 4.08 (d, J = 1.0 Hz, 3H), 3.39–3.28 (m, 4H), 1.80–1.71 (m, 4H), 1.70–1.60 (m, 2H). LCMS (ESI) 347.2 $[M + H]^+$. HPLC purity at 254 nm, 97.3%.

2-(4-Morpholinophenyl)quinoline-4-carboxylic acid (7).—Isatin (247 mg, 1.68 mmol), 1-(4-morpholinophenyl)ethan-1-one (200 mg, 0.98 mmol), and KOH (336 mg, 6.00 mmol) were dissolved in 7 mL of EtOH and 1 mL of H_2O. Following general protocol A, 2-(4-morpholinophenyl)quinoline-4-carboxylic acid was recovered as a red solid (132 mg, 0.40 mmol, 41%). ^{1}H NMR (400 MHz, DMSO-d_6) δ 8.60 (d, J = 8.5 Hz, 1H), 8.39 (s, 1H), 8.21 (d, J = 8.7 Hz, 2H), 8.10 (d, J = 8.4 Hz, 1H), 7.85–7.76 (m, 1H), 7.68–7.59 (m, 1H), 7.11 (d, J = 8.7 Hz, 2H), 3.77 (t, J = 4.8 Hz, 4H), 3.26 (t, J = 4.9 Hz, 4H). LCMS (ESI) 335.90 $[M + H]^+$, 333.15 $[M - H]^-$. HPLC purity at 254 nm, 98.8%.

2-(4-Isopropylphenyl)quinoline-4-carboxylic Acid (8).—Isatin (264 mg, 1.79 mmol), 1-(4-isopropylphenyl)ethan-1-one (0.27 mL, 1.62 mmol), and KOH (275 mg, 4.91 mmol) were dissolved in 7 mL of EtOH and 1 mL of H_2O. Following general protocol A, 2-(4-isopropylphenyl)quinoline-4-carboxylic acid was recovered as a yellow solid (130 mg, 0.45 mmol, 28%). ^{1}H NMR (400 MHz, DMSO-d_6) δ 8.65 (d, J = 8.3 Hz, 1H), 8.44 (s, 1H), 8.23 (d, J = 8.3 Hz, 2H), 8.16 (d, J = 8.5 Hz, 1H), 7.89–7.81 (m, 1H), 7.75–7.67 (m, 1H), 7.46 (d, J = 8.3 Hz, 2H), 3.09–2.94 (m, 1H), 1.28 (d, J = 6.9 Hz, **6**H). LCMS (ESI) 292.20 $[M + H]^+$, 290.15 $[M - H]^-$. HPLC purity at 254 nm, 95.8%.

2-(4-Isobutylphenyl)quinoline-4-carboxylic Acid (9).—Isatin (500 mg, 3.40 mmol), 1-(4-isobutylphenyl)ethan-1-one (0.57 mL, 3.08 mmol), and KOH (1.14 g, 20.4 mmol) were dissolved in 12 mL of EtOH + 2 mL of H_2O. Following general protocol A, 2-(4-isobutylphenyl)quinoline-4-carboxylic acid was recovered as a pink solid (101 mg, 0.33 mmol, 10% yield). ^{1}H NMR (300 MHz, DMSO-d_6) δ **8.68** (d, J = 8.4 Hz, 1H), 8.14 (d, J = 7.9 Hz, 2H), 8.03–7.94 (m, 2H), 7.66 (t, J = 7.6 Hz, 1H), 7.46 (t, J = 7.6 Hz, 1H), 7.33 (d, J = 7.9 Hz, 2H), 2.59–2.52 (m, 2H), 2.00–1.85 (m, 1H), 0.91 (d, J = **6.6** Hz, **6**H). LCMS (ESI) 306.10 $[M + H]^+$, 304.20 $[M - H]^-$. HPLC purity at 254 nm, 99.9%.

2-([1,1′-Biphenyl]-4-yl)quinoline-4-carboxylic Acid (11).—Isatin (168 mg, 1.14 mmol), 1-([1,1′-biphenyl]-4-yl)ethan-1-one (200 mg, 1.2 mmol), and KOH (230 mg, 4.11

mmol) were dissolved in 3 mL of EtOH with 1 mL of H_2O. Following general protocol A, 2-([1,1′-biphenyl]-4-yl)quinoline-4-carboxylic acid was recovered as a beige solid (74 mg, 0.23 mmol, 20% yield) after recrystallization from ethanol. ^{1}H NMR (300 MHz, CD_3OD-$\boldsymbol{d}_4$) $\boldsymbol{\delta}$ 8.46–8.36 (m, 1H), 8.19 (d, ***J*** = 8.4 Hz, 2H), 8.14–8.02 (m, 2H), 7.83–7.63 (m, 5H), 7.56 (ddd, ***J*** = 8.2, **6.8**, 1.2 Hz, 1H), 7.44 (t, ***J*** = 7.4 Hz, 2H), 7.40–7.28 (m, 1H). LCMS (ESI) 326.15 $[M + H]^+$, 324.10 $[M - H]^-$. HPLC purity at 254 nm, 98.9%.

Methyl 2-([1,1′-Biphenyl]-4-yl)quinoline-4-carboxylate (12).—Intermediate **58** (100 mg, 0.29 mmol), phenylboronic acid (53 mg, 0.43 mmol), K_2HPO_4 (151 mg, 0.87 mmol), and $Pd(PPh_3)_4$ (17 mg, 0.01 mmol) were dissolved in 2 mL of dioxane and 1 mL of H_2O. The mixture was heated to 130 °C for 1.5 h in a microwave reactor. Following general protocol D, methyl 2-([1,1′-biphenyl]-4-yl)quinoline-4-carboxylate was recovered as a white crystal (28 mg, 0.08 mmol, 28%). ^{1}H NMR (300 MHz, $CDCl_3$-$\boldsymbol{d}$) $\boldsymbol{\delta}$ 8.76 (dd, ***J*** = **8.6**, 1.3 Hz, 1H), 8.46 (s, 1H), 8.35–8.20 (m, 3H), 7.85–7.73 (m, 3H), 7.74–7.58 (m, 3H), 7.49 (t, ***J*** = 7.4 Hz, 2H), 4.09 (s, 3H). LCMS (ESI) 340.10 $[M + H]^+$. HPLC purity at 254 nm, 99.5%.

2-(4-(Pyridin-2-yl)phenyl)quinoline-4-carboxylic Acid (13).—Isatin (82 mg, 0.56 mmol), intermediate **63** (100 mg, 0.51 mmol), and KOH (112 mg, 2.00 mmol) were dissolved in 4 mL in EtOH with 1 mL of H_2O. Following general protocol A, 2-(4-(pyridin-2-yl)phenyl)quinoline-4-carboxylic acid was recovered as a tan solid (62 mg, 0.19 mmol, 37%). ^{1}H NMR (300 MHz, CD_3OD-$\boldsymbol{d}_4$) $\boldsymbol{\delta}$ 8.71–8.64 (m, 1H), 8.46 (d, ***J*** = 8.4 Hz, 1H), 8.31 (d, ***J*** = 8.1 Hz, 2H), 8.22–8.10 (m, 4H), 8.04–7.94 (m, 2H), 7.78 (t, ***J*** = 7.7 Hz, 1H), 7.61 (t, ***J*** = 7.7 Hz, 1H), 7.42 (t, ***J*** = 6.0 Hz, 1H). LCMS (ESI) 326.85 $[M + H]^+$, 324.85 $[M - H]^-$. HPLC purity at 254 nm, 99.4%.

2-(4-(Pyridin-3-yl)phenyl)quinoline-4-carboxylic Acid (14).—Compound **15 (8** mg, 0.02 mmol) and NaOH (45 mg, 1.13 mmol) was dissolved in a 1 mL of THF and 1 mL of H_2O. Following general protocol E, a white solid was collected from the vacuum oven to yield 2-(4-(pyridin-3-yl)phenyl)quinoline-4-carboxylic acid (2 mg, 6.13×10^{-3} mmol, 30%). ^{1}H NMR (400 MHz, DMSO-$\boldsymbol{d}_6$) $\boldsymbol{\delta}$ 9.24–9.20 (m, 1H), 8.82–8.78 (m, 1H), 8.67 (d, ***J*** = 8.5, 1.5, 0.6 Hz, 1H), 8.64–8.61 (m, 1H), 8.56 (s, 1H), 8.50 (d, ***J*** = 8.5 Hz, 2H), 8.21 (d, 1H), 8.05 (d, ***J*** = 8.5 Hz, 2H), 7.93–7.85 (m, 2H), 7.78–7.71 (m, 1H). LCMS (ESI) 326.90 $[M + H]^+$, 324.85 $[M - H]^-$. HPLC purity at 254 nm, 95.2%.

Methyl 2-(4-(Pyridin-3-yl)phenyl)quinoline-4-carboxylate (15).—Intermediate **58** (60 mg, 0.18 mmol), pyridin-3-yIboronic acid (23 mg, 0.19 mmol), $Pd(PPh_3)_4$ (10 mg), and K_2CO_3 (72 mg, 0.53 mmol) were combined in 3 mL of toluene and 1 mL of H_2O. The mixture was heated at 110 °C overnight. Following general protocol D, methyl 2-(4-(pyridin-3-yl)phenyl)quinoline-4-carboxylate was recovered as a white solid (20 mg, 0.06 mmol, 33%). ^{1}H NMR (300 MHz, $CDCl_3$-$\boldsymbol{d}$) $\boldsymbol{\delta}$ 8.92 (s, 1H), 8.74 (d, ***J*** = 8.5 Hz, 1H), 8.62 (d, ***J*** = 4.8 Hz, 1H), 8.40 (s, 1H), 8.29 (d, ***J*** = 8.2 Hz, 2H), 8.21 (d, ***J*** = 8.4 Hz, 1H), 7.91 (dd, ***J*** = 8.0, 2.0 Hz, 1H), 7.82–7.68 (m, 3H), 7.66–7.57 (m, 1H), 7.37 (dd, ***J*** = 7.9, 4.8 Hz, 1H), 4.23–3.94 (m, 3H). LCMS (ESI) 341.1 $[M + H]^+$. HPLC purity at 254 nm, 99.6%.

2-(4-(Pyridin-4-yl)phenyl)quinoline-4-carboxylic Acid (16).—Intermediate **72** (14 mg, 0.04 mmol) and NaOH (62 mg, 1.59 mmol) was dissolved in 1 mL of THF and 1 mL of H_2O. Following general protocol E, a white solid was collected from the vacuum oven to yield 2-(4-(pyridin-4-yl)phenyl)quinoline-4-carboxylic acid (2 mg, 6.13×10^{-3} mmol, 15%). ^{1}H NMR (400 MHz, DMSO-d_6) δ 8.72–8.66 (m, 3H), 8.39 (d, J = 8.3 Hz, 2H), 8.08 (s, 1H), 8.04–7.99 (m, 3H), 7.85–7.80 (m, 2H), 7.73–7.66 (m, 1H), 7.53–7.47 (m, 1H). LCMS (ESI) 326.85 $[M + H]^+$, 324.80 $[M - H]^-$. HPLC purity at 254 nm, 95.1%.

2-(4-(2-Methoxypyridin-3-yl)phenyl)quinoline-4-carboxylic Acid (17).—Intermediate **73** (15 mg, 0.04 mmol) and NaOH (63 mg, 1.62 mmol) were dissolved in 1 mL of THF and 1 mL of H_2O. Following general protocol E, 2-(4-(2-methoxypyridin-3-yl)phenyl)quinoline-4-carboxylic acid was recovered as a beige solid (12 mg, 0.03 mmol, 75%). ^{1}H NMR (400 MHz, DMSO-d_6) δ 8.65 (d, J = 8.5 Hz, 1H), 8.50 (s, 1H), 8.36 (d, J = 8.0 Hz, 2H), 8.25–8.14 (m, 2H), 7.89–7.82 (m, 2H), 7.76 (d, J = 7.9 Hz, 2H), 7.70 (t, J = 7.7 Hz, 1H), 7.13 (t, J = 6.2 Hz, 1H), 3.91 (s, 3H). LCMS (ESI) 357.1 $[M + H]^+$, 355.1 $[M - H]^-$. HPLC purity at 254 nm, 99.8%.

2-(2'-Methoxy-[1,1′-biphenyl]-4-yl)quinoline-4-carboxylic Acid (18).—Intermediate **74** (15 mg, 0.04 mmol) and NaOH **(68** mg, 1.74 mmol) were dissolved in 1 mL of THF and 1 mL of H_2O. Following general protocol E, 2-(2′-methoxy-[1,1′-biphenyl]-4-yl)quinoline-4-carboxylic acid was recovered as a beige solid (13 mg, 0.04 mmol, 100%). ^{1}H NMR (400 MHz, DMSO-d_6) δ 8.69–8.61 (m, 1H), 8.49 (s, 1H), 8.37–8.27 (m, 2H), 8.17 (d, J = 8.4 Hz, 1H), 7.89–7.82 (m, 1H), 7.73–7.65 (m, 3H), 7.41–7.34 (m, 2H), 7.17–7.12 (m, 1H), 7.10–7.04 (m, 1H), 3.79 (s, 3H). LCMS (ESI) 356.2 $[M + H]^+$, 354.1 $[M - H]^-$. HPLC purity at 254 nm, 98.6%.

2-(4-(Pyrimidin-5-yl)phenyl)quinoline-4-carboxylic Acid (19).—Isatin (56 mg, 0.38 mmol), intermediate **64** (75 mg, 0.38 mmol), and KOH (64 mg, 1.14 mmol) were dissolved in 3 mL of EtOH and 1 mL of H_2O. Following general protocol A, 2-(4-(pyrimidin-5-yl)phenyl)quinoline-4-carboxylic acid was recovered as a yellow solid (24 mg, 0.07 mmol, 18% yield). ^{1}H NMR (300 MHz, DMSO-d_6) δ 9.31–9.21 (m, 3H), **8.66** (d, J = 8.5 Hz, 1H), 8.56 (s, 1H), 8.48 (d, J = 8.3 Hz, 2H), 8.21 (d, J = 8.4 Hz, 1H), 8.05 (d, J = 8.4 Hz, 2H), 7.94–7.85 (m, 1H), 7.79–7.68 (m, 1H). LCMS (ESI) 328.15 $[M + H]^+$, 326.85 $[M - H]^-$. HPLC purity at 254 nm, 99.5%.

2-(4-(Pyridazin-3-yl)phenyl)quinoline-4-carboxylic Acid (20).—Isatin (203 mg, 1.38 mmol), intermediate **65** (273 mg, 1.38 mmol), and KOH (309 mg, 5.52 mmol) were dissolved in 10 mL of EtOH Following general protocol A, 2-(4-(pyridazin-3-yl)phenyl)quinoline-4-carboxylic acid was recovered as a tan solid (160 mg, 0.49 mmol, 36%). ^{1}H NMR (400 MHz, DMSO-d_6) δ 9.25 (dd, J = 4.8, 1.5 Hz, 1H), **8.66** (d, J = 8.5 Hz, 1H), 8.56 (s, 1H), 8.50 (d, J = 8.3 Hz, 2H), 8.42–8.29 (m, 3H), 8.20 (d, J = 8.4 Hz, 1H), 7.91–7.79 (m, 2H), 7.74–7.70 (m, 1H). LCMS (ESI) 327.85 $[M + H]^+$, 325.85 $[M - H]^-$. HPLC purity at 254 nm, 96.7%.

2-(4-(Pyrimidin-2-yl)phenyl)quinoline-4-carboxylic Acid (21).—Isatin (67 mg, 0.46 mmol), intermediate **66** (109 mg, 0.55 mmol), and KOH (103 mg, 1.84 mmol) were dissolved in 3 mL of EtOH and 1 mL of H_2O. Following general protocol A, 2-(4-(pyrimidin-2-yl)phenyl)quinoline-4-carboxylic acid was recovered as a tan solid (80 mg, 0.24 mmol, 52%). ^{1}H NMR (400 MHz, DMSO-d_6) δ 8.96 (d, J = 4.8 Hz, 2H), 8.67 (d, J = 8.2 Hz, 1H), 8.61–8.54 (m, 3H), 8.50–8.46 (m, 2H), 8.20 (d, J = 8.4 Hz, 1H), 7.90–7.84 (m, 1H), 7.75–7.69 (m, 1H), 7.50 (t, J = 4.8 Hz, 1H). LCMS 328.10 $[M + H]^+$, 326.10 $[M - H]^-$. HPLC purity at 254 nm, 96.8%

2-(4-(2-(Trifluoromethyl)pyridin-3-yl)phenyl)quinoline-4-carboxylicAcid (22).—(2-(Trifluoromethyl)pyridin-3-yl)boronic acid (190 mg, 1.12 mmol), 1-(4-bromophenyl)ethan-1-one (200 mg, 1.02 mmol), K_2CO_3 (563 mg, 4.08 mmol), and $Pd(PPh_3)_4$ (118 mg, 10% mol) were dissolved in dioxane (10 mL) and heated to reflux overnight. The solvent was concentrated, and the residue was partitioned between EtOAc and H_2O. Product was extracted with EtOAc (3×), poured over a silica pad, and eluted with additional EtOAc. The elution was concentrated for use in the next step. 1-(4-(2-(Trifluoromethyl)pyridin-3-yl)phenyl)ethan-1-one, isatin (160 mg, 1.02 mmol), and KOH (227 mg, 4.06 mmol) were dissolved in 5 mL of EtOH and 1 mL of H_2O. The mixture was stirred under refluxing conditions for 24 h and then concentrated. Residue was redissolved in 1 M KOH and washed with EtOAc (3×). The aqueous layer was acidified with AcOH until precipitant formation was observed, pH 3–4. The solid was collected and washed with Et_2O and 2-propanol to yield 2-(4-(2-(trifluoromethyl)pyridin-3-yl)phenyl)quinoline-4-carboxylic acid as a tan solid (39 mg, 0.10 mmol, 10% yield over two steps). ^{1}H NMR (400 MHz, DMSO-d_6) δ 8.83 (dd, J = 4.7, 1.5 Hz, 1H), 8.71–8.66 (m, 1H), 8.55 (s, 1H), 8.43 (d, J = 8.4 Hz, 2H), 8.21 (d, J = 8.4 Hz, 1H), 8.05–8.02 (m, 1H), 7.92–7.82 (m, 2H), 7.77–7.71 (m, 1H), 7.59 (d, J = 8.1 Hz, 2H). LCMS (ESI) 395.10 $[M + H]^+$, 393.10 $[M - H]^-$. HPLC purity at 254 nm, 99.8%.

2-(4-(4-(Trifluoromethyl)pyridin-3-yl)phenyl)quinoline-4-carboxylic Acid (23).—Isatin (220 mg, 1.50 mmol), intermediate **67** (235 mg, 0.89 mmol), and KOH (300 mg, 5.36 mmol) were dissolved in 10 mL of absolute EtOH. Following general protocol A, 2-(4-(4-(trifluoromethyl)pyridin-3-yl)phenyl)quinoline-4-carboxylic acid was recovered as a tan solid (**88** mg, 0.22 mmol, 25%). ^{1}H NMR (400 MHz, DMSO-d_6) δ 8.97–8.90 (m, 1H), 8.80 (s, 1H), 8.69 (d, J = 8.5 Hz, 1H), 8.58–8.53 (m, 1H), 8.47–8.40 (m, 2H), 8.21 (d, J = 8.4 Hz, 1H), 7.95–7.85 (m, 2H), 7.74 (t, 1H), 7.62 (d, J = 8.0 Hz, 2H). LCMS (ESI) 394.90 $[M + H]^+$, 392.85 $[M - H]^-$. HPLC purity at 254 nm, 97.1%.

Methyl 2-(4-(4-(Trifluoromethyl)pyridin-3-yl)phenyl)quinoline-4-carboxylate (24).—Compound **23** (30 mg, 0.08 mmol) was dissolved in anhydrous MeOH with a catalytic amount of H_2SO_4 (30 drops). Following general protocol B, methyl 2-(4-(4-(trifluoromethyl)pyridin-3-yl)phenyl)quinoline-4-carboxylate was recovered as a white solid (19 mg, 0.05 mmol, 63%). ^{1}H NMR (400 MHz, $CDCl_3$-d) δ 8.90–8.73 (m, 3H), 8.50 (s, 1H), 8.34 (d, J = 8.2 Hz, 2H), 8.31–8.25 (m, 1H), 7.82 (ddd, J = 8.5, **6.8**, 1.5 Hz, 1H), 7.71–7.65 (m, 2H), 7.56 (d, J = 8.0 Hz, 2H), 4.12 (s, 3H). LCMS (ESI) 409.1 $[M + H]^+$. HPLC purity at 254 nm, 99.9%.

2-(4-(4-Methylpyridin-3-yl)phenyl)quinoline-4-carboxylic Acid (25).—Isatin (140 mg, 0.95 mmol), intermediate **68** (200 mg, 0.95 mmol), and KOH (320 mg, 5.71 mmol) were dissolved in 4 mL of EtOH and 2 mL of H_2O. Following general protocol A, 2-(4-(4-methylpyridin-3-yl)phenyl)quinoline-4-carboxylic acid was recovered as a beige solid (85 mg, 0.25 mmol, 26% yield). ^{1}H NMR (300 MHz, DMSO-$\boldsymbol{d}_6$) $\boldsymbol{\delta}$ 8.85–8.74 (m, 2H), **8.68** (d, ***J*** = 8.5 Hz, 1H), 8.56 (s, 1H), 8.48 (d, ***J*** = 8.1 Hz, 2H), 8.20 (d, ***J*** = 8.4 Hz, 1H), 7.95–7.84 (m, 2H), 7.78–7.68 (m, 3H), 2.53 (s, 4H). LCMS (ESI) 341.20 $[M + H]^+$, 339.15 $[M - H]^-$. HPLC purity at 254 nm, 99.8%.

2-(4-(2-Methylpyridin-3-yl)phenyl)quinoline-4-carboxylic Acid (26).—Isatin (173 mg, 1.18 mmol), intermediate **69** (249 mg, 1.18 mmol), and KOH (394 mg, 7.04 mmol) were dissolved in 4 mL of EtOH and 2 mL of H_2O. Following general protocol A, 2-(4-(2-methylpyridin-3-yl)phenyl)quinoline-4-carboxylic acid recovered as a tan solid, (228 mg, 0.67 mmol, 57% yield). ^{1}H NMR (400 MHz, DMSO-$\boldsymbol{d}_6$) $\boldsymbol{\delta}$ 8.75–8.68 (m, 1H), 8.50 (dd, ***J*** = 4.9, 1.7 Hz, 1H), 8.38–8.32 (m, 2H), 8.19 (s, 1H), 8.09–8.02 (m, 1H), 7.77–7.68 (m, 2H), 7.62–7.51 (m, 3H), 7.35 (dd, ***J*** = 7.7, 4.8 Hz, 1H), 2.51 (s, **8**H). LCMS (ESI) 341.20 $[M + H]^+$, 339.10 $[M - H]^-$. HPLC purity at 254 nm, 99.6%.

2-(4-(6-Fluoropyridin-3-yl)phenyl)quinoline-4-carboxylic Acid (27).—Intermediate **75** (27 mg, 0.08 mmol) and LiOH (45 mg, 1.95 mmol) were dissolved in 1 mL of dioxane and 1 mL of H_2O. Following general protocol E, 2-(4-(6-fluoropyridin-3-yl)phenyl)quinoline-4-carboxylic acid was recovered as a tan solid (21 mg, 0.06 mmol, 75%). ^{1}H NMR (300 MHz, CD_3OD-$\boldsymbol{d}_4$) $\boldsymbol{\delta}$ 8.63–8.56 (m, 1H), 8.46 (d, 1H), 8.38–8.27 (m, 3H), 8.19–8.08 (m, 2H), 7.91–7.83 (m, 2H), 7.78 (t, ***J*** = 8.5, 6.9, 1.5 Hz, 1H), 7.61 (t, ***J*** = 8.3, 6.9, 1.3 Hz, 1H), 7.22 (dd, ***J*** = **8.6**, 2.6 Hz, 1H). LCMS (ESI) 345.2 $[M + H]^+$, 343.1 $[M - H]^-$. HPLC purity at 254 nm, 95.8%.

2-(4-(2-Fluoropyridin-3-yl)phenyl)quinoline-4-carboxylic Acid (28).—Intermediate **76** (23 mg, 0.06 mmol) and LiOH (45 mg, 1.95 mmol) were dissolved in 1 mL of dioxane and 1 mL of H_2O. Following general protocol E, 2-(4-(2-fluoropyridin-3-yl)phenyl)quinoline-4-carboxylic acid was recovered as a white solid (17 mg, 0.05 mmol, 72%). ^{1}H NMR (300 MHz, CD_3OD-$\boldsymbol{d}_4$) $\boldsymbol{\delta}$ 8.49 (d, ***J*** = 8.2 Hz, 1H), 8.30 (d, ***J*** = 8.4 Hz, 2H), 8.26–8.13 (m, 4H), 7.86–7.75 (m, 3H), 7.63 (t, ***J*** = 7.6 Hz, 1H), 7.53–7.46 (m, 1H). LCMS (ESI) 345.10 $[M + H]^+$, 343.05 $[M - H]^-$. HPLC purity at 254 nm, 99.8%.

2-(4-(2-Chloropyridin-3-yl)phenyl)quinoline-4-carboxylic Acid (29).—Intermediate **77** (76 mg, 0.20 mmol) and 115 mg of KOH were dissolved in 2 mL of THF and 2 mL of H_2O. The mixture was stirred at 35 °C for 1 h. Following general protocol E, 2-(4-(2-chloropyridin-3-yl)phenyl)quinoline-4-carboxylic acid was recovered as a tan solid (34 mg, 0.09 mmol, 45%). ^{1}H NMR (400 MHz, DMSO-$\boldsymbol{d}_6$) $\boldsymbol{\delta}$ 8.69–8.63 (m, 1H), 8.52 (s, 1H), 8.49–8.45 (m, 1H), 8.41 (d, ***J*** = 8.3 Hz, 2H), 8.18 (d, ***J*** = 8.4 Hz, 1H), 7.99–7.95 (m, 1H), 7.90–7.83 (m, 1H), 7.74–7.66 (m, 3H), 7.59–7.53 (m, 1H). LCMS (ESI) 361.5 $[M + H]^+$ 359.05 $[M - H]^-$ HPLC purity at 254 nm, 98.6%.

2-(4-(2-Chloro-6-methylpyridin-3-yl)phenyl)quinoline-4-carboxylic Acid (30).— Intermediate **78** (70 mg, 0.18 mmol) was dissolved in 3 mL of dioxane and 1 mL of H_2O with LiOH **(86** mg, 1.87 mmol). Following general protocol E, 2-(4-(2-chloro-6-methylpyridin-3-yl)phenyl)quinoline-4-carboxylic acid was recovered as a white solid **(22** mg, 33%). ^{1}H NMR (300 MHz, DMSO-$\boldsymbol{d}_6$) $\boldsymbol{\delta}$ 8.67 (d, ***J*** = 8.5 Hz, 1H), 8.54 (s, 1H), 8.42 (d, ***J*** = 8.1 Hz, 2H), 8.20 (d, ***J*** = 8.4 Hz, 1H), 7.93–7.84 (m, 2H), 7.79–7.66 (m, 3H), 7.43 (d, ***J*** = 7.6 Hz, 1H), 2.53 (s, 3H). LCMS (ESI) 375.10 $[M + H]^+$, 373.05 $[M - H]^-$. HPLC purity at 254 nm, 99.8%.

2-(4-(1H-Imidazol-1-yl)phenyl)quinoline-4-carboxylic Acid (31).—Isatin (265 mg, 1.80 mmol), 1-(4-(1***H***-imidazol-1-yl)phenyl)ethan-1-one (200 mg, 1.08 mmol), and KOH (242 mg, 4.32 mmol) were dissolved in 7 mL of EtOH and 1 mL of H_2O. Following general protocol A, 2-(4-(1***H***-imidazol-1-yl)phenyl)quinoline-4-carboxylic acid was recovered as a tan solid (116 mg, 0.36 mmol, 33%). ^{1}H NMR (400 MHz, DMSO-$\boldsymbol{d}_6$) $\boldsymbol{\delta}$ 8.64 (dd, ***J*** = 8.5, 1.4 Hz, 1H), 8.50 (s, 1H), 8.49–8.40 (m, 3H), 8.22–8.14 (m, 1H), 7.92–7.82 (m, 4H), 7.75–7.66 (m, 1H), 7.18 (s, 1H). LCMS (ESI) 315.90 $[M + H]^+$, 313.85 $[M - H]^-$. HPLC purity at 254 nm, 95.4%.

2-([1,1′-Biphenyl]-4-yl)-3-methylquinoline-4-carboxylic Acid (32).—Isatin (200 mg, 1.36 mmol), 1-([1,1′-biphenyl]-4-yl)propan-1-one (237 mg, 1.13 mmol), and KOH (266 mg, 4.75 mmol) were dissolved in 5 mL of EtOH and 2 mL of H_2O. Following general protocol A, 2-([1,1′-biphenyl]-4-yl)-3-methylquinoline-4-carboxylic acid was recovered as a tan solid **(8** mg, **0.02** mmol, **2**%) after trituration with diethyl ether and 2-propanol and then recrystallization from EtOH ^{1}H NMR (300 MHz, DMSO-$\boldsymbol{d}_6$) $\boldsymbol{\delta}$ 8.08 (d, ***J*** = 8.2 Hz, 1H), 7.87–7.66 (m, 9H), 7.52 (t, ***J*** = 7.5 Hz, 2H), 7.42 (t, ***J*** = 7.3 Hz, 1H), 2.46 (s, 3H). LCMS (ESI) 340.15 $[M + H]^+$, 338.10 $[M - H]^-$. HPLC purity at 254 nm, 97.5%.

2-(4-(2-Fluoropyridin-3-yl)phenyl)-3-methylquinoline-4-carboxylic Acid (33).— Intermediate **79** (30 mg, 0.08 mmol) and LiOH (60 mg, 2.50 mmol) were dissolved in 3 mL of dioxane and 3 mL of H_2O. The mixture was heated to 100 °C for 1.5 h. Following general protocol E, 2-(4-(2-fluoropyridin-3-yl)phenyl)-3-methylquinoline-4-carboxylic acid was recovered following purification by preparative reverse-phase chromatography as a white solid (9 mg, 0.03 mmol, 38%). ^{1}H NMR (300 MHz, DMSO-$\boldsymbol{d}_6$) $\boldsymbol{\delta}$ 8.32–8.20 (m, 2H), 8.11–8.5 (m, 1H), 7.86–7.77 (m, **6**H), 7.74–7.66 (m, 1H), 7.57–7.51 (m, 1H), 2.46 (s, 3H). LCMS (ESI) 359.1 $[M + H]^+$, 357.2 $[M - H]^-$. HPLC purity at 254 nm, 99.8%.

2-(4-(2-Fluoro-6-methylpyridin-3-yl)phenyl)-3-methylquinoline-4-carboxylic Acid (34).—Intermediate **80** (22 mg, 0.06 mmol) was dissolved in 1 mL of DCM and 1 mL of 1 M BBr_3 in DCM. Following general protocol F, 2-(4-(2-fluoro-6-methylpyridin-3-yl)phenyl)-3-methylquinoline-4-carboxylic acid was recovered as a white solid (13 mg, 0.03 mmol, 50%) following purification by preparative reversephase chromatography. ^{1}H NMR (300 MHz, CD_3OD-$\boldsymbol{d}_4$) $\boldsymbol{\delta}$ 8.12–8.06 (m, 1H), 8.06–8.00 (m, 2H), 7.82–7.68 (m, 5H), 7.65–7.58 (m, 1H), 7.38–7.32 (m, 1H), 2.56 (s, 3H), 2.47 (s, 3H). LCMS (ESI) 373.15 $[M + H]^+$, 371.15 $[M - H]^-$. HPLC purity at 254 nm, 97.5%.

2-(4-(2-Chloropyridin-3-yl)phenyl)-3-methylquinoline-4-carboxylic Acid (35).— Intermediate **81** (33 mg, 0.09 mmol) was dissolved in 1.5 mL of DCM and 1 mL of 1 M BBr_3 in DCM Following general protocol F, 2-(4-(2-chloropyridin-3-yl)phenyl)-3-methylquinoline-4-carbozylic acid was recovered as a white solid (24 mg, 0.06 mmol, **66**%) following purification by preparative reverse-phase chromatography. ^{1}H NMR (300 MHz, DMSO-$\boldsymbol{d}_6$) $\boldsymbol{\delta}$ 8.48 (dd, $\boldsymbol{J}$ = 4.7, 1.9 Hz, 1H), 8.04–7.98 (m, 1H), 7.95–7.83 (m, 2H), 7.73–7.55 (m, **6**H), 7.53–7.45 (m, 1H), 2.35 (s, 3H). LCMS (ESI) 375.10 [M + H]$^+$, 373.10 [M − H]$^-$. HPLC purity at 254 nm, 99.9%.

2-(4-(2-Chloro-6-methylpyridin-3-yl)phenyl)-3-methylquinoline-4-carboxylic Acid (36).—Intermediate **82** (10 mg, 0.02 mmol) was dissolved in 1 mL of DCM and 1 mL of 1 M BBr_3 in DCM Following general protocol F, 2-(4-(2-chloro-6-methylpyridin-3-yl)phenyl)-3-methylquinoline-4-carboxylic acid was recovered as a white solid (l mg, 2.5 × 10^{-3} mmol, 10%) following purification via preparative reverse-phase chromatography. ^{1}H NMR (400 MHz, CD_3OD-$\boldsymbol{d}_4$) $\boldsymbol{\delta}$ 8.16 (d, $\boldsymbol{J}$ = 8.4 Hz, 1H), 8.07 (d, $\boldsymbol{J}$ = 8.5 Hz, 1H), 7.95 (t, $\boldsymbol{J}$ = 7.5 Hz, 1H), 7.88–7.77 (m, 4H), 7.76–7.72 (m, 2H), 7.44–7.40 (m, 1H), 2.61 (s, 3H), 2.54 (s, 3H). LCMS (ESI) 389.15 [M + H]$^+$, 387.15 [M − H]$^-$. HPLC purity at 254 nm, 99.9%.

6-Fluoro-2-(4-(2-fluoropyridin-3-yl)phenyl)-3-methylquinoline-4-carboxylic Acid (37).—Intermediate **83** (34 mg, 0.09 mmol) was dissolved in 1 mL of DCM and 1 mL of 1 M BBr_3 in DCM Following general protocol F, 6-fluoro-2-(4-(2-fluoropyridin-3-yl)phenyl)-3-methylquinoline-4-carboxylic acid was recovered as a white solid (15 mg, 0.04 mmol, 44%) following purification by preparative reversephase chromatography. ^{1}H NMR (400 MHz, DMSO-$\boldsymbol{d}_6$) $\boldsymbol{\delta}$ 8.29 (d, $\boldsymbol{J}$ = 4.8 Hz, 1H), 8.27–8.19 (m, 1H), 8.06–8.00 (m, 1H), 7.80–7.71 (m, 4H), 7.65–7.57 (m, 1H), 7.57–7.48 (m, 2H), 2.38 (s, 3H). LCMS (ESI) 377.15 [M + H]$^+$, 375.10 [M − H]$^-$. HPLC purity at 254 nm, 98.4%.

6-Chloro-2-(4-(2-fluoropyridin-3-yl)phenyl)-3-methylquinoline-4-carboxylic Acid (38).—Intermediate **87** (18 mg, 0.04 mmol) was dissolved in 1 mL of DCM and 1 mL of 1 M BBr_3 in DCM Following general protocol F, 6-chloro-2-(4-(2-fluoropyridin-3-yl)phenyl)-3-methylquinoline-4-carboxylic acid was recovered as a white solid (3 mg, 0.01 mmol, 25%) following purification by preparative reversephase chromatography. ^{1}H NMR (300 MHz, CD_3OD-$\boldsymbol{d}_4$) $\boldsymbol{\delta}$ 8.27–8.16 (m, 2H), 8.04–7.97 (m, 2H), 7.85–7.78 (m, 2H), 7.75–7.66 (m, 3H), 7.52–7.45 (m, 1H), 2.48 (s, 3H). LCMS (ESI) 393.10 [M + H]$^+$, 391.10 [M − H]$^-$. HPLC purity at 254 nm, 95.5%.

2-(4-(2-Chloropyridin-3-yl)phenyl)-3,6-dimethylquinoline-4-carboxylic Acid (39).—Intermediate **90** (17 mg, 0.04 mmol) was dissolved in 1 mL of DCM and 1 mL of 1 M BBr_3 in DCM Following general protocol F, 2-(4-(2-Chloropyridin-3-yl)phenyl)-3,6-dimethylquinoline-4-carboxylic acid was recovered as a white film (2 mg, 5.15 × 10^{-3} mmol, 4%) following purification by preparative reverse-phase chromatography. ^{1}H NMR (300 MHz, CD_3OD-$\boldsymbol{d}_4$) $\boldsymbol{\delta}$ 8.05 (t, $\boldsymbol{J}$ = **8.6** Hz, 2H), 7.91–7.63 (m, 7H), 7.41 (d, $\boldsymbol{J}$ = 7.8 Hz, 1H), 2.60 (s, 3H), 2.49 (s, 3H). LCMS (ESI) 389.1 [M + H]$^+$, 387.2 [M − H]$^-$. HPLC purity at 254 nm, 98.4%.

6-Fluoro-2-(4-(2-fluoro-6-methylpyridin-3-yl)phenyl)-3-methylquinoline-4-carboxylic Acid (40).—Intermediate **84** (17 mg, 0.04 mmol) was dissolved in 1 mL of DCM and 1 mL of 1 M BBr_3 in DCM. Following general protocol F, 6-fluoro-2-(4-(2-fluoro-6-methylpyridin-3-yl)phenyl)-3-methylquinoline-4-carboxylic acid was recovered as a white solid (16 mg, 0.04 mmol, 99% yield) upon trituration with ethanol. ^{1}H NMR (400 MHz, CD_3OD-$\boldsymbol{d}_4$) $\boldsymbol{\delta}$ 8.12–8.2 (m, 2H), 7.82–7.75 (m, 2H), 7.73–7.59 (m, 3H), 7.59–7.50 (m, 1H), 7.37–7.31 (m, 1H), 2.56 (s, 3H), 2.47 (s, 3H). LCMS (ESI) 391.15 $[M + H]^+$, 389.15 $[M - H]^-$. HPLC purity at 254 nm, 97.8%.

2-(4-(2-Chloropyridin-3-yl)phenyl)-6-fluoro-3-methylquinoline-4-carboxylic Acid (41).—Intermediate **85 (6** mg, 1.47×10^{-2} mmol) was dissolved in 1 mL of DCM and 1 mL of 1 M BBr_3 in DCM Following general protocol F, 2-(4-(2-chloropyridin-3-yl)phenyl)-6-fluoro-3-methylquinoline-4-carboxylic acid was recovered as a white film (5 mg, 1.27×10^{-2} mmol, **86**%) following purification by preparative reverse-phase chromatography. ^{1}H NMR (400 MHz, DMSO-$\boldsymbol{d}_6$) $\boldsymbol{\delta}$ 8.53–8.45 (m, 1H), 8.18–8.11 (m, 1H), 8.06–7.96 (m, 1H), 7.79–7.71 (m, 3H), 7.69–7.63 (m, 2H), 7.62–7.55 (m, 1H), 7.55–7.46 (m, 1H), 2.46 (s, 3H). LCMS (ESI) 393.10 $[M + H]^+$, 391.10 $[M - H]^-$. HPLC purity at 254 nm, 95.7%.

6-Chloro-2-(4-(2-chloropyridin-3-yl)phenyl)-3-methylquinoline-4-carboxylic Acid (42).—Intermediate **88** (21 mg, 0.05 mmol) was dissolved in 1 mL of DCM and 1 mL of 1 M BBr_3 in DCM. Following general protocol F, 6-chloro-2-(4-(2-chloropyridin-3-yl)phenyl)-3-methylquinoline-4-carboxylic acid was recovered as a white solid after purification by preparative reverse-phase chromatography (l mg, 2.44×10^{-3} mmol, 5%). ^{1}H NMR (500 MHz, CD_3OD-$\boldsymbol{d}_4$) $\boldsymbol{\delta}$ 8.42 (d, $\boldsymbol{J}$ = 4.9 Hz, 1H), 8.03 (d, $\boldsymbol{J}$ = 9.0 Hz, 1H), 7.98–7.94 (m, 2H), 7.76–7.66 (m, 5H), 7.53 (dd, $\boldsymbol{J}$ = 7.7, 4.8 Hz, 1H), 2.49 (s, 3H). LCMS (ESI) 409.05 $[M + H]^+$, 407.10 $[M - H]^-$. HPLC purity at 254 nm, 98.1%.

2-(4-(2-Chloro-6-methylpyridin-3-yl)phenyl)-6-fluoro-3-methylquinoline-4-carboxylic Acid (43).—Intermediate **86** (13 mg, 0.03 mmol) was dissolved in 1 mL of DCM and 1 mL of 1 M BBr_3 in DCM. Following general protocol F, 2-(4-(2-chloro-6-methylpyridin-3-yl)phenyl)-6-fluoro-3-methylquinoline-4-carboxylic acid was purified via reverse phase preparative chromatography (7 mg, 0.02 mmol, **66**%). ^{3}H NMR (300 MHz, CD_3OD-$\boldsymbol{d}_4$) $\boldsymbol{\delta}$ 8.09–8.01 (m, 1H), 7.89–7.81 (m, 1H), 7.72–7.60 (m, 5H), 7.59–7.50 (m, 1H), 7.40 (d, $\boldsymbol{J}$ = 7.7 Hz, 1H), 2.60 (s, 3H), 2.48 (s, 3H). LCMS (ESI) 407.10 $[M + H]^+$, 405.10 $[M - H]^-$. HPLC purity at 254 nm, 95.1%.

6-Chloro-2-(4-(2-chloro-6-methylpyridin-3-yl)phenyl)-3-methylquinoline-4-carboxylic Acid (44).—Intermediate **89** (28 mg, 0.06 mmol) was dissolved in 1 mL of DCM and 1 mL of 1 M BBr_3 in DCM. Following general protocol F, 6-chloro-2-(4-(2-chloro-6-methylpyridin-3-yl)phenyl)-3-methylquinoline-4-carboxylic acid was recovered as a white solid (1 mg, 2.37×10^{-3} mmol, 3%). ^{1}H NMR (400 MHz, DMSO-$\boldsymbol{d}_6$) $\boldsymbol{\delta}$ 8.13–8.10 (m, 1H), 7.90–7.80 (m, 3H), 7.79–7.73 (m, 2H), 7.66–7.61 (m, 2H), 7.45–7.40 (m, 1H), 2.54 (s, 3H), 2.47 (s, 3H). LCMS (ESI) 424.8 $[M + H]^+$, 422.2 $[M - H]^-$. HPLC purity at 254 nm, 95.1%.

2-([1,1′-Biphenyl]-4-yl)-3-methyl-1,8-naphthyridine-4-carboxylic Acid (45).— Intermediate **97** (40 mg, 0.14 mmol), 1-([1,1′-biphenyl]-4-yl)propan-1-one (25 mg, 0.12 mmol), and KOtBu (78 mg, 0.7 mmol) were dissolved in 2 mL of anhydrous EtOH Following general protocol I, 2-([1,1′-biphenyl]-4-yl)-3-methyl-1,8-naphthyridine-4-carboxylic acid was recovered as a white solid (9 mg, 0.03 mmol, 21%). ^{1}H NMR (400 MHz, DMSO-$\boldsymbol{d}_6$) $\boldsymbol{\delta}$ 9.14 (s, 1H), 8.32 (dd, $\boldsymbol{J}$ = 8.4, 1.9 Hz, 1H), 7.90–7.84 (m, 2H), 7.82–7.78 (m, 4H), 7.76–7.70 (m, 1H), 7.56–7.50 (m, 2H), 7.46–7.40 (m, 1H), 2.51 (s, 3H). LCMS 341.15 [M + H]$^+$, 339.20 [M − H]$^-$. HPLC purity at 254 nm, 99.3%.

2-([1,1′-Biphenyl]-4-yl)-3-methyl-1,7-naphthyridine-4-carboxylic Acid (46).— Intermediate **98** (198 mg, 0.71 mmol), 1-([1,1′-biphenyl]-4-yl)propan-1-one (119 mg, 0.57 mmol), and KOH (112, 1.99 mmol) were dissolved in 10 mL of anhydrous EtOH Following general protocol I, 2-([1,1′-biphenyl]-4-yl)-3-methyl-1,7-naphthyridine-4-carboxylic acid was purified as a white solid (26 mg, 0.08 mmol, **11**%). ^{1}H NMR (400 MHz, DMSO-$\boldsymbol{d}_6$) $\boldsymbol{\delta}$ 9.44 (s, 1H), 8.73–8.61 (m, 1H), 7.88–7.82 (m, 2H), 7.81–7.77 (m, 4H), 7.74 (d, $\boldsymbol{J}$ = 5.7 Hz, 1H), 7.56–7.50 (m, 2H), 7.46–7.41 (m, 1H), 2.51 (s, 3H). LCMS (ESI) 341.2 [M + H]$^+$, 339.1 [M − H]$^-$. HPLC purity at 254 nm, 97.1%.

2-([1,1′-Biphenyl]-4-yl)-3-methyl-1,6-naphthyridine-4-carboxylic Acid (47).— Intermediate **99** (81 mg, 0.29 mmol), 1-([1,1′-biphenyl]-4-yl)propan-1-one (62 mg, 0.29 mmol), and KOH (49 mg, 0.87 mmol) were dissolved in 4 mL of anhydrous EtOH Following general protocol I, 2-([1,1′-biphenyl]-4-yl)-3-methyl-1,6-naphthyridine-4-carboxylic acid was recovered as an amorphous solid **(6** mg, **0.02** mmol, 7%). ^{1}H NMR (400 MHz, CD_3OD-$\boldsymbol{d}_4$) $\boldsymbol{\delta}$ 9.38 (s, 1H), **8.66** (d, $\boldsymbol{J}$ = 6.0 Hz, 1H), 7.95 (d, $\boldsymbol{J}$ = 6.0 Hz, 1H), 7.88–7.82 (m, 2H), 7.79–7.68 (m, 4H), 7.55–7.47 (m, 2H), 7.46–7.36 (m, 1H), 2.53 (s, 3H). LCMS (ESI) 341.1 [M + H]$^+$, 339.2 [M − H]$^-$. HPLC purity at 254 nm, 96.5%.

2-([1,1′-Biphenyl]-4-yl)-3-methyl-6-(trifluoromethyl)-1,7-naphthyridine-4-carboxylic Acid (48).—Intermediate **100** (118 mg, 0.34 mmol), 1-([1,1′-biphenyl]-4-yl)propan-1-one (71 mg, 0.34 mmol), and KOH (76 mg, 1.36 mmol) were dissolved in 5 mL of anhydrous EtOH. Following general protocol I, 2-([1,1′-biphenyl]-4-yl)-3-methyl-6-(trifluoromethyl)-1,7-naphthyridine-4-carboxylic acid (4 mg, 0.01 mmol, 3%) was recovered as a clear oil. ^{1}H NMR (300 MHz, CD_3OD-$\boldsymbol{d}_4$) $\boldsymbol{\delta}$ 9.42 (s, 1H), 8.29 (s, 1H), 7.84 (d, $\boldsymbol{J}$ = 8.3 Hz, 2H), 7.77–7.70 (m, 4H), 7.50 (t, $\boldsymbol{J}$ = 7.6 Hz, 2H), 7.39 (t, $\boldsymbol{J}$ = 7.5 Hz, 1H), 2.57 (s, 3H). LCMS (ESI) 409.2 [M + H]$^+$, 407.2 [M − H]$^-$. HPLC purity at 254 nm, 97.2%.

2-(4-(2-Chloropyridin-3-yl)phenyl)-3-methyl-1,7-naphthyridine-4-carboxylic Acid (49).—Intermediate **98** (32 mg, 0.12 mmol) intermediate 63 (28 mg, 0.12 mmol), and KOH (60 mg, 1.07 mmol) were dissolved in 2 mL of anhydrous EtOH Following general protocol I, 2-(4-(2-chloropyridin-3-yl)phenyl)-3-methyl-1,7-naphthyridine-4-carboxylic acid (4 mg, 0.03 mmol, **8**%) was recovered as a white solid. ^{1}H NMR (300 MHz, CD_3OD-$\boldsymbol{d}_4$) $\boldsymbol{\delta}$ 9.34 (s, 1H), 8.57 (d, $\boldsymbol{J}$ = 5.8 Hz, 1H), 8.48–8.42 (m, 1H), 8.02–7.91 (m, 2H), 7.80–7.65 (m, 4H), 7.59–7.51 (m, 1H), 2.55 (s, 3H). LCMS (ESI) 376.1 [M + H]$^+$, 374.1 [M − H]$^-$. HPLC purity at 254 nm, 96.0%.

2-(4-(2-Chloro-6-methylpyridin-3-yl)phenyl)-3-methyl-1,7-naphthyridine-4-carboxylic Acid (50).—Intermediate **98 (66** mg, 0.24 mmol), intermediate 64 (62 mg, 0.24 mmol), and KOH (60 mg, 1.07 mmol) were dissolved in 3 mL of anhydrous EtOH Following general protocol I, 2-(4-(2-chloro-6-methylpyridin-3-yl)phenyl)-3-methyl-1,7-naphthyridine-4-carboxylic acid (2 mg, 0.03 mmol, 4%). ^{1}H NMR (300 MHz, CD_3OD-$\boldsymbol{d}_4$) $\boldsymbol{\delta}$ 9.88 (s, 1H), 8.80 (d, ***J*** = 6.5 Hz, 1H), 8.57 (d, ***J*** = **6.6** Hz, 1H), 7.88 (dd, ***J*** = 10.8, 7.8 Hz, 3H), 7.72 (d, ***J*** = 7.9 Hz, 2H), 7.45 (d, ***J*** = 7.8 Hz, 1H), 2.76 (s, 3H), 2.62 (s, 3H). LCMS (ESI) 390.1 $[M + H]^+$, 388.1 $[M - H]^-$. HPLC purity at 254 nm, 95.0%.

2-(4-(2-Chloropyridin-3-yl)phenyl)-3-methyl-6-(trifluoromethyl)-1.7-naphthyridine-4-carboxylic Acid (51).—Intermediate **102** **(8** mg, 1.9×10^{-2} mmol) and NaOH (44 mg, 1.15 mmol) were dissolved in dioxane and water then heated to 60 °C overnight. Upon completion, the mixture was concentrated to a residue and the corresponding carboxylic acid was used for the next step without purification. The residue was combined with (2-chloropyridin-3-yl)boronic acid **(6** mg, 0.03 mmol), Na_2CO_3 **(8** mg, 0.08 mmol), and $Pd(PPh_3)_4$ (l mg) and dissolved in 0.5 mL of dioxane and 0.5 mL of H_2O. The mixture was heated to 110 °C for 3 h Upon completion, the mixture was concentrated, redissolved in 0.5 M NH_3 in MeOH, and purified via reverse-phase preparatory chromatography to yield 2-(4-(2-chloropyridin-3-yl)phenyl)-3-methyl-6-(trifluoromethyl)-1,7-naphthyridine-4-carboxylic acid as a white film (2 mg, 4.5×10^{-2} mmol, 46% over 2 steps). ^{1}H NMR (400 MHz, CD_3OD-$\boldsymbol{d}_4$) $\boldsymbol{\delta}$ 9.50 (s, 1H), 8.47–8.43 (m, 1H), 8.30 (s, 1H), 8.01–7.94 (m, 1H), 7.81 (d, ***J*** = 8.3 Hz, 2H), 7.72 (d, ***J*** = 8.2 Hz, 2H), 7.58–7.53 (m, 1H), 2.64 (s, 3H). LCMS (ESI) 444.2 $[M + H]^+$, 442.2 $[M - H]^-$. HPLC purity at 254 nm, 98.9%.

2-(2'-Fluoro-[1,1'-biphenyl]-4-yl)-3-methyl-6-(trifluoromethyl)-1.7-naphthyridine-4-carboxylic Acid (52).—Intermediate **91** **(8** mg, 0.02 mmol) and KOH (61 mg, 1.08 mmol) were dissolved in 0.5 mL of THF and 0.5 mL of H_2O. The mixture was heated to 50 °C for 4 h. Following general protocol E, 2-(2′-fluoro-[1,1′-biphenyl]-4-yl)-3-methyl-6-(trifluoromethyl)-1,7-naphthyridine-4-carboxylic acid was recovered Sallowing reverse-phase preparatory chromatography (5 mg, 0.01 mmol, 50%). ^{1}H NMR (300 MHz, CD_3OD-$\boldsymbol{d}_4$) $\boldsymbol{\delta}$ 9.48 (s, 1H), 8.29 (s, 1H), 7.78 (s, 4H), **7.66–7.57** (m, 1H), 7.44 (q, ***J*** = 6.3, 5.8 Hz, 1H), 7.37–7.21 (m, 2H), 2.63 (s, 3H). LCMS (ESI) 427.1 $[M + H]^+$, 425.2 $[M - H]^-$. HPLC purity at 254 nm, 98.4%.

2-(4-Bromophenyl)quinoline-4-carboxylic Acid (53).—Isatin (5.00 g, 34.0 mmol), 1-(4-bromophenyl)ethan-1-one (6.70 g, 34.0 mmol), and KOH (11.4 g, 204 mmol) were dissolved in 55 mL of EtOH and 24 mL of H_2O. Following general protocol A, 2-(4-bromophenyl)quinoline-4-carboxylic acid was recovered as a yellow solid (9.02 g, 27.7 mmol, 81%). ^{1}H NMR (300 MHz, DMSO-$\boldsymbol{d}_6$) $\boldsymbol{\delta}$ **8.68** (d, ***J*** = 8.3 Hz, 1H), 8.20 (d, ***J*** = 8.5 Hz, 2H), 8.08 (s, 1H), 8.02 (d, ***J*** = 8.4 Hz, 1H), 7.72 (dd, ***J*** = 12.5, 8.1 Hz, 3H), 7.53 (t, ***J*** = 7.6 Hz, 1H). MS (ESI) 328.0 $[M + H]^+$.

2-(4-Bromophenyl)-3-methylquinoline-4-carboxylic Acid (54).—Isatin (5.00 g, 34.0 mmol), 1-(4-bromophenyl)propan-1-one (7.41 g, 34.7 mmol), and KOH (11.4 g, 204 mmol)

were dissolved in 55 mL of EtOH and 24 mL of H_2O. Following general protocol A, 2-(4-bromophenyl)-3-methylquinoline-4-carboxylic acid was recovered as a white solid (8.73 g, 25.6 mmol, 75%) upon recrystallization in EtOH ^{1}H NMR (300 MHz, DMSO-d_6) δ 8.03 (d, J = 8.5 Hz, 1H), 7.81–7.56 (m, 7H), 2.36 (s, 3H). MS (ESI) 342.00, 343.95 $[M + H]^+$, 342.00, 340.00 $[M - H]^-$.

2-(4-Bromophenyl)-6-fluoro-3-methylquinoline-4-carboxylic Acid (55).—5-Fluoroisatin (1.00 g, 6.06 mmol), 1-(4-bromophenyl)propan-1-one (1.29 g, 6.06 mmol), and KOH (1.02 g, 18.2 mmol) were dissolved in 10 mL of EtOH and 3 mL of H_2O. Following general protocol A, 2-(4-bromophenyl)-6-fluoro-3-methylquinoline-4-carboxylic acid was recovered as a beige solid (853 mg, 2.38 mmol, 39%). ^{1}H NMR (500 MHz, DMSO-d_6) δ = 8.14–8.10 (m, 1H), 7.73–7.67 (m, 3H), 7.57 (d, J = 8.1 Hz, 2H), 7.51–7.47 (m, 1H), 2.39 (s, 3H). MS (ESI+) 360.00, 361.95 $[M + H]^+$ 358.10, 360.15 $[M - H]^-$.

2-(4-Bromophenyl)-6-chloro-3-methylquinoline-4-carboxylic Acid (56).—5-Chloroisatin (1.00 g, 5.49 mmol), 1-(4-bromophenyl)propan-1-one (1.20 g, 5.63 mmol), and KOH (1.23 g, 22.0 mmol) were dissolved in 20 mL of EtOH and 10 mL of H_2O. Following general protocol A, 2-(4-bromophenyl)-6-chloro-3-methylquinoline-4-carboxylic acid was recovered as a tan solid (1.57 g, 4.18 mmol, 76%). ^{1}H NMR (400 MHz, DMSO-d_6) δ 8.13 (d, J = **8.8** Hz, 1H), 7.88–7.81 (m, 2H), 7.79–7.75 (m, 2H), 7.68–7.62 (m, 2H), 2.47 (s, 3H). MS (ESI) 376.0, 377.9 $[M + H]^+$.

2-(4-Bromophenyl)-3,6-dimethylquinoline-4-carboxylic Acid (57).—5-Methylisatin (1.00 g, 6.21 mmol), 1-(4-bromophenyl)propan-1-one (1.32 g, 6.20 mmol), and KOH (1.39 g, 24.8 mmol) were dissolved in 10 mL of EtOH and 3 mL of H_2O. Following general protocol A, 2-(4-bromophenyl)-3,6-dimethylquinoline-4-carboxylic acid was recovered as a tan solid (1.14 g, 3.20 mmol, 52%). ^{1}H NMR (400 MHz, DMSO-d_6) δ 8.07 (d, J = **8.6** Hz, 1H), 7.79–7.70 (m, 3H), 7.66–7.60 (m, 3H), 2.56 (s, 3H), 2.38 (s, 3H). MS (ESI) 356.0 $[M + H]^+$.

Methyl 2-(4-Bromophenyl)quinoline-4-carboxylate (58).—Intermediate **53** (9.00 g, 27.4 mmol), Cs_2CO_3 (10.8 g, 33.3 mmol), and MeI (3.48 mL, 55.4 mmol) were stirred at room temperature in 139 mL of DMF overnight Following general protocol C, methyl 2-(4-bromophenyl)quinoline-4-carboxylate (4.07 g, 11.9 mmol, 43%) was recovered as a white solid. ^{1}H NMR (300 MHz, $CDCl_3$-d) δ 8.79–8.71 (m, 1H), 8.36 (s, 1H), 8.25–8.17 (m, 1H), 8.14–8.06 (m, 2H), 7.83–7.74 (m, 1H), 7.71–7.61 (m, 3H), 4.09 (s, 3H). MS (ESI) 342.0 $[M + H]^+$.

Methyl 2-(4-Bromophenyl)-3-methylquinoline-4-carboxylate (59).—Intermediate **54** (8.73 g, 25.6 mmol), Cs_2CO_3 (9.98 g, 30.7 mmol), and MeI (3.22 mL, 51.2 mmol) were stirred at room temperature in 140 mL of DMF overnight. Following general protocol C, methyl 2-(4-bromophenyl)-3-methylquinoline-4-carboxylate (7.55 g, 21.2 mmol, 83%) was recovered as a white cake-like powder. ^{1}H NMR (300 MHz, $CDCl_3$-d) δ 8.15 (d, J = **8.6** Hz, 1H), 7.78–7.69 (m, 2H), 7.70–7.57 (m, 3H), 7.47 (d, J = 7.5 Hz, 2H), 4.12 (s, 3H), 2.41 (s, 3H). MS (ESI) 356.0, 357.9 $[M + H]^+$.

Methyl 2-(4-Bromophenyl)-6-fluoro-3-methylquinoline-4-carboxylate (60).— Intermediate **55** (853 mg, 2.38 mmol), Cs_2CO_3 (928 mg, 2.86 mmol), and MeI (0.3 mL, 4.76 mmol) were stirred at room temperature in 12 mL of DMF overnight. Following general protocol C, methyl 2-(4-bromophenyl)-6-fluoro-3-methylquinoline-4-carboxylate recovered (636 mg, 1.71 mmol, 71%) as a solid. ^{1}H NMR (300 MHz, $CDCl_3$-***d***) ***δ*** 8.13 (dd, ***J*** = 9.2, 5.4 Hz, 1H), 7.70–7.63 (m, 2H), 7.54–7.43 (m, 3H), 7.42–7.35 (m, 1H), 4.11 (s, 3H), 2.42 (s, 3H). MS (ESI) 374.0, 376.0 $[M + H]^+$.

Methyl 2-(4-Bromophenyl)-6-chloro-3-methylquinoline-4-carboxylate (61).— Intermediate **56** (1.57 g, 4.18 mmol), Cs_2CO_3 (1.63 g, 5.02 mmol), and MeI (0.53 mL, 8.36 mmol) were stirred at room temperature in 40 mL of DMF overnight. Following general protocol C, methyl 2-(4-bromophenyl)-6-chloro-3-methylquinoline-4-carboxylate (1.21 g, 3.13 mmol, 75%) was recovered as an orange solid. ^{1}H NMR (300 MHz, $CDCI_3$-***d***) ***δ*** 8.07 (d, ***J*** = 9.0 Hz, 1H), 7.75–7.71 (m, 1H), 7.66 (d, ***J*** = 8.1 Hz, 3H), 7.49–7.42 (m, 2H), 4.13 (s, 2H), 2.42 (s, 3H). MS (ESI) 389.9, 392.0 $[M + H]^+$.

Methyl 2-(4-Bromophenyl)-3,6-dimethylquinoline-4-carboxylate (62).— Intermediate **57** (1.14 g, 3.08 mmol), Cs_2CO_3 (1.20 g, 3.69 mmol), and MeI (0.38 mL, 6.16 mmol) were stirred at room temperature in 40 mL of DMF overnight. Following general protocol C, methyl 2-(4-bromophenyl)-3,6-dimethylquinoline-4-carboxylate (1.06 g, 2.87 mmol, 93%) was recovered as an orange solid. ^{1}H NMR (300 MHz, $CDCI_3$-***d***) ***δ*** 8.03 (d, ***J*** = **8.6** Hz, 1H), 7.68–7.60 (m, 2H), 7.59–7.53 (m, 1H), 7.50–7.42 (m, 3H), 4.12 (s, 3H), 2.57 (s, 3H), 2.39 (s, 3H). MS (ESI) 370.0, 371.9 $[M + H]^+$.

1-(4-(Pyridin-2-yl)phenyl)ethan-1-one (63).—(4-AcetyIphenyl)boronic acid (1.04 g, 6.34 mmol), 2-iodopyridine (0.52 mL, 4.85 mmol), K_2CO_3 (2.68 g, 19.4 mmol), and $Pd(PPh_3)_4$ (280 mg) were dissolved in 10 mL of dioxane and 1 mL of H_2O. The reaction was heated to 100 °C overnight. Following general protocol D, 1-(4-(pyridin-2-yl)phenyl)ethan-1-one was recovered as a white solid (185 mg, 0.93 mmol, 19%). ^{1}H NMR (400 MHz, $CDCl_3$-***d***) ***δ*** 8.78–8.74 (m, 1H), 8.15–8.06 (m, 4H), 7.84–7.80 (m, 2H), 7.34–7.29 (m, 1H), 2.67 (s, 3H). MS (ESI) 198.0 $[M + H]^+$.

1-(4-(Pyrimidin-5-yl)phenyl)ethan-1-one (64).—(4-Acetylphenyl)boronic acid (155 mg, 0.94 mmol), 5-bromopyrimidine (100 mg, 0.63 mmol), K_2HPO_3 (219 g, 1.26 mmol), and $Pd(OAc)_2$ (2 mg) were dissolved in 10 mL of ethylene glycol. The reaction was heated to 80 °C for 4 h. Following general protocol D, 1-(4-(pyrimidin-5-yl)phenyl)ethan-1-one was recovered as a white solid (104 mg, 0.52 mmol, 55%). ^{1}H NMR (300 MHz, $CDCl_3$-***d***) ***δ*** 9.33 (s, 1H), 9.05 (s, 2H), 8.14 (d, ***J*** = 8.3 Hz, 2H), 7.72 (d, ***J*** = 8.3 Hz, 2H), 2.69 (s, 3H). MS (ESI) 199.0 $[M + H]^+$.

1-(4-(Pyridazin-3-yl)phenyl)ethan-1-one (65).—(4-Acetylphenyl)boronic acid (670 mg, 4.08 mmol), 3-bromopyridazine (500 mg, 3.15 mmol), K_2CO_3 (1.74 g, 12.6 mmol), and $Pd(PPh_3)_4$ (182 mg) were dissolved in 10 mL of dioxane and 1 mL of H_2O. The reaction was heated to 100 °C overnight. Following general protocol D, 1-(4-(pyridin-2-yl)phenyl)ethan-1-one was recovered as a white solid (301 mg, 1.52 mmol, 48%). ^{1}H NMR

(400 MHz, $CDCl_3$-***d***) ***δ*** 8.12–8.05 (m, 2H), 7.97–7.89 (m, 1H), 7.77–7.70 (m, 2H), 7.00–6.91 (m, 1H), 2.69 (s, 3H). MS (ESI) 199.2 $[M + H]^+$.

1-(4-(Pyrimidin-2-yl)phenyl)ethan-1-one (66).—(4-Acetylphenyl)boronic acid (1.08 g, 6.60 mmol), 2-bromopyrimidine (700 mg, 4.40 mmol), K_2CO_3 (2.43 g, 17.6 mmol), and $Pd(PPh_3)_4$ (254 mg) were dissolved in 10 mL of dioxane. The reaction was heated to 100 °C for 10 h. Following general protocol D, 1-(4-(pyrimidin-2-yl)phenyl)ethan-1-one was recovered as a white solid (109 mg, 0.55 mmol, 13%). ^{1}H NMR (400 MHz, $CDCl_3$-***d***) ***δ*** 8.87 (d, ***J*** = 4.8 Hz, 2H), 8.60–8.54 (m, 2H), 8.12–8.07 (m, 2H), 7.30–7.26 (m, 1H), 2.69 (s, 3H). MS (ESI) 199.1 $[M + H]^+$.

1-(4-(4-(Trifluoromethyl)pyridin-3-yl)phenyl)ethan-1-one (67).—(4-Acetylphenyl)boronic acid (100 mg, 0.44 mmol), 3-bromo-4-(trifluoromethyl)pyridine (109 mg, 0.66 mmol), K_2HPO_4 (230 mg, 1.32 mmol), and $Pd(PPh_3)_4$ (25 mg) were dissolved in 2 mL of dioxane and 1 mL of H_2O. The mixture was heated to 130 °C for 1.5 h in a microwave reactor. Following general protocol D, l-(4-(4-(trifluoromethyl)pyridin-3-yl)phenyl)ethan-1-one was recovered as a dear oil (60 mg, 0.23 mmol, 53%). ^{1}H NMR (300 MHz, $CDCl_3$-***d***) ***δ*** 8.87–8.81 (m, 1H), **8.66** (s, 1H), 8.11–8.02 (m, 2H), 7.66 (d, ***J*** = 5.1 Hz, 1H), 7.46 (d, ***J*** = 8.1 Hz, 2H), 2.67 (s, 3H). MS (ESI) 266.0 $[M + H]^+$.

1-(4-(4-Methylpyridin-3-yl)phenyl)ethan-1-one (68).—(4-Acetylphenyl)boronic acid (570 mg, 3.47 mmol), 3-bromo-4-methylpyridine (0.20 mL, 1.79 mmol), Na_2CO_3 (1.47 g, 13.9 mmol), and $Pd(PPh_3)_4$ (200 mg) were dissolved in 10 mL of toluene and 1 mL of H_2O. The reaction was heated to 120 °C for 10 h. Following general protocol D, 1-(4-(4-methylpyridin-3-yl)phenyl)ethan-1-one was recovered (368 mg, 1.74 mmol, 97%) as a white solid. ^{1}H NMR (300 MHz, $CDCl_3$-***d***) ***δ*** 8.38–8.27 (m, 2H), 7.93 (d, ***J*** = 8.0, 1.6 Hz, 2H), 7.31 (d, ***J*** = 8.1, 1.6 Hz, 2H), 7.09 (d, ***J*** = 5.1 Hz, 1H), 2.52 (s, 3H), 2.17 (s, 3H). MS (ESI) 212.1 $[M + H]^+$.

1-(4-(2-Methylpyridin-3-yl)phenyl)ethan-1-one (69).—(4-Acetylphenyl)boronic acid (570 mg, 3.47 mmol), 3-bromo-2-methylpyridine (0.20 mL, 1.73 mmol), Na_2CO_3 (1.47 g, 13.88 mmol), and $Pd(PPh_3)_4$ (200 mg) were dissolved in 10 mL of toluene and 1 mL of H_2O. The reaction was heated to 120 °C for 10 h. Following general protocol D, 1-(4-(2-methylpyridin-3-yl)phenyl)ethan-1-one was recovered as an oil (249 mg, 1.18 mmol, **68**%). ^{1}H NMR (400 MHz, $CDCl_3$-***d***) ***δ*** 8.57–8.54 (m, 1H), 8.09–8.04 (m, 2H), 7.58–7.53 (m, 1H), 7.47–7.42 (m, 2H), 7.27–7.22 (m, 1H), 2.67 (s, 3H), 2.54 (s, 3H). MS (ESI) 212.1 $[M + H]^+$.

1-(4-(2-Chloropyridin-3-yl)phenyl)propan-1-one (70).—4′-Bromo-propiophenone (300 mg, 1.41 mmol), 2-chloropryidine-3-boronic acid (332 mg, 2.11 mmol), K_2HPO_4 (736 mg, 4.23 mmol), and $Pd(PPh_3)_4$ (81 mg) were added to a microwave vial in 2 mL of dioxane and 1 mL of H_2O. The mixture was heated to 100 °C for 12 h. Following general protocol D, 1-(4-(2-chloropyridin-3-yl)phenyl)propan-1-one was recovered as a white solid (134 mg, 0.55 mmol, 39%). ^{1}H NMR (300 MHz, $CDCl_3$-*d*) *δ* 8.43 (dd, *J* = 4.8, 1.9 Hz, 1H), 8.06 (d,

2H), 7.71 (dd, *J* = 7.5, 1.9 Hz, 1H), 7.56 (d, 2H), 7.41–7.34 (m, 1H), 3.06 (q, *J* = 7.2 Hz, 2H), 1.25 (t, *J* = 7.2 Hz, 3H). MS (ESI) 246.0 $[M + H]^+$.

1-(4-(2-Chloro-6-methylpyridin-3-yl)phenyl)propan-1-one (71).—4′-Bromopropiophenone (220 mg, 1.03 mmol), (2-chloro-6-methylpyridin-3-yl)boronic acid (264 mg, 1.54 mmol), K_2HPO_4 (538 mg, 3.9 mmol), and $Pd(PPh_3)_4$ (60 mg, 5% mmol) were dissolved in 2 mL of dioxane and 1 mL of H_2O. The mixture was heated to 130 °C for 1.5 h in a microwave reactor. Following general protocol D, 1-(4-(2-chloro-6-methylpyridin-3-yl)phenyl)propan-1-one was recovered as a white solid (137 mg, 0.53 mmol, 51%). ^{1}H NMR (300 MHz, $CDCl_3$-*d*) δ 8.07–7.99 (m, 2H), 7.59–7.49 (m, 3H), 7.19 (d, *J* = 7.7 Hz, 1H), 3.4 (q, *J* = 7.2 Hz, 2H), 2.58 (s, 3H), 1.24 (t, *J* = 7.2 Hz, 3H). MS (ESI) 260.0 $[M + H]^+$.

Methyl 2-(4-(Pyridin-4-yl)phenyl)quinoline-4-carboxylate (72).—Intermediate **58** (100 mg, 0.29 mmol), 4-pyridineboronic acid pinacol ester (84 mg, 0.41 mmol), $Pd(PPh_3)_4$ (17 mg), and K_2CO_3 (151 mg, 0.87 mmol) were dissolved in 2 mL of dioxane and 1 mL of H_2O. The mixture was heated to 130 °C for 1.5 h in a microwave reactor. Following general protocol D, methyl 2-(4-(pyridin-4-yl)phenyl)quinoline-4-carboxylate was recovered as an off-white solid (34 mg, 0.10 mmol, 34%). ^{1}H NMR (300 MHz, $CDCl_3$-*d*) δ 8.80–8.67 (m, 3H), 8.44 (s, 1H), 8.39–8.30 (m, 2H), 8.28–8.20 (m, 1H), 7.79 (dd, *J* = 8.8, 6.7 Hz, 3H), 7.70–7.55 (m, 3H), 4.09 (s, 3H). LCMS (ESI) 341.1 $[M + H]^+$. HPLC purity at 254 nm, 99.6%.

Methyl 2-(4-(2-Methoxypyridin-3-yl)phenyl)quinoline-4-carboxylate (73).—Intermediate **58** (200 mg, 0.59 mmol), (2-methoxypyridin-3-yl)boronic acid (108 mg, 0.70 mmol), K_2CO_3 (326 mg, 2.36 mmol), and $Pd(PPh_3)_4$ (67 mg) were dissolved in 5 mL of toluene and 2 mL of H_2O. The mixture was heated to reflux overnight Following general protocol D, methyl 2-(4-(2-methoxypyridin-3-yl)phenyl)quinoline-4-carboxylate was recovered as an off-white solid (15 mg, 0.04 mmol, 7%). ^{1}H NMR (300 MHz, $CDCl_3$-*d*) δ 8.78 (d, *J* = 8.5 Hz, 1H), 8.48 (s, 1H), 8.34–8.19 (m, 4H), 7.86–7.61 (m, 5H), 7.08–7.00 (m, 1H), 4.11 (s, 3H), 4.03 (s, 3H). MS (ESI) 371.1 $[M + H]^+$.

Methyl 2-(2′-Methoxy-[1,1′-biphenyl]-4-yl)quinoline-4-carboxylate (74).—Intermediate **58** (l40 mg, 0.41 mmol), (2-methoxyphenyl)boronic acid (87 mg, 0.57 mmol), K_2CO_3 (250 mg, 1.81 mmol), and $Pd(PPh_3)_4$ (26 mg) were dissolved in 6 mL of anhydrous dioxane. The mixture was heated to reflux overnight. Following general protocol D, methyl 2-(2′-methoxy-[1,1′-biphenyl]-4-yl)quinoline-4-carboxylate (14 mg, 0.04 mmol, 10%). ^{1}H NMR (300 MHz, $CDCl_3$-*d*) δ 8.848.75 (m, 1H), 8.49 (s, 1H), 8.35–8.25 (m, 3H), 7.84–7.73 (m, 3H), 7.69–7.62 (m, 1H), 7.46–7.35 (m, 2H), 7.15–7.01 (m, 2H), 4.11 (s, 3H), 3.87 (s, 2H). MS (ESI) 370.1 $[M + H]^+$.

Methyl 2-(4-(6-Fluoropyridin-3-yl)phenyl)quinoline-4-carboxylate (75).—Intermediate **58** (50 mg, 0.15 mmol), (6-fluoropyridin-3-yl)boronic acid (35 mg, 0.25 mmol), K_2HPO_4 (73 mg, 0.42 mmol), and $Pd(PPh_3)_4$ (8 mg, 7.0×10^{-3} mmol) were dissolved in 1 mL of dioxane and 0.5 mL of H_2O. The mixture was heated to 130 °C for 1.5 h in a microwave reactor. Following general protocol D, methyl 2-(4-(6-fluoropyridin-3-

yl)phenyl)quinoline-4-carboxylate was recovered as a beige solid (45 mg, 0.13 mmol, 93% yield). ^{1}H NMR (300 MHz, $CDCl_3$-*d*) δ 8.82–8.74 (m, 1H), 8.56–8.49 (m, 1H), 8.46 (s, 1H), 8.40–8.31 (m, 2H), 8.26 (d, *J* = 8.5, 0.9 Hz, 1H), 8.10–8.01 (m, 1H), 7.85–7.77 (m, 1H), 7.76–7.62 (m, 3H), 7.06 (dd, *J* = 8.5, 3.0 Hz, 1H). MS (ESI) 359.0 [M + H]$^+$.

Methyl 2-(4-(2-Fluoropyridin-3-yl)phenyl)quinoline-4-carboxylate (76).— Intermediate **58** (50 mg, 0.15 mmol), (2-fluoropyridin-3-yl)boronic acid (34 mg, 0.24 mmol), K_2HPO_4 (73 mg, 0.42 mmol) and $Pd(PPh_3)_4$ (**8** mg, 7.0 × 10^{-3} mmol) were dissolved in 1 mL of dioxane and 0.5 mL of H_2O. The mixture was heated to 130 °C for 1.5 h in a microwave reactor. Following general protocol D, methyl 2-(4-(2-fluoropyridin-3-yl)phenyl)quinoline-4-carboxylate was recovered as a white solid (45 mg, 0.13 mmol, 93% yield). ^{1}H NMR (300 MHz, $CDCl_3$-***d***) ***δ*** 8.78 (d, ***J*** = **8.6**, 1.3 Hz, 1H), 8.47 (s, 1H), 8.37–8.31 (m, 2H), 8.30–8.19 (m, 1H), 8.02–7.92 (m, 1H), 7.85–7.63 (m, 5H), 7.38–7.31 (m, 1H). MS (ESI) 359.1 [M + H]$^+$

Methyl 2-(4-(2-Chloropyridin-3-yl)phenyl)quinoline-4-carboxylate (77).— Intermediate **58** (150 mg, 0.44 mmol), (2-chloropyridin-3-yl)boronic acid (110 mg, 0.71 mmol), K_2CO_3 (243 mg, 1.76 mmol), and $Pd(PPh_3)_4$ (25 mg) were dissolved in 5 mL of dioxane and 1 mL of H_2O. The mixture was heated to reflux overnight. Following general protocol D, methyl 2-(4-(2-chloropyridin-3-yl)phenyl)quinoline-4-carboxylate was recovered as an off-white solid (76 mg, 0.20 mmol, 45%). ^{1}H NMR (300 MHz, $CDCl_3$-*d*) δ 8.79 (d, *J* = 8.5 Hz, 1H), 8.50–8.43 (m, 2H), 8.33 (d, *J* = 8.1 Hz, 2H), 8.27 (d, *J* = 8.4 Hz, 1H), 7.85–7.73 (m, 2H), 7.68 (dd, *J* = 8.4, 6.5 Hz, 3H), 7.40–7.34 (m, 1H), 4.11 (s, 3H). MS (ESI) 375.0 [M + H]$^+$.

Methyl 2-(4-(2-Chloro-6-methylpyridin-3-yl)phenyl)quinoline-4-carboxylate (78).—Intermediate **58** (132 mg, 0.39 mmol), (2-chloro-6-methylpyridin-3-yl)boronic acid (100 mg, 0.58 mmol), K_2HPO_4 (204 mg, 1.17 mmol), and $Pd(PPh_3)_4$ (23 mg) were dissolved in 5 mL of dioxane and 1 mL of H_2O. The mixture was heated to reflux overnight. Following general protocol D, methyl 2-(4-(2-chloro-6-methylpyridin-3-yl)phenyl)quinoline-4-carboxylate (109 mg, 0.29 mmol, 74%). ^{1}H NMR (300 MHz, $CDCl_3$-*d*) δ 8.83–8.74 (m, 1H), 8.47 (s, 1H), 8.35–8.22 (m, 3H), 7.86–7.77 (m, 1H), 7.72–7.61 (m, 4H), 7.21 (d, *J* = 7.6 Hz, 1H), 4.10 (s, 3H), 2.63 (s, 3H). MS (ESI) 389.1 [M + H]$^+$.

Methyl 2-(4-(2-Fluoropyridin-3-yl)phenyl)-3-methylquinoline-4-carboxylate (79).—Intermediate **59** (100 mg, 0.28 mmol), (2-fluoropyridin-3-yl)boronic acid (60 mg, 0.42 mmol), K_2HPO_4 (146 mg, 0.84 mmol), and $Pd(PPh_3)_4$ (16 mg, 0.01 mmol) were dissolved in 2 mL of dioxane and 1 mL of H_2O. The mixture was heated to 130 °C for 1.5 h in a microwave reactor. Following general protocol D, methyl 2-(4-(2-fluoropyridin-3-yl)phenyl)-3-methylquinoline-4-carboxylate was recovered as a white solid (82 mg, 0.22 mmol, 79%). ^{1}H NMR (300 MHz, $CDCl_3$-*d*) δ 8.26–8.22 (m, 1H), 8.20–8.15 (m, 1H), 7.98–7.90 (m, 1H), 7.78–7.67 (m, 6H), 7.64–7.56 (m, 1H), 7.35–7.29 (m, 1H), 4.12 (s, 3H), 2.48 (s, 3H). MS (ESI) 373.1 [M + H]$^+$.

Methyl 2-(4-(2-Fluoro-6-methylpyridin-3-yl)phenyl)-3-methylquinoline-4-carboxylate (80).—Intermediate **59** (50 mg, 0.13 mmol), (2-fluoro-6-methylpyridin-3-

yl)boronic acid (31 mg, 0.20 mmol), K_2HPO_4 (73 mg, 0.42 mmol), and $Pd(PPh_3)_4$ (7 mg, 6.0×10^{-3} mmol) were dissolved in 1 mL of dioxane and 0.5 mL of H_2O. The mixture was heated to 130 °C for 1.5 h in a microwave reactor. Following general protocol D, methyl 2-(4-(2-fluoro-6-methylpyridin-3-yl)phenyl)-3-methylquinoline-4-carboxylate was recovered as a white solid (22 mg, 0.06 mmol, 43%). ^{1}H NMR (300 MHz, $CDCl_3$-*d*) δ 8.17 (d *J* = 8.6, 1.5 Hz, 1H), 7.89–7.79 (m, 1H), 7.78–7.66 (m, 6H), 7.60 (t, *J* = 7.3, 6.9, 1.3 Hz, 1H), 7.18 (d, *J* = 7.6, 1.8 Hz, 1H), 4.13 (s, 3H), 2.59 (s, 3H), 2.48 (s, 3H). MS (ESI) 387.2 $[M + H]^+$.

Methyl 2-(4-(2-Chloropyridin-3-yl)phenyl)-3-methylquinoline-4-carboxylate (81).—Intermediate **59** (50 mg, 0.14 mmol), (2-chloropyridin-3-yl)boronic acid (31 mg, 0.20 mmol), K_2HPO_4 (78 mg, 0.45 mmol), and $Pd(PPh_3)_4$ (8 mg) were dissolved in 2 mL of dioxane and 1 mL of H_2O. The mixture was heated to 130 °C for 1.5 h in a microwave reactor. Following general protocol D, methyl 2-(4-(2-chloropyridin-3-yl)phenyl)-3-methylquinoline-4-carboxylate was recovered as a white solid (25 mg, 0.06 mmol, 43%). ^{1}H NMR (300 MHz, $CDCl_3$-*d*) δ 8.47–8.42 (m, 1H), 8.19 (d *J* = 8.5 Hz, 1H), 7.80–7.58 (m, 8H), 7.42–7.33 (m, 1H), 4.13 (s, 3H), 2.50 (s, 3H). MS (ESI) 389.1 $[M + H]^+$.

Methyl 2-(4-(2-Chloro-6-methylpyridin-3-yl)phenyl)-3-methylquinoline-4-catboxylate (82).—Intermediate **59** (100 mg, 0.28 mmol), (2-chloro-6-methylpyridin-3-yl)boronic acid (72 mg, 0.42 mmol), K_2HPO_4 (146 mg, 0.84 mmol), and $Pd(PPh_3)_4$ (16 mg, 0.01 mmol) were dissolved in 2 mL of dioxane and 1 mL of H_2O. The mixture was heated to 130 °C for 1.5 h in a microwave reactor. Following general protocol D, methyl 2-(4-(2-chloro-6-methylpyridin-3-yl)phenyl)-3-methylquinoline-4-carboxylate was recovered as a white solid (43 mg, 0.10 mmol, 39%). ^{1}H NMR (300 MHz, $CDCl_3$-*d*) δ 8.21–8.15 (m, 1H), 7.78–7.70 (m, 2H), 7.70–7.57 (m, 6H), 7.21 (d, *J* = 7.7 Hz, 1H), 4.13 (s, 3H), 2.62 (s, 3H), 2.49 (s, 3H). MS (ESI) 403.1 $[M + H]^+$.

Methyl 6-Fluoro-2-(4-(2-fluoropyridin-3-yl)phenyl)-3-methylquinoline-4-carboxylate (83).—Intermediate **60** (50 mg, 0.13 mmol), (2-fluoropyridin-3-yl)boronic acid (31 mg, 0.22 mmol), K_2HPO_4 (68 mg, 0.39 mmol), and $Pd(PPh_3)_4$ (7 mg, 6.0×10^{-3} mmol) were dissolved in 1 mL of dioxane and 0.5 mL of H_2O. The mixture was heated to 130 °C for 1.5 h in a microwave reactor. Following general protocol D, methyl 6-fluoro-2-(4-(2-fluoropyridin-3-yl)phenyl)-3-methylquinoline-4-carboxylate was recovered as a white solid (34 mg, 0.09 mmol, 69%). ^{1}H NMR (300 MHz, $CDCl_3$-*d*) δ 8.28–8.24 (m, 1H), 8.17 (dd, *J* = 9.2, 5.5 Hz, 1H), 8.01–7.91 (m, 1H), 7.78–7.66 (m, 4H), 7.56–7.46 (m, 1H), 7.44–7.32 (m, 2H), 4.13 (s, 3H), 2.49 (s, 3H). MS (ESI) 291.1 $[M + H]^+$.

Methyl 6-Fluoro-2-(4-(2-fluoro-6-methylpyridin-3-yl)phenyl)-3-methylquinoline-4-carboxylate (84).—Intermediate **60** (50 mg, 0.13 mmol), (2-fluoro-6-methylpyridin-3-yl)boronic acid (30 mg, 0.20 mmol), K_2HPO_4 (68 mg, 0.39 mmol), and $Pd(PPh_3)_4$ (7 mg, 6.0×10^{-3} mmol) were dissolved in 1 mL of dioxane and 0.5 mL of H_2O. The mixture was heated to 130 for 1.5 h in a microwave reactor. Following general protocol D, methyl 6-fluoro-2-(4-(2-fluoro-6-methylpyridin-3-yl)phenyl)-3-methylquinoline-4-carboxylate was recovered as a white solid. (17 mg, 0.04

mmol, 31%). ^{1}H NMR (300 MHz, $CDCl_3$-*d*) *δ* 8.17 (dd, *J* = 9.2, 5.5 Hz, 1H), 7.88–7.80 (m, 1H), 7.75–7.64 (m, 4H), 7.55–7.46 (m, 1H), 7.44–7.38 (m, 1H), 7.18 (d, *J* = 7.6, 1.8 Hz, 1H), 4.13 (s, 3H), 2.59 (s, 3H), 2.49 (s, 3H). MS (ESI) 405.1 $[M + H]^+$.

Methyl 2-(4-(2-Chloropyridin-3-yl)phenyl)-6-fluoro-3-methylquinoline-4-carboxylate (85).—Intermediate **60** (960 mg, 2.67 mmol), (2-chloropyridin-3-yl)boronic acid (503 mg, 3.20 mmol), K_2HPO_4 (1.34 g, 7.70 mmol), and $Pd(PPh_3)_4$ (80 mg) were dissolved in 10 mL of dioxane and 4 mL of H_2O. The mixture was heated to reflux overnight Following general protocol D, methyl 2-(4-(2-chloropyridin-3-yl)phenyl)-6-fluoro-3-methylquinoline-4-carboxylate was recovered as a white solid (385 mg, 0.95 mmol, 36%). ^{1}H NMR (300 MHz, $CDCI_3$-*d*) *δ* 8.49–8.43 (m, 1H), 8.22–8.11 (m, 1H), 7.77–7.59 (m, 5H), 7.56–7.48 (m, 1H), 7.45–7.34 (m, 2H), 4.13 (s, 3H), 2.50 (s, 3H). MS (ESI) 407.1 $[M + H]^+$.

Methyl 2-(4-(2-Chloro-6-methylpyridin-3-yl)phenyl)-6-fluoro-3-methylquinoline-4-carboxylate (86).—Intermediate **60** (1.00 g, 2.68 mmol), (2-chloro-6-methylpyridin-3-yl)boronic acid (688 mg, 4.02 mmol), K_2HPO_4 (1.40 g, 8.04 mmol), and $Pd(PPh_3)_4$ (155 mg) were dissolved in 11 mL of dioxane and 3 mL of H_2O. The mixture was heated to reflux overnight. Following general protocol D, methyl 2-(4-(2-chloro-6-methylpyridin-3-yl)phenyl)-6-fluoro-3-methylquinoline-4-carboxylate was recovered as a white solid (474 mg, 1.13 mmol, 42%). ^{1}H NMR (300 MHz, $CDCI_3$-*d*) *δ* 8.20–8.13 (m, 1H), 7.68–7.57 (m, 5H), 7.56–7.45 (m, 1H), 7.43–7.36 (m, 1H), 7.21 (d, *J* = 7.7 Hz, 1H), 4.12 (s, 3H), 2.61 (s, 3H), 2.49 (s, 3H). MS (ESI) 421.1 $[M + H]^+$.

Methyl 6-Chloro-2-(4-(2-fluoropyridin-3-yl)phenyl)-3-methylquinoline-4-carboxylate (87).—Intermediate **61** (50 mg, 0.13 mmol), (2-fluoropyridin-3-yl)boronic acid (31 mg, 0.22 mmol), K_2HPO_4 (68 mg, 0.39 mmol), and $Pd(PPh_3)_4$ (7 mg, 6.0×10^{-3} mmol) were dissolved in 1 mL of dioxane and 0.5 mL of H_2O. The mixture was heated to 130 °C for 1.5 h in a microwave reactor. Following general protocol D, methyl 6-chloro-2-(4-(2-fluoropyridin-3-yl)phenyl)-3-methylquinoline-4-carboxylate was recovered as a yellow solid (19 mg, 0.05 mmol, 38%). ^{1}H NMR (300 MHz, $CDCl_3$-*d*) *δ* 8.33–8.21 (m, 1H), 8.10 (d, *J* = 8.9 Hz, 1H), 7.96 (t, *J* = 8.2 Hz, 1H), 7.78–7.64 (m, 6H), 7.40–7.31 (m, 1H), 4.14 (s, 3H), 2.49 (s, 3H). MS (ESI) 407.1 $[M + H]^+$.

Methyl 6-Chloro-2-(4-(2-chloropyridin-3-yl)phenyl)-3-methylquinoline-4-carboxylate (88).—Intermediate **61** (50 mg, 0.13 mmol), ***(2-***chloropyridin-3-yl)boronic acid (34 mg, 0.22 mmol), K_2HPO_4 (68 mg, 0.39 mmol), and $Pd(PPh_3)_4$ (7 mg, 6.0×10^{-3} mmol) were dissolved in 1 mL of dioxane and 0.5 mL of H_2O. The mixture was heated to 130 °C for 1.5 h in a microwave reactor. Following general protocol D, methyl 6-chloro-2-(4-(2-fluoropyridin-3-yl)phenyl)-3-methylquinoline-4-carboxylate was recovered as a tan solid (4 mg, 0.01 mmol, 8%). ^{1}H NMR (400 MHz, $CDCl_3$-***d***) ***δ*** 8.49–8.44 (m, 1H), 8.12 (d, ***J*** = 8.9, 0.5 Hz, 1H), 7.77–7.73 (m, 2H), 7.72–7.66 (m, 3H), 7.64–7.60 (m, 2H), 7.42–7.35 (m, 1H), 4.15 (s, 3H), 2.51 (s, 3H). MS (ESI) 423.0 $[M + H]^+$.

Methyl 6-Chloro-2-(4-(2-chloro-6-methylpyridin-3-yl)phenyl)-3-methylquinoline-4-carboxylate (89).—Intermediate **61** (50 mg, 0.13 mmol), (2-

chloro-6-methylpyridin-3-yl)boronic acid (35 mg, 0.20 mmol), K_2HP0_4 (**68** mg, 0.39 mmol), and $Pd(PPh_3)_4$ (7 mg, 6.0×10^{-3} mmol) were dissolved in 1 mL of dioxane and 0.5 mL of H_2O. The mixture was heated to 130 °C for 1.5 h in a microwave reactor. Following general protocol D, methyl 6-chloro-2-(4-(2-chloro-6-methylpyridin-3-yl)phenyl)-3-methylquinoline-4-carboxylate was recovered as a solid (28 mg, 0.06 mmol, 46%). ^{1}H NMR (300 MHz, $CDCl_3$-***d***) ***δ*** 8.11 (d, ***J*** = 8.9 Hz, 1H), 7.75 (d, ***J*** = 2.2 Hz, 1H), 7.70–7.58 (m, **6**H), 7.22 (d, ***J*** = 7.7 Hz, 1H), 4.14 (s, 3H), 2.63 (s, 3H), 2.49 (s, 3H). MS (ESI) 437.1, 438.9 $[M + H]^+$.

Methyl 2-(4-(2-Chloropyridin-3-yl)phenyl)-3,6-dimethylquinoline-4-carboxylate (90).—Intermediate **62** (50 mg, 0.14 mmol), (2-chloropyridin-3-yl)boronic acid (35 mg, 0.23 mmol), K_2HP0_4 (**68** mg, 0.39 mmol), and $Pd(PPh_3)_4$ (7 mg, 6.0×10^{-3} mmol) were dissolved in 1 mL of dioxane and 0.5 mL of H_2O. The mixture was heated to 130 °C for 1.5 h in a microwave reactor. Following general protocol D, methyl 2-(4-(2-chloropyridin-3-yl)phenyl)-3,6-dimethylquinoline-4-carboxylate was recovered an off-white solid (9 mg, 0.02 mmol, 16%) upon recrystallization in EtOH. ^{1}H NMR (400 MHz, $CDCl_3$-***d***) ***δ*** 8.45 (dd, ***J*** = 4.8, 1.9 Hz, 1H), 8.08 (d, ***J*** = **8.6** Hz, 1H), 7.75 (dd, ***J*** = 7.5, 1.9 Hz, 1H), 7.71–7.68 (m, 2H), 7.64–7.56 (m, 3H), 7.51–7.48 (m, 1H), 7.37 (dd, ***J*** = 7.6, 4.8 Hz, 1H), 4.14 (s, 3H), 2.58 (d ***J*** = 1.0 Hz, 3H), 2.48 (s, 3H). MS (ESI) 403.10 $[M + H]^+$.

Methyl 2-(2′-Fluoro-[1,1′-biphenyl]-4-yl)-3-methyl-6-(trifluoromethyl)-1,7-naphthyridine-4-carboxylate (91).—Intermediate **102** (14 mg, 0.03 mmol), 2-fluorophenyIboronic acid (7 mg, 0.05 mmol), K_2HPO_4 (17 mg, 0.10 mmol), and $Pd(PPh_3)_4$ (1 mg) were dissolved in 1 mL of dioxane and 1 mL of H_2O. The mixture was heated to 130 °C for 1.5 h in a microwave reactor. Following general protocol D, methyl 2-(2′-fluoro-[1,1′-biphenyl]-4-yl)-3-methyl-6-(tri-fluoromethyl)-1,7-naphthyridine-4-carboxylate was recovered (11 mg, 0.02, **66**%). ^{1}H NMR (300 MHz, $CDCl_3$-***d***) ***δ*** 9.65 (s, 1H), 8.07 (s, 1H), 7.80–7.68 (m, 4H), 7.58–7.49 (m, 1H), 7.46–7.36 (m, 1H), 7.31 (s, OH), 7.27–7.18 (m, 1H), 4.18 (s, 3H), 2.62 (s, 3H). MS (ESI) 441.2 $[M + H]^+$.

N-(Pyridin-2-yl)pivalamide (92).—2-Aminopyridine (1.00 g, 10.6 mmol), triethylamine (1.85 mL, 13.3 mmol), and pivaloyl chloride (1.44 mL, 11.7 mmol) were combined in 18 mL of anhydrous DCM following general protocol G. Product was recrystallized by addition of hexane to generate ***N***-(pyridin-**2**-yl)pivalamide as white needles (1.81 g, 10.2 mmol, 96%). ^{1}H NMR (400 MHz, $CDCl_3$-***d***) ***δ*** 8.26–8.18 (m, 3H), 7.66 (ddd, ***J*** = **8.6**, 7.3, 1.9 Hz, 1H), 7.03–6.95 (m, 1H), 1.29 (d, ***J*** = 1.9 Hz, 9H). MS (ESI) 179.1 $[M + H]^+$.

N-(Pyridin-3-yl)pivalamide (93).—3-Aminopyridine (1.00 g, 10.6 mmol), triethylamine (1.85 mL, 13.3 mmol), and pivaloyl chloride (1.44 mL, 11.7 mmol) were combined in 18 mL of anhydrous DCM following general protocol G. Product was recrystallized by addition of hexane to generate ***N***-(pyridin-3-yl)pivalamide as a tan solid (1.56 g, 10.6mmol, 83%). ^{1}H NMR (400 MHz, $CDCI_3$-***d***) ***δ*** 8.57 (d, ***J*** = 2.6 Hz, 1H), 8.38–8.33 (m, 1H), 8.22–8.16 (m, 1H), 7.49 (s, 1H), 7.31–7.25 (m, 1H), 1.35 (s, 9H). MS (ESI) 179.1 $[M + H]^+$.

N-(Pyridin-4-yl)pivalamide (94).—4-Aminopyridine (1.00 g, 10.6 mmol), triethylamine (1.85 mL, 13.3 mmol), and pivaloyl chloride (1.44 mL, 11.7 mmol) were combined in 18 mL of anhydrous DCM following general protocol G. Product was recrystallized by addition of hexane to generate ***N***-(pyridin-4-yl)pivalamide as white needles (991 mg, 5.57 mmol, 53%). ^{1}H NMR (400 MHz, $CDCl_3$-***d***) ***δ*** 8.57 (d, ***J*** = 2.6Hz, 1H), 8.36 (dd, ***J***= 4.7, 1.5 Hz, 1H), 8.24–8.18 (m, 1H), 7.50–7.41 (m, 1H), 7.32–7.24 (m, 1H), 1.36 (d, ***J*** = 1.5 Hz, 9H). MS (ESI) 179.1 $[M + H]^+$.

N-(6-(Trifluoromethyl)pyridin-3-yl)pivalamide (95).—*6*-(Trifluoromethyl)pyridin-3-amine (1.00 g, 6.17 mmol), diisopropyle-thyamine (1.35 mL, 7.71 mmol), and pivaloyl chloride (0.83 mL, 6.78 mmol) were combined in 17 mL of anhydrous DCM following general protocol G. Product was recrystallized by addition of hexane to generate ***N***-(6-(trifluoromethyl)pyridin-3-yl)pivalamide as a white powder (1.48 g, 6.04 mmol, 98%). ^{1}H NMR (300 MHz, $CDCl_3$-***d***) ***δ*** 8.64–8.61 (m, 1H), 8.35 (dd, ***J*** = **8.6**, 2.5 Hz, 1H), 7.82 (s, 1H), 7.60 (d, ***J*** = **8.6** Hz, 1H), 1.31 (s, 9H). MS (ESI) 245.2 $[M + H]^+$.

tert-Butyl (6-(Trifluoromethyl)pyridin-3-yl)carbamate (96).—This protocol was adapted from Hughes et al.[49] 6-(Trifluoromethyl)-pyridin-3-amine (4.00 g, 24.7 mmol) and di-***tert***-butyl-dicarbonate (6.73 g, 30.9 mmol) were refluxed in 50 mL of anhydrous dioxane. After 24 h, 1.00 g (4.59 mmol) of additional di-tert-butyl-dicarbonate was added and the mixture was stirred at reflux for another 24 h. After 48 h, the reaction mixture was quenched by the addition of cold H_2O and extracted with EtOAc. The organic layer was dried with $MgSO_4$ filtered, and concentrated before purifying via silica chromatography. ***tert***-Butyl (6-(trifluoromethyl)pyridin-3-yl)carbamate was recovered as a white powder (2.45 g, 9.35 mmol, 38%). ^{1}H NMR (300 MHz, $CDCl_3$-***d***) ***δ*** 8.62 (d, ***J*** = 2.5 Hz, 1H), 8.35 (dd, ***J*** = **8.6**, 2.5 Hz, 1H), 7.82 (s, 1H), 7.60 (d, ***J*** = **8.6** Hz, 1H), 1.31 (s, 9H). MS (ESI) 263.2 $[M + H]^+$.

Ethyl 2-Oxo-2-(2-pivalamidopyridin-3-yl)acetate (97).—Following general protocol H, intermediate **92** (816 mg, 4.58 mmol), TMEDA (1.38 mL, 9.16 mmol), 1.6 M n-BuLi (5.73 mL, 9.16 mmol), and diethyl oxalate (1.03 mL, 9.16 mmol) were combined in 12 mL of anhydrous diethyl ether. Ethyl 2-oxo-2-(2-pivalamidopyridin-3-yl)-acetate was recovered as a yellow oil (136 mg, 0.48 mmol, 10%). ^{1}H NMR (400 MHz, $CDCl_3$-***d***) ***δ*** 9.86 (s, 1H), 8.59–8.48 (m, 1H), 8.03 (dt, ***J*** = 7.8, 1.6 Hz, 1H), 7.13 (ddd, ***J*** = 7.9, 4.8, 1.3 Hz, 1H), 4.36 (qd, ***J*** = 7.2, 1.2 Hz, 2H), 1.37 (td, ***J*** = 7.1, 1.2 Hz, 3H), 1.29 (s, 9H). MS (ESI) 277.3 $[M - H]^-$.

Ethyl 2-Oxo-2-(3-pivalamidopyridin-4-yl)acetate (98).—Following general protocol H, intermediate **93** (1.00 g, 5.62 mmol), TMEDA (2.10 mL, 14.1 mmol), 1.6 M ***n***-BuLi (8.75 mL, 14.1 mmol), and diethyl oxalate (2.29 mL, 16.7 mmol) were combined in 17 mL of anhydrous diethyl ether. Ethyl 2-oxo-2-(2-pivalamidopyridin-3-yl)-acetate was recovered as an off-white solid (564 mg, 2.39 mmol, 43%). ^{1}H NMR (400 MHz, $CDCl_3$-***d***) ***δ*** 10.84 (s, 1H), 10.16 (s, 1H), 8.52 (d, ***J*** = 5.1 Hz, 1H), 7.58 (d, ***J*** = 5.2 Hz, 1H), 4.50 (q, ***J*** = 7.1 Hz, 2H), 1.46 (t, ***J*** = 7.2 Hz, 3H), 1.38 (s, 9H). MS (ESI) 277.2 $[M - H]^-$.

Ethyl 2-Oxo-2-(4-pivalamidopyridin-3-yl)acetate (99).—*Following* general protocol H, intermediate ***94*** (1.00 g, 5.62 mmol), 1.6 M *n*-BuLi (7.4 mL, 11.8 mmol), and diethyl oxalate (2.29 mL, 16.8 mmol) were combined in 16 mL of anhydrous diethyl ether. TMEDA was not utilized. Ethyl 2-oxo-2-(4-pivalamidopyridin-3-yl)acetate was recovered as an off-white solid (796 mg, 2.86 mmol, 51%). ^{1}H NMR (400 MHz, $CDCl_3$-*d)* δ 9.78 (s, 1H), 8.37 (d, J = 5.8 Hz, 1H), 8.26 (d, J = 5.8 Hz, 1H), 8.20 (s, 1H), 4.18–4.02 (m, 2H), 1.27 (s, 9H), 1.12 (t, J = 7.1 Hz, 3H). MS (ESI) 277.2 $[M - H]^-$.

Ethyl 2-Oxo-2-(5-pivalamido-2-(trifluoromethyl)pyridin-4-yl)-acetate (100).— Following general protocol H, intermediate **95** (1.00 g, 4.07 mmol), TMEDA (1.53 mL, 10.2 mmol), 1.6 M ***n***-BuLi (6.35 mL, 10.2 mmol), and diethyl oxalate (1.66 mL, 12.2 mmol) were combined in 12 mL of anhydrous diethyl ether. Ethyl 2-oxo-2-(5-pivalamido-2-(trifluoromethyl)pyridin-4-yl) acetate was recovered as a yellow oil (188 mg, 0.54 mmol, 13%). ^{1}H NMR (300 MHz, $CDCl_3$-***d***) $\boldsymbol{\delta}$ 11.07 (s, 1H), 10.25 (s, 1H), 8.02 (s, 1H), 4.53 (q, ***J*** = 7.1 Hz, 2H), 1.47 (t, ***J*** = 7.2 Hz, 3H), 1.38 (s, 9H). MS 345.1 $[M - H]^-$.

Ethyl 2-(5-((tert-Butoxycarbonyl)amino)-2-(trifluoromethyl)pyridin-4-yl)-2-oxoacetate (101).—Following general protocol H, intermediate **96** (1.00 g, 3.82 mmol), TMEDA (1.20 mL, 8.02 mmol), 1.6 M ***n***-BuLi (5.01 mL, 8.02 mmol), and diethyl oxalate (1.55 mL, 11.4 mmol) were dissolved in 13 mL of anhydrous diethyl ether. Ethyl 2-(5-((***tert***-butoxycarbonyl)amino)-2-(trifluoromethyl)pyridin-4-yl)-2-oxoacetate was recovered as a yellow oil (44 mg, 0.17 mmol, 1%). ^{1}H NMR (300 MHz, $CDCl_3$-***d***) $\boldsymbol{\delta}$ 8.51–8.47 (m, 1H), 7.65–7.58 (m, 1H), 6.98 (s, 1H), 4.35 (q, ***J*** = 7.1 Hz, 2H), 1.52 (s, 9H), 1.37 (t, ***J*** = 7.1 Hz, 2H). MS (ESI) 363.2 $[M + H]^+$.

Methyl 2-(4-Bromophenyl)-3-methyl-6-(trifluoromethyl)-1,7-naphthyridine-4-carboxylate (102).—Intermediate **101** (1.38 g, 3.82 mmol) was dissolved in 10 mL DCM and 1 mL of trifluoroacetic acid. The mixture was stirred at room temperature for 2 h before being concentrated to a residue. 1-(4-Bromophenyl)propan-1-one (813 mg, 3.82 mmol) and KOH (856 mg, 15.3 mmol) were added to the residue, and the mixture was dissolved in 15 mL of anhydrous EtOH. In a sealed vial, the mixture was heated to 100 °C overnight. Upon completion, the mixture was concentrated and the residue was redissolved in 1 M KOH, washed with EtOAc, and precipitated from aqueous layer by addition of HC1 until the pH was 2–3 and precipitant was collected. The dried precipitant was dissolved in 5 mL of THF and 1 mL of MeOH under an argon atmosphere and chilled to 0 °C. A 2.0 M solution of TMS-diazomethane in THF (0.4 mL, 0.8 mmol) was added to the mixture, and the solution was allowed to warm to room temperature over 2 h. The mixture was quenched by the addition of acetic acid, concentrated, redissolved in EtOAc, and washed with brine **(3×).** The organic layer was dried with $MgSO_4$ filtered, concentrated, and purified by silica chromatography to yield methyl 2-(4-bromophenyl)-3-methyl-6-(trifluoromethyl)-l,7-naphthyridine-4-carboxylate (32 mg, 0.08 mmol, 2% overall yield). ^{1}H NMR (300 MHz, $CDCl_3$-*d*) δ 9.60 (s, 1H), 8.05 (s, 1H), 7.75–7.67 (m, 2H), 7.56–7.47 (m, 2H), 4.17 (s, 3H), 2.54 (s, 3H). MS (ESI) 425.0, 427.0 $[M + H]^+$.

Molecular Modeling.

To offer rationalizations of SAR trends, select synthesized molecules were analyzed by molecular docking using AutoDock Vina 1.5.6.[50] The PDB file of DHODH (1D3G) was downloaded from the Protein Data Bank and was prepared for docking by fixing missing bonds or atoms, adding polar hydrogens and Kollman charges, and removing water molecules. The protein was validated by first removing the cocrystallized brequinar analogue followed by docking it in the same binding site. The coordinates to be used as the center of the grid box were determined by calculating the centroid of the brequinar analogue using BIOVIA Discovery Studio Visualizer.[51] The compounds were drawn using ChemDraw Ultra and converted to 3D structures, with their geometries optimized by the semiemperical MM2 method, and were converted to pdbqt files using AutoDock Tools.

DHODH Expression and Purification.

DHODH expression and purification followed the same protocol as described by Madak et al.[52] The DHODH construct was kindly provided by the De Brabander lab from UT Southwestern.[1] Briefly, DHODH was expressed in *E. coli* Rosetta 2 (DE3) in LB medium with ampicillin (100 μg/mV) and 0.1 mM FMN. Cells were grown at 37 °C to OD_{600} = 0.6, then induced with 1 mM IPTG for 3 h. Cells were harvested by centrifugation, and the pellet was resuspended in lysis buffer (50 mM Tris-HCI, pH 8.5, 300 mM NaCl, 10% glycerol, 5 mM β-mercaptoethanol, 10 mM imidazole, 2% Triton X-100, 0.5 mM FMN, 200 μM PMSF, 1 mg/mL lysozyme). The cell suspension was incubated on ice for 2 h, followed by sonication. The cleared supernatant was incubated with Ni-NTA resin for 1 h at 4 °C and then loaded onto a column. The column was washed with wash buffer (50 mM Tris-HCI, pH 8.5, 300 mM NaCI, 10% glycerol, 5 mM β-mercaptoethanol, 25 mM imidazole, 0.1 mM FMN), and DHODH was eluted with elution buffer (wash buffer containing 300 mM imidazole). Buffer exchange was carried out using an Amicon concentrator into storage buffer (100 mM HEPES, pH 8.0, 150 mM NaCI, 10% glycerol), and DHODH was stored at −80 °C.

DHODH Inhibition Assay.

DHODH activity was monitored as previously described with some modifications.[2] First, 1 μL of test compound (50×) or DMSO, 60 nM DHODH, 100 μM DCIP, and 20 μM COQ_{10} (final concentrations for 50 μL) in the assay buffer **(100** mM HEPES pH 8.0,150 mM NaCI, 10% glycerol, **0.1%** Triton X-100) in a total of 40 μL were incubated together for **30** min. The assay was started by the addition of 10 μL of dihydroorotate to a final concentration of 200 μM. The reduction of DCIP was measured by monitoring the absorbance at 600 nm over **1** h at room temperature using a microplate reader (BMG Labtech). Data were exported to Microsoft Excel for analysis, and IC_{50} values were determined using GraphPad Prism6.

General Protocol for Preparation of Cells.

HCT-116 and MIA PaCa-2 cells were grown in RPMI 1640 supplemented and with 10% fetal bovine serum (FBS). HL-60 was grown in IMDM supplemented with 20% FBS. All cell lines were incubated in the standard conditions of 37 °C and 5% CO_2. Cancer cells were

purchased from NCI Developmental Therapeutics Program and ATCC (Manassas, VA). For uridine rescue experiments, cells were seeded in medium containing dialyzed FBS (Gibco).

Biological Evaluation in Cell Proliferation Assays.

For the MTT assay, cells were seeded at 3000–7500 cells per well in a 96-well plate in 180 μL of cell culture medium and incubated overnight Compounds were added the following day and were incubated with the cells for 72 h. Post-treatment, thiazolyl blue tetrazolium bromide (MTT) (AMRESCO) was added to a final concentration of 300 μg/mL and incubated at 37 °C for 3.5 h. The media containing compound and MTT was discarded and 100 μL of DMSO was added to dissolve the insoluble formazan. The plates were shaken at room temperature for 15 min. A microplate reader (Molecular Devices) was then used to obtain the absorbance at 570 nm. Data were evaluated using GraphPad Prism**6** software. For colony formation assays, cells were seeded at 200 cells per well in 180 μL of cell culture medium and were allowed to attach overnight. Compounds were added the next day and were incubated with the cells for either 24 h or for the duration of the assay (seven days). Once colonies had formed in the DMSO-treated wells, cells were stained with a 0.05% crystal violet solution (2% formaldehyde, 40% methanol in distilled water), washed with water to remove excess stain, and imaged with Odyssey Imaging Systems (LI-COR Biosciences, Lincoln, NE).

Pharmacokinetic Studies.

PK data was generated by the University of Michigan PK core. The study utilized (18) female CD-1 mice with a triple dose design. The inhibitor at 2 mg/mL in PBS containing 20% DMSO and 50% PEG-400 was given by IV injection (10 mg/kg) and oral (PO) 20 mg/kg. At the given time points (0.083, 0.167, 0.25, 0.5, 1, 2, 4, 7, 16, and 24 h), blood samples were collected using heparinized calibrated pipettes. Samples were centrifuged at 15000 rpm for 10 min. Subsequently, blood plasma was collected from the upper layer. The plasma was frozen at −80 °C for later analysis.

Thermodynamic Solubility Studies.

Thermodynamic solubility was evaluated by Analiza (Cleveland, OH) using their standard protocol. In short, solubility was calculated using a CLND detector. Compounds were dissolved in 450 μL of PBS pH 7.4 and shaken overnight at room temperature. The solution was filtered through a 0.45 μm filter and injected directly into the CLND. Concentrations were determined via calibration curves to assess thermodynamic solubility in solution.

Crystallography.

Cloning, Expression, Purification of DHODH.—The gene for N-terminally truncated human DHODH (residues 33–396) was subcloned into pMCSG26 LIC site using pET22b-DHODH (residues 30–396) as the template with the following 3’ and 5’ primers (GTCTCTCCCATGGGAGATGAGCGTTTCTATGCTGAACAC and TGGTGGTGCCCAGCTTCCAGCCTCCGATGATCTGCTCCAATGG).

The C-terminally tagged construct (DHODH-His_6) was transformed into *Escherichia coli* Rosetta 2 (DE3) cells. Transformed cells were grown in Terrific Broth containing 100 μg/mL

ampicillin at 37 °C to an OD600 of 0.6. Expression was induced by addition of 0.4 mM IPTG. Cells were incubated at 25 °C overnight, harvested by centrifugation at 6700g, and the pellet stored at −80 °C.

Purification of DHODH was performed as published with modifications.[46] The thawed pellet was resuspended in 160 mL of lysis buffer containing 50 mM HEPES pH 8.0, 300 mM NaCI, 10% glycerol, 10 mM imidazole, 0.05% (v/v) THESIT (Sigma Aldrich), 200 ***μ***M phenylmethylsulfoxide, supplemented with a protease inhibitor cocktail (complete EDTA-free, Sigma Aldrich). Resuspended cells were lysed by sonication and centrifuged at 34000***g***. The resulting supernatant was added to 10 mL of Ni NTA Superflow resin (Qiagen) pre-equilibrated with lysis buffer. After the lysate was incubated with Ni NTA resin for 1 h at 4 °C, the resin was washed with lysis buffer containing 20 mM imidazole and the protein eluted with lysis buffer containing 400 mM imidazole. Eluent was loaded onto a HiLoad 16/60 Superdex 75 column (GE Healthcare) pre-equilibrated with 50 mM HEPES pH 7.8, 300 mM NaCI, 10% glycerol, 10 mM DTT, and 40 mM Anzergent 3–10 (Anatrace). Fractions corresponding to DHODH were pooled and 200 mM HEGA-8 (Anatrace) was added before concentrating protein to 18–22 mg/mL.

Crystallization, Data Collection, and Structure Determination.—DHODH was incubated with 2 mM L-dihydroorotate and 1 mM inhibitor at 4 °C for 2 h and crystallized by sitting drop vapor diffusion at 20 °C. Protein was mixed in a 1:1 ratio with well solution containing 1.7–2.2 M ammonium sulfate, 1.4–1.5 M NaCl, 0.1 M sodium acetate pH 5.3, and 10 mM DTT. Prior to data collection, crystals were cryoprotected in well solution supplemented with **20**% ethylene glycol (DHODH:**43**) or silica oil (DHODH:**46**) and flash-cooled in liquid nitrogen. Diffraction data were collected on the Advanced Photon Source LS-CAT beamline 21-ID-G (Supporting Information, Table 2**).** All data were processed with HKL2000,[53] and both structures were solved by molecular replacement in Phaser[54] using a previous structure of DHODH (PDB 4IGH) absent its ligands as the search model. Iterative model building and refinement were performed using COOT[55] and PHENIX,[56] respectively. Ligand restraints were generated in eLBOW.[57]

The structure of DHODH with inhibitor 43 (PDB **6**CJF) was solved to 1.63 **Å** in the space group of PI. The structure contained two chains of protein in the asymmetric unit, with an RMSD of 0.337 **Å** between chains based on SSM superpositioning in COOT. In chain A, residues 33–396 were modeled with the exception of two disordered loop regions corresponding to residues 69–73 and 214–225. Similarly, residues 36–396 of chain B were modeled with the exception of the same two disordered loop regions, which included residues 69–75 and 216–223. In both chains, several peptide residues corresponding to the linker between the protein C-terminal histidine tag were also ordered.

The structure of DHODH with inhibitor 46 (PDB **6**CJG) was solved to 2.85 **Å** in the space group $P3_221$, with one chain of protein in the asymmetric unit. Residues 34–396 were modeled with the exception of two disordered loop regions 71–73 and 218–223.

Supplementary Material

Refer to Web version on PubMed Central for supplementary material.

ACKNOWLEDGMENTS

We thank Dr. Larisa Yeomans and Dr. Tanpreet Kaur for assistance evaluating NMR spectroscopy. We thank Analiza for their solubility assay assistance. We also thank the Pharmacokinetic Core at the University of Michigan for PK evaluation services. C.RC. is a trainee of the University of Michigan Pharmacological Sciences Training Program (PSTP, T32-GM007767). Use of the Advanced Photon Source, an Office of Science User Facility operated for the U.S. Department of Energy (DOE) Office of Science by Argonne National Laboratory, was supported by the U.S. DOE under contract no. DE-AC02-06CH11357. Use of the LS-CAT Sector 21 was supported by the Michigan Economic Development Corporation and the Michigan Technology Tri-Corridor (grant 085P1000817).

ABBREVIATIONS USED

DHODH	dihydroorotate dehydrogenase
TRAIL	tumor necrosis factor related apoptosis inducing ligand
PTEN	phosphatase and tensin homologue
SAR	structure activity relationship
PK	pharmacokinetic
LipE	lipophilic ligand efficiency
tPSA	total polar surface area
BBr_3	boron tribromide
PCC	pyridinium chlorochromate
TMEDA	tetramethylethylenediamine
LCMS	liquid chromatography–mass spectrometry

REFERENCES

(1). Munier-Lehmann H; Vidalain P-O; Tangy F; Janin YL On dihydroorotate dehydrogenases and their inhibitors and uses. J. Med. Chem. 2013, 56 (8), 3148–3167. [PubMed: 23452331]

(2). Vyas VK; Ghate M Recent developments in the medicinal chemistry and therapeutic potential of dihydroorotate dehydrogenase (DHODH) inhibitors. Mini-Rev. Med. Chem. 2011, 11 (12), 1039–1055. [PubMed: 21861807]

(3). Mohamad Fairus AK; Choudhary B; Hosahalli S; Kavitha N; Shatrah O Dihydroorotate dehydrogenase (DHODH) inhibitors affect ATP depletion, endogenous ROS and mediate S-phase arrest in breast cancer cells. Biochimie 2017, 135, 154–163. [PubMed: 28196676]

(4). Reis RAG; Calil FA; Feliciano PR_; Pinheiro MP; Nonato MC The dihydroorotate dehydrogenases: past and present Arch. Biochem. Biophys. 2017, 632, 175–191. [PubMed: 28666740]

(5). Lolli ML; Sainas S; Pippione AC; Giorgis M; Boschi D; Dosio F Use of dihydroorotate dehydrogenase (hDHODH) inhibitors in autoimmune diseases and new perspectives in cancer therapy. Recent Pat. Anti-Cancer Drug Discovery 2018, 13 (l), 86–105. [PubMed: 29119937]

(6). Brown KK; Spinelli JB; Asara JM; Toker A Adaptive reprogramming of de novo pyrimidine synthesis is a metabolic vulnerability in triple-negative breast cancer. Cancer Discovery 2017, 7 (4), 391–399. [PubMed: 28255083]

(7). Sharma A; Janocha AJ; Hill BT; Smith MR; Erzurum SC; Almasan A Targeting mTORCl-mediated metabolic addiction overcomes fhidarabine resistance in malignant B cells. Mol. Cancer Res. 2014, 12 (9), 1205–1215. [PubMed: 25061101]

(8). Dietrich S; Kramer OH; Hahn E; Schafer C; Giese T; Hess M; Tretter T; Rieger M; Hullein J; Zenz T; Ho AD; Dreger P; Luff T Lefhmomide induces apoptosis in fludarabine-resistant and clinically refractory CLL cells. Clin. Cancer Res. 2012, 18 (2), 417–431. [PubMed: 22072733]

(9). He T; Haapa-Paananen S; Kaminskyy VO; Kohonen P; Fey V; Zhivotovsky B; Kallioniemi O; Perala M Inhibition of the mitochondrial pyrimidine biosynthesis enzyme dihydroorotate dehydrogenase by doxorubicin and brequinar sensitizes cancer cells to TRAIL-induced apoptosis. Oncogene 2014, 33 (27), 3538–3549. [PubMed: 24013224]

(10). Mathur D; Stratikopoulos E; Ozturk S; Steinbach N; Pegno S; Schoenfeld S; Yong R; Murty VV; Asara JM; Cantley LC; Parsons R PTEN regulates glutamine flux to pyrimidine synthesis and sensitivity to dihydroorotate dehydrogenase inhibition. Cancer Discovery 2017, 7 (4), 380–390. [PubMed: 28255082]

(11). White RM; Cech J; Ratanasirintrawoot S; Lin CY; Rahl PB; Burke CJ; Langdon E; Tomlinson ML; Mosher J; Kaufinan C; Chen F; Long HK; Kramer M; Datta S; Neuberg D; Granter S; Young RA; Morrison S; Wheeler GN; Zon LI DHODH modulates transcriptional elongation in the neural crest and melanoma. Nature 2011, 471 (7339), 518–522. [PubMed: 21430780]

(12). Sykes DB; Kfoury YS; Mercier FE; Wawer MJ; Law JM; Haynes MK; Lewis TA; Schajnovitz A, Jain E; Lee D; Meyer H; Pierce KA, Tolliday NJ,. Waller A,. Ferrara SJ; Eheim AL; Stoeckigt D; Maxcy KL; Cobert JM; Bachand J; Szekely BA; Mukherjee S; Sklar LA,. Kotz JD; Clish CB; Sadreyev RI; Clemons PA; Janzer A,. Schreiber SL; Scadden DT Inhibition of dihydroorotate dehydrogenase overcomes differentiation blockade in acute myeloid leukemia. Cell 2016, 167, 171–186. [PubMed: 27641501]

(13). Cody R; Stewart D; DeFomi M; Moore M; Dallaire B; Azamia N; Gyves J Multicenter phase II study of brequinar sodium in patients with advanced breast cancer. Am. J. Clin. Oncol. 1993, 16 (6), 526–528. [PubMed: 8256771]

(14). Dodion PF; Wagener T; Stoter G; Drozd A; Lev LM; Skovsgaard T; Renard J; Cavalli F Phase II trial with brequinar (DUP-785, NSC 368390) in patients with metastatic colorectal cancer: a study of the Early Clinical Trials Group of the EOR.TC. Ann Oncol 1990, I (1), 79–80.

(15). Urba S; Doroshow J; Cripps C; Robert F; Velez-Garcia E; Dallaire B; Adams D; Carlson R; Grillo-Lopez A; Gyves J Multicenter phase II trial of brequinar sodium in patients with advanced squamous-cell carcinoma of the head and neck. Cancer Chemother. Pharmacol. 1992, 31 (2), 167–169. [PubMed: 1451236]

(16). Moore M; Maroun J; Robert F; Natale R; Neidhart J; Dallaire B; Sisk R; Gyves J Multicenter phase II study of brequinar sodium in patients with advanced gastrointestinal cancer. Invest. New Drugs 1993, 11 (l), 61–65. [PubMed: 8349438]

(17). Maroun J; Ruckdeschel J; Natale R; Morgan R; Dallaire B; Sisk R; Gyves J Multicenter phase II study of brequinar sodium in patients with advanced lung cancer. Cancer Chemother. Pharmacol. 1993, 32 (1), 64–66. [PubMed: 8384937]

(18). Natale R; Wheeler R; Moore M; Dallaire B; Lynch W; Carlson R; Grillo-Lopez A; Gyves J Multicenter phase II trial of brequinar sodium in patients with advanced melanoma. Ann Oncol 1992, 3 (8), 659–660. [PubMed: 1450049]

(19). King SY; Basista AM; Torosian G Self-association and solubility behaviors of a novel anticancer agent, brequinar sodium. J. Pharm. Sci. 1989, 78 (2), 95–100. [PubMed: 2715943]

(20). Joshi AS; King SY; Zajac BA; Makowka L; Sher LS; Kahan BD; Menkis AH; Stiller CR; Schaefle B; Kornhauser DM Phase I safety and pharmacokinetic studies of brequinar sodium after single ascending oral doses in stable renal, hepatic, and cardiac allograft recipients. J. Clin. Pharmacol. 1997, 37 (12), 1121–1128. [PubMed: 9506007]

(21). Fragoso YD; Brooks JB Leflunomide and teriflunomide: altering the metabolism of pyrimidines for the treatment of autoimmune diseases. Expert Rev. Clin. Pharmacol. 2015, 8 (3), 315–320.

(22). Leflunomide in Treating Patients With Relapsed or Refractory Multiple Myeloma. ClinicalTrials.gov, U.S. National Institutes of Health: Bethesda, MD, July 27, 2015,https://clinicaltrials.gov/show/NCT02509052 (accessed November 2017).

(23). Leflunomide + Vemurafenib in V600 Mutant Met Melanoma. ClinicalTrials.gov, U.S. National Institutes of Health: Bethesda, MD, June 5, 2012; https://clinicaltrials.gov/show/NCT01611675 (accessed November 2017).

(24). Baban B; Liu JY; Mozaffari MS Aryl hydrocarbon receptor agonist, leflunomide, protects the ischemic-reperfused kidney: role of Tregs and stem cells. Am J Physiol Regul Integr Comp Physiol 2012, 303 (11), R1136–1146. [PubMed: 23100028]

(25). Ramadoss P; Marcus C; Perdew GH Role of the aryl hydrocarbon receptor in drug metabolism. Expert Opin. Drug Metab. Toxicol 2005, I (1), 9–21.

(26). Sainas S; Pippione AC; Giorgis M; Lupino E; Goyal P; Ramondetti C; Buccinna B; Piccinini M; Braga RC; Andrade CH; Andersson CH; Moritzer AC; Friemann R; Mensa S; Al-Karadaghi S; Boschi D; Lolli ML Design, synthesis, biological evaluation and x-ray structural studies of potent human dihydroorotate dehydrogenase inhibitors based on hydroylated azole scaffolds. Eur. J. Med. Chem. 2017, 129, 287–302. [PubMed: 28235702]

(27). Liu S; Neidhardt E, A-Grossman TH; Ocain T; Clardy J Structures of human dihydroorotate dehydrogenase in complex with antiproliferative agents. Structure 2000, 8 (l), 25–33. [PubMed: 10673429]

(28). Chen SF; Papp LM; Ardecky RJ; Rao GV; Hesson DP; Forbes M; Dexter DL Structure-activity relationship of quinoline carboxylic acids: a new class of inhibitors of dihydroorotate dehydrogenase. Biochem. Pharmacol. 1990, 40 (4), 709–714. [PubMed: 2386542]

(29). Davis JP; Copeland RA Histidine to alanine mutants of human dihydroorotate dehydrogenase: identification of a brequinar-resistant mutant enzyme. Biochem. Pharmacol. 1997, 54 (4), 459–465. [PubMed: 9313772]

(30). Baumgartner R; Walloschek M; Kralik M; Gotschlich A; Tasler S; Mies J; Leban J Dual binding mode of a novel series of DHODH inhibitors. J. Med. Chem. 2006, 49, 1239–1247. [PubMed: 16480261]

(31). Bissantz C; Kuhn B; Stahl M A medicinal chemist's guide to molecular interactions. J. Med. Chem. 2010, 53 (14), 5061–5084. [PubMed: 20345171]

(32). Maag H In Prodrugs: Challenges and Rewards Part I; Stella VJB, Borchardt R, Hageman MJ, Oliyai R, Maag H, Tilley JW, Eds.; Springer-Verlag: New York, 2007.

(33). Hopkins AL; Keserii GM; Leeson PD; Rees DC; Reynolds CH The role of ligand efficiency metrics in drug discovery. Nat. Rev. Drug Discovery 2014, 13, 105. [PubMed: 24481311]

(34). Shvekhgeimer MG-A The Pfitzinger reaction. (Review). Chem. Heterocycl Compd. 2004, 40 (3), 257–294.

(35). Sriram R; Sesha Sai Pavan Kumar CN; Raghunandan N; Ramesh V; Sarangapani M; Rao VJ AlCLl3/PCC-SiO2-promoted oxidation of azaindoles and indoles. Synth. Commun. 2012, 42 (23), 3419–3428.

(36). Kumar CNSSP; Devi CL; Rao VJ; Palaniappan S Use of pyridinium chlorochromate and reusable polyaniline salt catalyst combination for the oxidation of indoles. Synlett 2008,13, 2023–2027.

(37). Stockmann V; Fiksdahl A Synthesis of novel 1,7-naphthyridines by Friedländer condensation of pyridine substrates. Journal of Heterocyclic Chemistry 2011, 48 (6), 1383–1387.

(38). Zong R; Zhou H; Thummel RP Direct access to 4-carboxy-1,8-naphthyridines and related compounds through Pfitzinger-type chemistry. J. Org. Chem. 2008, 73 (11), 4334–4337. [PubMed: 18461999]

(39). Turner JA Regiospecffic electrophilic substitution of aminopyridines: ortho lithiation of 2-, 3-, and 4-(pivaloylamino)-pyridines. J. Org. Chem. 1983, 48 (20), 3401–3408.

(40). Hewawasam P; Meanwell NA A general method for the synthesis of isatins: Preparation of regiospecffically functionalized isatins from anilines. Tetrahedron Lett. 1994, 35 (40), 7303–7306.

(41). Peters GJ; Sharma SL; Laurensse E; Pinedo HM Inhibition of pyrimidine de novo synthesis by DUP-785 (NSC 368390). Invest. New Drugs 1987, 5 (3), 235–244. [PubMed: 2822596]

(42). Chen SF; Ruben RL; Dexter DL Mechanism of action of the novel anticancer agent 6-fluoro-2-(2′-fluoro-1,1′-biphenyl-4-yl)-3-methyl-4-quinolinecarboxylic acid sodium salt (NSC 368390): inhibition of de novo pyrimidine nucleotide biosynthesis. Cancer Res. 1986, 46 (10), 5014–5019. [PubMed: 3019518]

(43). Ishikawa M; Hashimoto Y Improvement in aqueous solubility in small molecule drug discovery programs by disruption of molecular planarity and symmetry. J. Med. Chem. 2011, 54, 1539–1554. [PubMed: 21344906]

(44). Rydberg P; Gloriam DE; Zaretzki J; Breneman C; Olsen L SMARTCyp: a 2D method for prediction of cytochrome P450-mediated drug metabolism. ACS Med. Chem. Lett. 2010, I (3), 96–100.

(45). Hail N Jr.; Chen P; Rower J; Bushman LR Teriflunomide encourages cytostatic and apoptotic effects in premahgnant and malignant cutaneous kératinocytes. Apoptosis 2010, 15, 1234–1246. [PubMed: 20544286]

(46). Das P; Deng X; Zhang L; Roth MG; Fontoura BM; Phillips MA; De Brabander JK SAR based optimization of a 4-quinoline carboxylic acid analog with potent anti-viral activity. ACS Med. Chem. Lett. 2013, 4 (6), 517–521.

(47). Walse B; Dufe VT; Svensson B; Fritzson I; Dahlberg L; Khairoullina A; Wellmar U; Al-Karadaghi S The structures of human dihydroorotate dehydrogenase with and without inhibitor reveal conformational flexibility in the inhibitor and substrate binding sites. Biochemistry 2008, 47 (34), 8929–8936. [PubMed: 18672895]

(48). Estel L; Linard F; Marsais F; Godard A; Quéguiner G Synthesis of ortho-substituted aminopyridines: metalation of pivaloy-lamino derivatives. J. Heterocycl. Chem. 1989, 26 (l), 105–112.

(49). Hughes RO; Rogier DJ; Jacobsen EJ; Walker JK; Machines A; Bond BR; Zhang LL; Yu Y; Zheng Y; Rumsey JM; Walgren JL; Curtiss SW; Fobian YM; Heasley SE; Cubbage JW; Moon JB; Brown DL; Acker BA; Maddux TM; Tollefson MB; Mischke BV; Owen DR; Freskos JN; Molyneaux JM; Benson AG; Blevis-Bal RM Design, synthesis, and biological evaluation of 3-[4-(2-hydroxyethyl)piperazin-1-yl]-7-(6-methoxypyridin-3-yl)-1 -(2-propoxyethyl) pyrido[3,4-b]pyrazin-2(1H)-one, a potent, orally active, brain penetrant inhibitor of phosphodiesterase 5 (PDE5). J. Med. Chem. 2010, 53 (6), 2656–2660. [PubMed: 20196613]

(50). Trott O; Olson AJ AutoDock Vina: improving the speed and accuracy of docking with a new scoring function, efficient optimization and multithreading. J. Comput. Chem. 2010, 31, 455–461. [PubMed: 19499576]

(51). BIOVIA, Discovery Studio Modeling Environment, Release 2017; Dassault Systèmes: San Diego, 2016.

(52). Madak JT; Cuthbertson CR; Chen W; Showalter HD; Neamati N Design, synthesis, and characterization of brequinar conjugates as probes to study DHODH inhibition. Chem. - Eur. J 2017, 23 (56), 13875–13878. [PubMed: 28833638]

(53). Otwinowski Z; Minor W Processing of x-ray diffraction data collected in oscillation mode. Methods Enzymol. 1997, 276, 307–326.

(54). McCoy AJ; Grosse-Kunstleve RW; Adams PD; Winn MD; Storoni LC; Read RJ Phaser crystallographic software. J. Appl. Crystallogr. 2007, 40, 658–674. [PubMed: 19461840]

(55). Emsley P; Lohkamp B; Scott WG; Cowtan K Features and development of Coot. Acta Crystallogr., Sect. D: Biol Crystallogr. 2010, 66, 486–501. [PubMed: 20383002]

(56). Adams PD; Afonine PV; Bunkoczi G; Chen VB; Davis IW; Echols N; Headd JJ; Hung LW; Kapral GJ; Grosse-Kunsdeve RW; McCoy AJ; Moriarty NW; Oeffner R; Read RJ; Richardson DC; Richardson JS; Terwilliger TC; Zwart PH PHENIX: a comprehensive Python-based system for macromolecular structure solution. Acta Crystallogr., Sect. D: Biol Crystallogr. 2010, 66, 213–221. [PubMed: 20124702]

(57). Moriarty NW; Grosse-Kunstleve RW; Adams PD Electronic ligand builder and optimization workbench (eLBOW): a tool for ligand coordinate and restraint generation. Acta Crystallogr., Sect. D: Biol Crystallogr. 2009, 65, 1074–1080. [PubMed: 19770504]

(58). de Forni M; Armand J-P; Fontana X; Recondo G; Domenge C; Carde P; Chabot GG; Gouyette A; Barbu M Phase I and pharmacokinetic study of brequinar (DUP 785; NSC 368390) in cancer patients. Eur. J. Cancer 1993, 29, 983–988.

(59). Noe DA; Rowinsky EK; Shen H-SL; Clarke BV; Grodiow LB; McGuire WB; Hantel A; Adams DB; Abeloff MD; Ettinger DS; Donehower RC Phase I and pharmacokinetic study of brequinar sodium (NSC 368390). Cancer Res. 1990, 50, 4595–4599. [PubMed: 2369734]

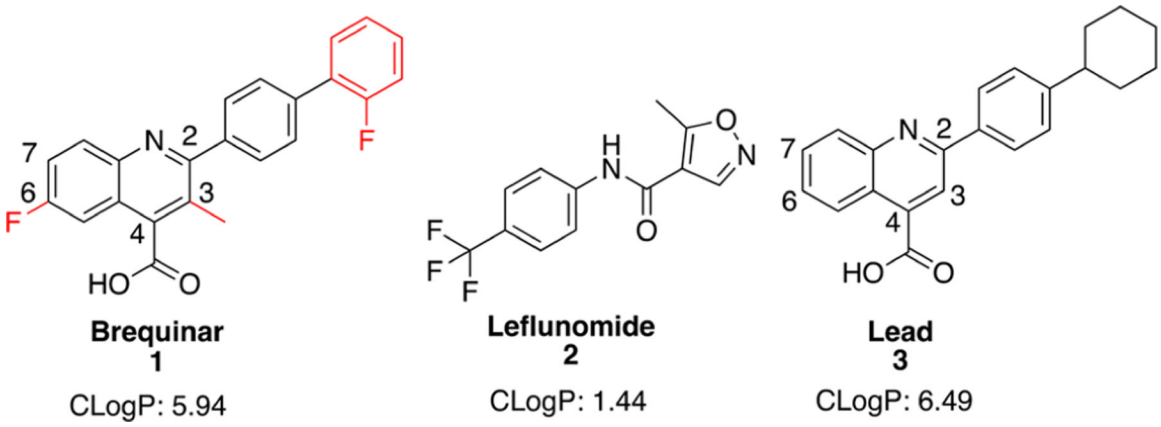

Figure 1.
Selected DHODH inhibitors.

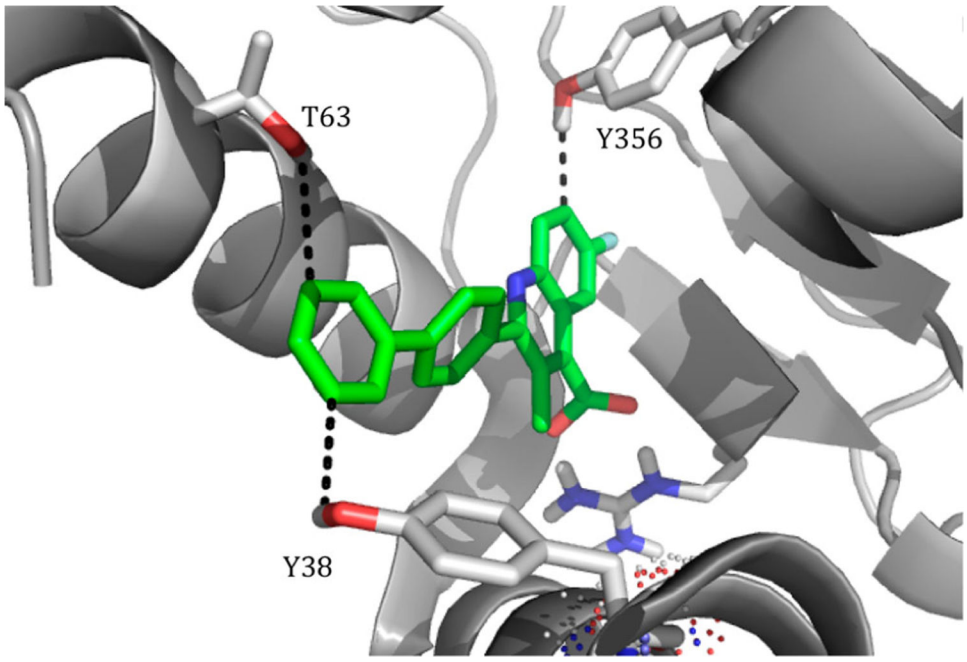

Figure 2.

Cocrystal structure of a brequinar analogue in DHODH. Proposed interactions are depicted. Y356 is 2.5 Å from C7 of the quinoline ring; Y38 and T63 are 3.7 and 3.9 Å, respectively, from the ***meta***-position of the distal phenyl ring. Measurements were calculated from the hydrogen of side chain hydroxyl groups. Figure generated using PDB 1D3G, resolution 1.6 Å.

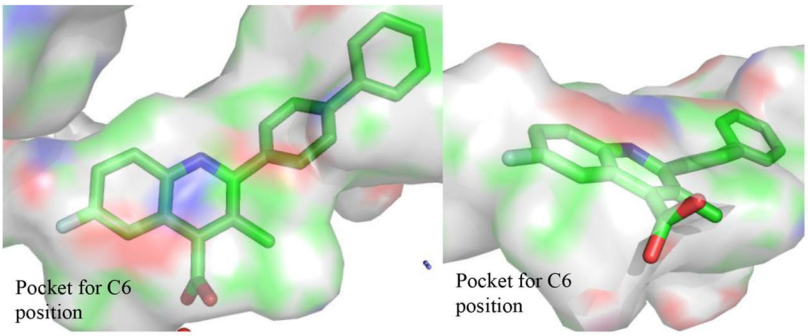

Figure 3.

Depicted binding cavity of a brequinar analogue from PDB 1D3G. The pocket for a C***6*** substituent is shown.

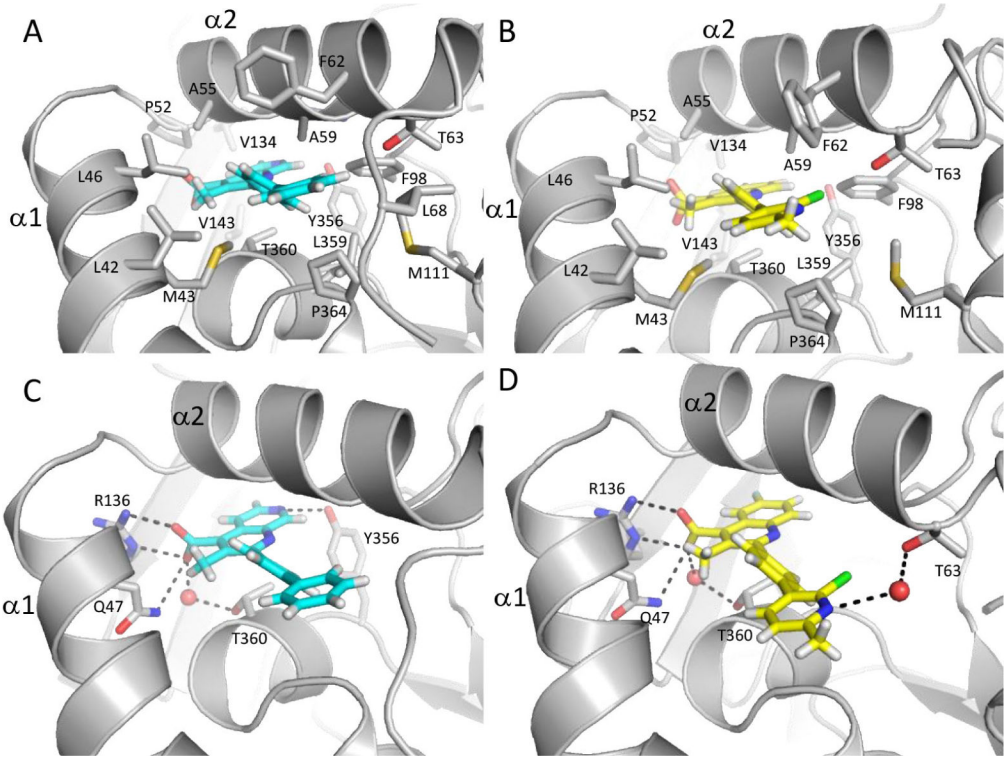

Figure 4.

Noncovalent interactions of DHODH with ***46*** (cyan, PDB **6**CJG) and **43** (yellow, PDB **6**CJF). (A) and (B) display hydrophobic interactions and (C) and (D) hydrogen-bonding interactions (dashed lines). **43** shown as modeled in predominant conformation. Nitrogen is shown in blue, oxygen in red, sulfur in yellow, chlorine in green, fluorine in light blue, and hydrogens in white.

A

Compound	IC_{50} (μM)
1	0.544 ± 0.051
11	3.51 ± 1.9
26	11.6 ± 0.74
29	7.12 ± 2.0
35	15.3 ± 7.3
41	9.28 ± 2.2
43	4.81 ± 0.40
46	7.08 ± 3.2
48	2.67 ± 0.22
52	0.401 ± 0.32

B

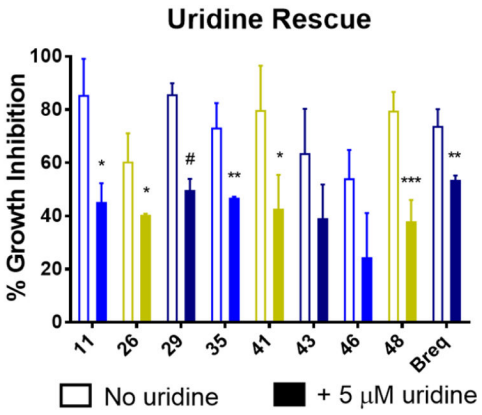

Figure 5.

Activity of DHODH inhibitors in a leukemia cell line. (A) IC_{50} values of select analogues in HL-60. Compounds were assayed for antiproliferative effects in an MTT assay containing complete medium. (B) Uridine supplementation rescues cell growth inhibition induced by select optimized analogues. Compounds were assayed at twice their IC_{50} values for antiproliferative effects in an MTT assay with medium containing dialyzed FBS ± 5 ***μM*** uridine. Data are represented as the mean and standard deviation from three independent experiments. * $p < 0.05$, ** $p < 0.01$, *** $p < 0.005$, # $p < 0.001$.

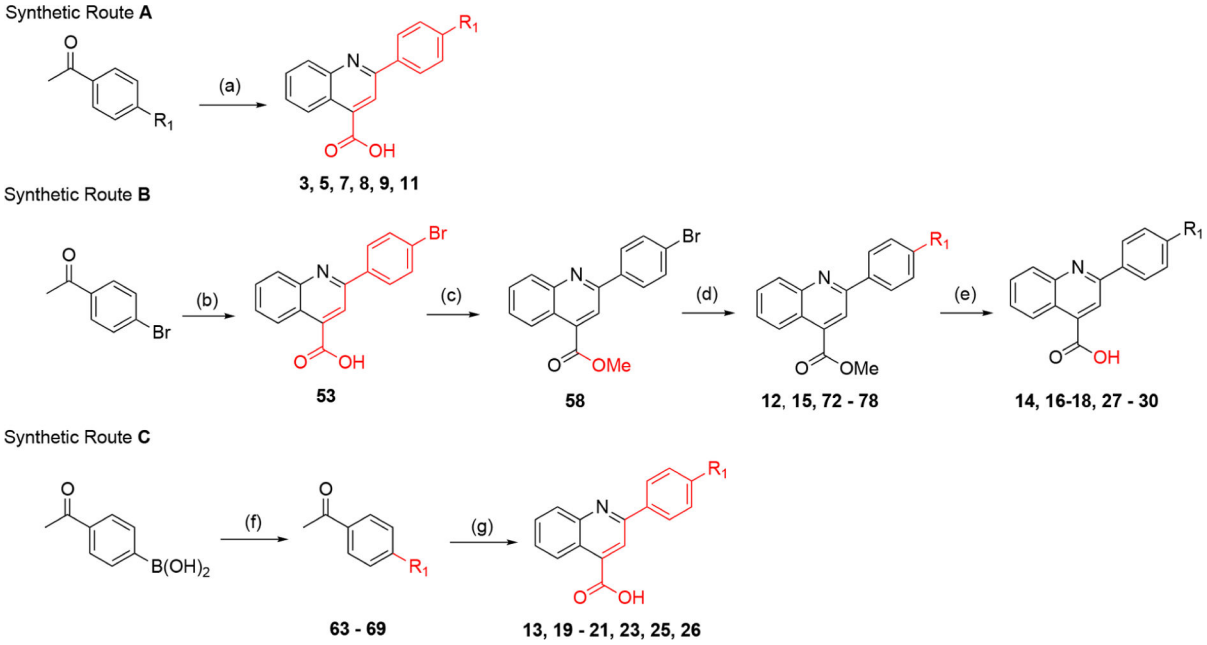

Scheme 1. Synthesis of Quinoline Analogues without a C3 Methyl Group[a]

[a]Reagents and conditions. Route **A:** (a) isatin, KOH, EtOH/H_2O reflux, 12–48 h (10–41%). Route **B:** (b) isatin, KOH, EtOH/H_2O, 12–48 h (81%); (c) MeI, Cs_2CO_3 DMF, rt, overnight (43%); (d) R_1-boronic acid/ester, $Pd(PPh_3)_4$, K_2HPO_4, dioxane/H_2O, 130 °C, 1.5 h (7–93%); (e) LiOH or NaOH, THF/H_2O, rt, overnight (15–100%). Route **C:** (f) R_1-halogen, $Pd(PPh_3)_4$, K_2HPO_4, dioxane/H_2O, 130 °C, 1.5 h (13–97%); (g) isatin, KOH, EtOH/H_2O, reflux; 12–48 h (18–57%).

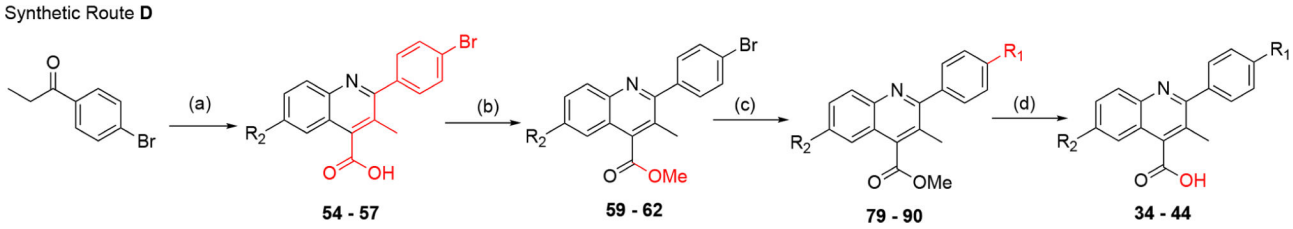

Scheme 2. Synthesis of Quinoline Analogues with a C3 Methyl Substituent[a]

[a]Reagents and conditions. Route **D:** (a) R_2-isatin, KOH, EtOH/H_2O, reflux; 12–48 h (39–76%); (b) MeI, Cs_2CO_3, DMF, rt, overnight (71–93%); (c) R_1-boronic acid, $Pd(PPh_3)_4$, K_2HPO_4, dioxane/H_2O, 130 °C, 1.5 h (8–79%); (d) BBr_3, DCM, rt, 2–24 h (3–99%).

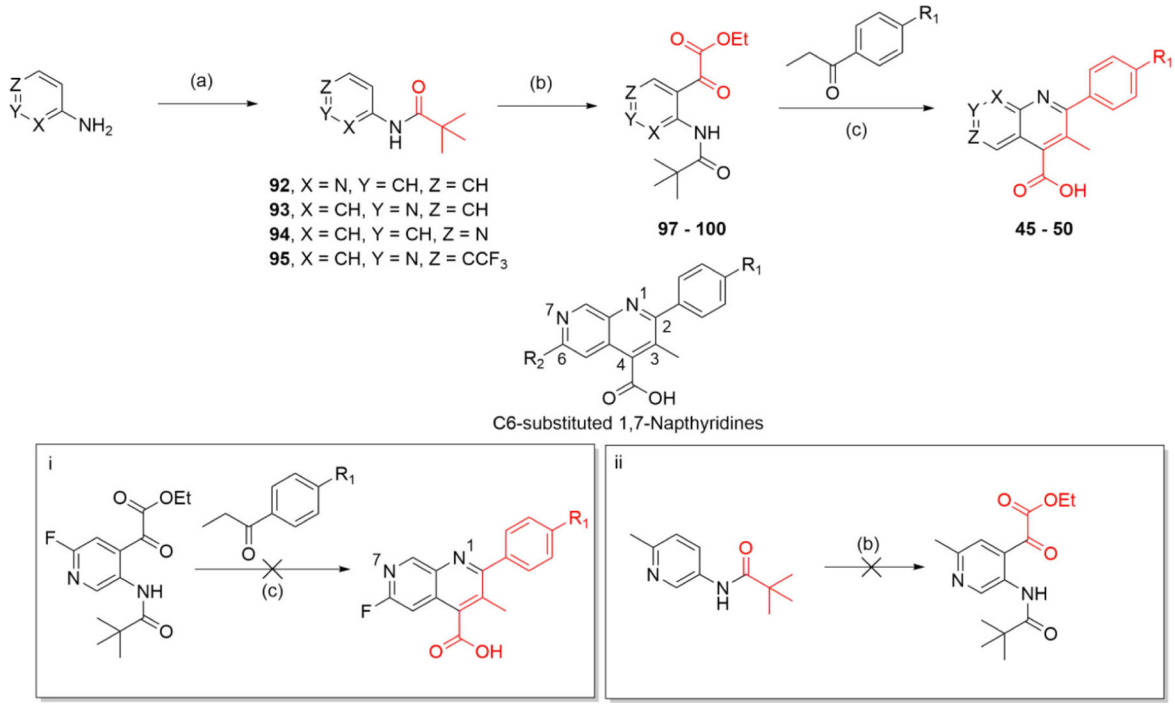

Scheme 3. Synthesis of Naphthyridine Core Analogues[a]

[a]Reagents and conditions. Route **E**: (a) PivCl, DIPEA, DCM, rt, 12 h (53–98%); (b) (1) *n*-BuLi, TMEDA, Et_2O, −78 to 10 °C (15 min to 2.5 h), (2) diethyl oxalate, Et_2O, −78 °C to rt, 1.5 h (1–51%); (c) KOH, EtOH, 100 °C, 12–48 h (3–21%).

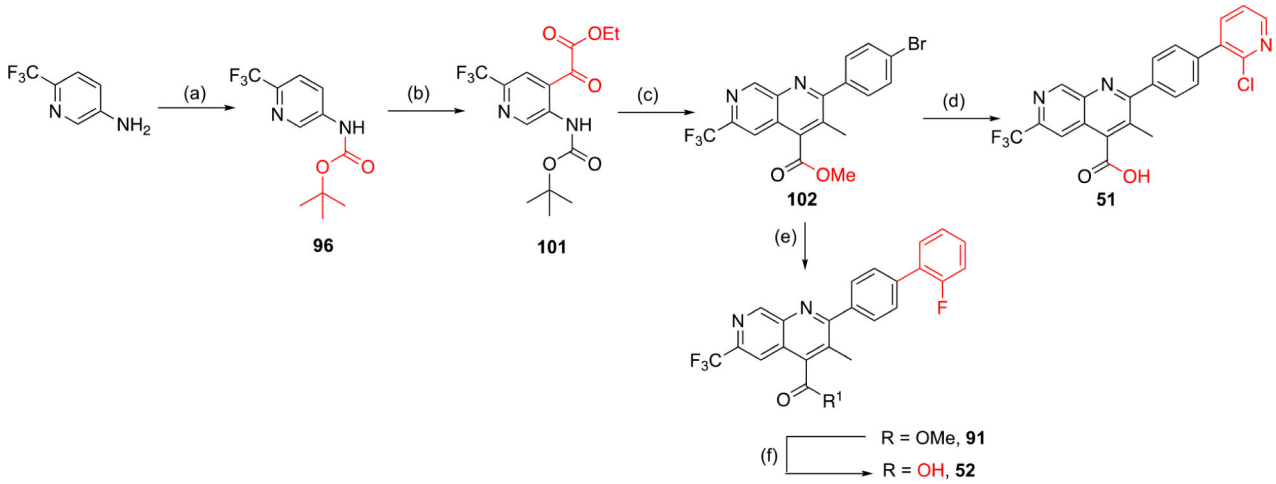

Scheme 4. Alternate Synthesis of Naphthyridine Core Analogues[a]

[a]Reagents and conditions. Route F: (a) Boc_2O, *p*-dioxane, reflux 72 h (36%); (b) (1) *n*-BuLi, TMEDA, Et_2O, −78 to **10** °C (15 min to 2.5 h), (**2**) diethyl oxalate, Et_2O, −78 °C to rt, 1.5 h (l%); (c) (1) TFA, DCM, rt, 2 h, (2) 4′-bromopropiophenone, KOH, EtOH, 100 °C, 24 h, (3) TMS-diazomethane, THF, MeOH, rt, 2 h (2% over three steps), (d) (1) NaOH, dioxane, 60 °C, overnight, (2) 2-chloropyridine-3-boronic acid, $Pd(PPh_3)_4$, K_2HPO_4, dioxane/H_2O, 130 °C, 1.5 h (46% over two steps); (e) 2-fluorophenylboronic acid, $Pd(PPh_3)_4$, K_2HPO_4 dioxane/H_2O, 130 °C, 1.5 h (**66**%); (f) KOH, THF/H_2O, 50 °C, 4 h (50%).

Table 1.

Biological Activity of Quinolone R_2 Carboxylic Acids and Methyl Esters with Selected R_1 Substituents[a]

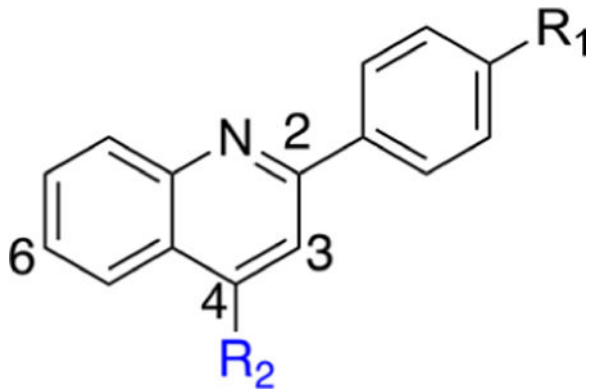

#	R_1	R_2	DHODH Assay IC_{50} (μM)	cLogP	LipE	MTT Assay HCT-116 IC_{50} (μM)	MIA PaCa-2 IC_{50} (μM)
1 (Breq)			0.00730 ± 0.0031	5.94	2.20	0.679 ± 0.19	1.69 ± 0.69
3	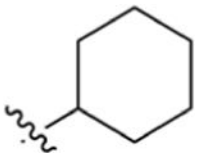	CO_2H	0.250 ± 0.11	6.49	0.11	4.22 ± 0.85	5.88 ± 3.9
4	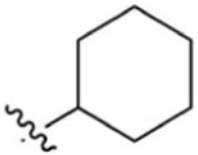	CO_2Me	>200	6.72	NA	42.6 ± 22	37.1 ± 11

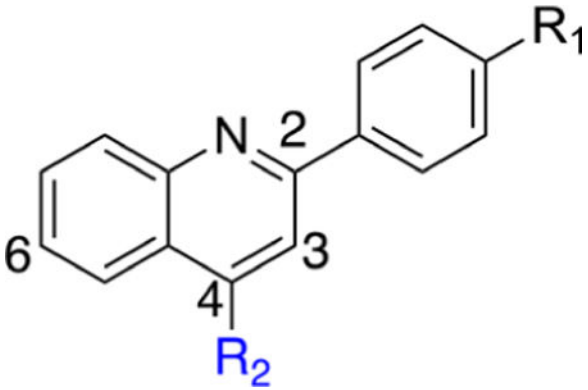

#	R_1	R_2	DHODH Assay IC_{50} (μM)	cLogP	LipE	MTT Assay HCT-116 IC_{50} (μM)	MTT Assay MIA PaCa-2 IC_{50} (μM)
5	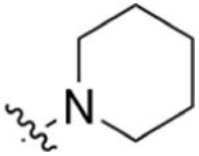	CO_2H	8.07 ± 1.1	4.71	0.38	7.23 ± 1.8	16.7 ± 4.5
6	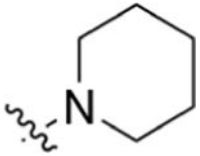	CO_2Me	>200	4.93	NA	38.2 ± 5.5	31.8 ± 6.0
7	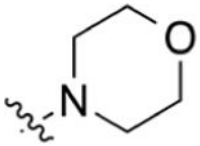	CO_2H	>200	3.23	NA	> 100	> 100

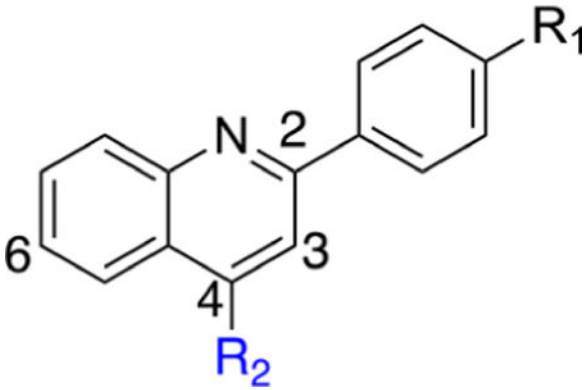

#	R_1	R_2	DHODH Assay IC_{50} (μM)	cLogP	LipE	MTT Assay HCT-116 IC_{50} (μM)	MIA PaCa-2 IC_{50} (μM)
8	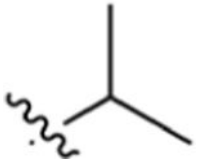	CO_2H	3.41 ± 0.43	5.30	0.17	19.1 ± 4.1	24.2 ± 5.2
9	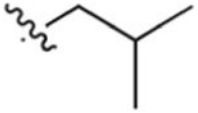	CO_2H	1.04 ± 0.76	5.83	0.15	8.00 ± 1.9	14.5 ± 7.3
10	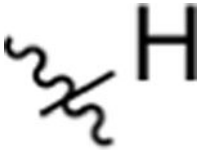	CO_2H	144 ± 32	3.87	−0.03	> 100	> 100
11	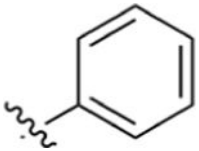	CO_2H	0.0510 ± 0.027	5.76	1.53	0.344 ± 0.18	2.16 ± 1.3

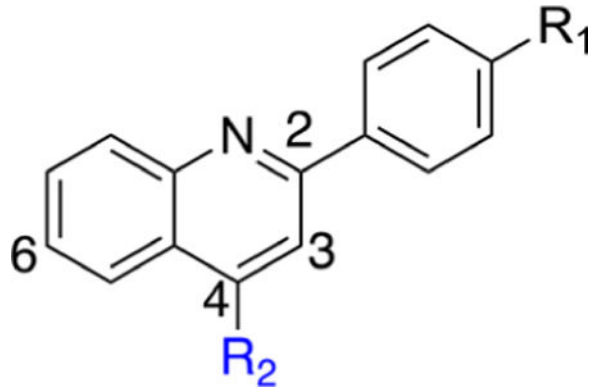

#	R_1	R_2	DHODH Assay IC_{50} (μM)	cLogP	LipE	MTT Assay HCT-116 IC_{50} (μM)	MIA PaCa-2 IC_{50} (μM)
12	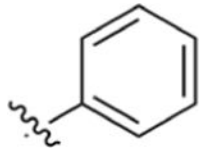	CO_2Me	>200	5.98	NA	6.90 ± 2.5	11.5 ± 6.0

[a]Data for cLogP values was predicted using ChemBioDraw Professional 16. Lipophilic ligand efficiency (LipE) calculated LipE = $-pIC_{50}$ (M) – cLogP.[33]

Table 2.

Biological Activity of Quinolone R_2 Carboxylic Acids and Methyl Esters with R_1 Pyridine and Pyrimidine Moieties[a]

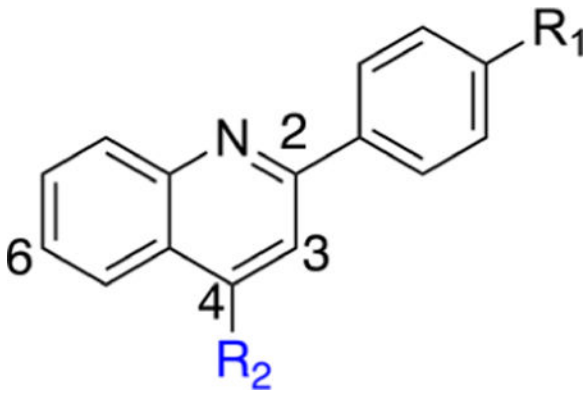

#	R_1	R_2	DHODH Assay IC_{50} (μM)	cLogP	LipE	MTT Assay HCT-116 IC_{50} (μM)	MTT Assay MIA PaCa-2 IC_{50} (μM)
13	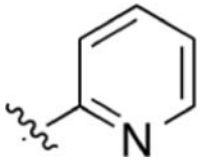	CO_2H	10.1 ± 2.4	4.47	0.53	39.6 ± 14	49.3 ± 36
14	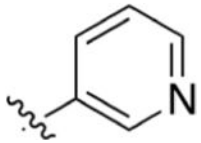	CO_2H	0.391 ± 0.090	4.26	2.15	20.9 ± 6.4	32.8 ± 7.0
15	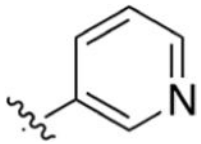	CO_2Me	>200	4.49	NA	6.15 ± 2.9	6.43 ± 3.0

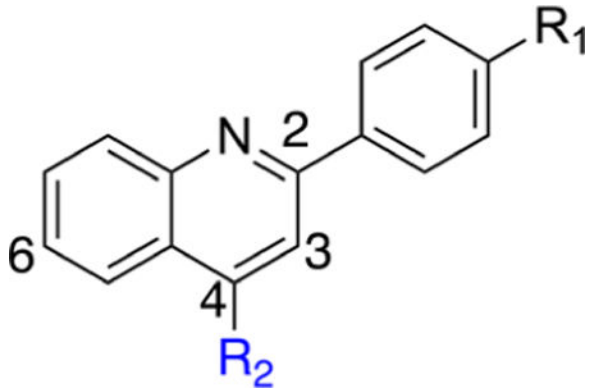

#	R_1	R_2	DHODH Assay IC_{50} (μM)	cLogP	LipE	MTT Assay HCT-116 IC_{50} (μM)	MIA PaCa-2 IC_{50} (μM)
16	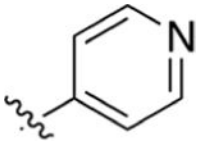	CO_2H	7.55 ± 1.3	4.26	0.86	33.6 ± 2.6	68.1 ± 27
17	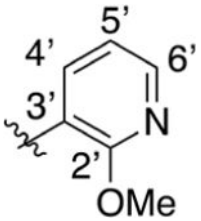	CO_2H	0.165 ± 0.086	4.02	2.76	5.60 ± 0.88	13.6 ± 2.7
18	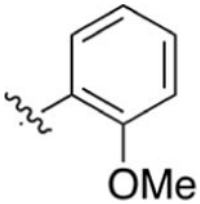	CO_2H	0.127 ± 0.022	5.12	1.78	2.85 ± 1.1	7.45 ± 2.8

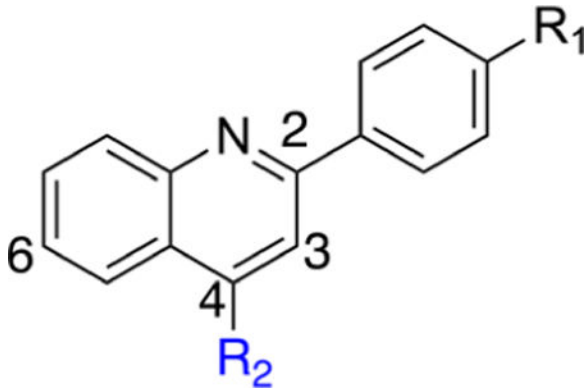

#	R_1	R_2	DHODH Assay IC_{50} (μM)	cLogP	LipE	MTT Assay HCT-116 IC_{50} (μM)	MIA PaCa-2 IC_{50} (μM)
19	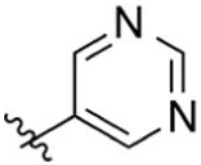	CO_2H	>200	2.76	NA	>50	>50
20	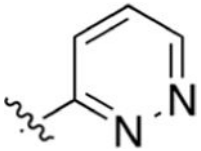	CO_2H	8.21 ± 2.8	3.24	1.85	> 50	>50
21	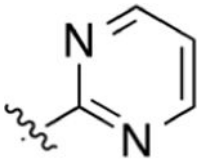	CO_2H	>200	2.97	NA	>50	>50

[a]Data for cLogP values was predicted using ChemBioDraw Professional 16. Lipophilic ligand efficiency (LipE) calculated LipE = $-pIC_{50}$ (M) – cLogP.[33]

Table 3.

Biological Activity of Quinolone R_2 Carboxylic Acids and Methyl Esters with R_1 Substituted Pyridines[a]

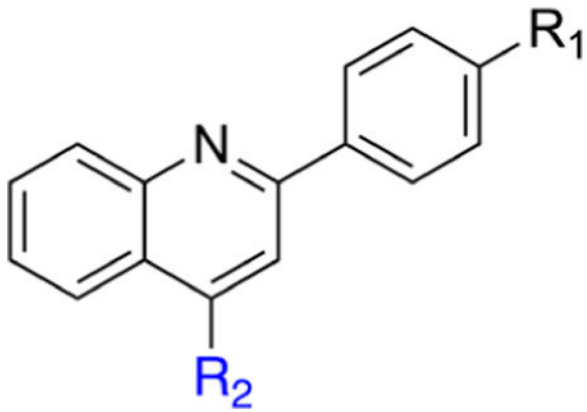

#	R_1	R_2	DHODH Assay IC_{50} (μM)	cLogP	LipE	MTT Assay HCT-116 IC_{50} (μM)	MIA PaCa-2 IC_{50} (μM)
22	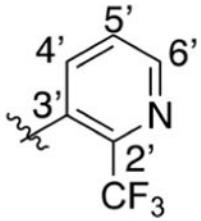	CO_2H	0.148 ± 0.021	5.14	1.69	4.63 ± 1.1	8.84 ± 3.8
23	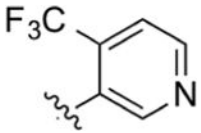	CO_2H	1.43 ± 0.76	5.14	0.70	3.87 ± 1.0	8.71 ± 3.2

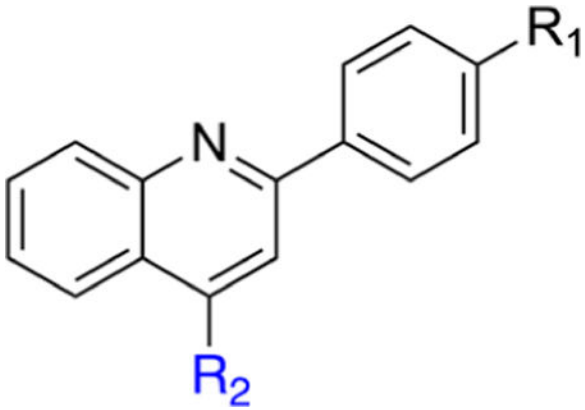

#	R_1	R_2	DHODH Assay IC_{50} (μM)	cLogP	LipE	MTT Assay HCT-116 IC_{50} (μM)	MIA PaCa-2 IC_{50} (μM)
24	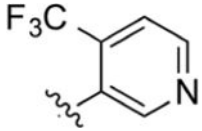	CO_2Me	>50	5.37	NA	NT[b]	NT
25	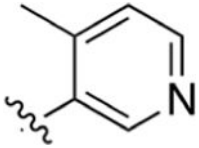	CO_2H	0.373 ± 0.22	4.46	1.97	10.8 ± 2.7	17.9 ± 5.9
26	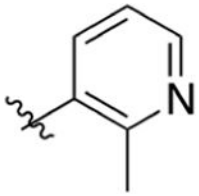	CO_2H	0.0221 ± 0.020	4.46	3.20	10.0 ± 0.85	18.2 ± 6.0

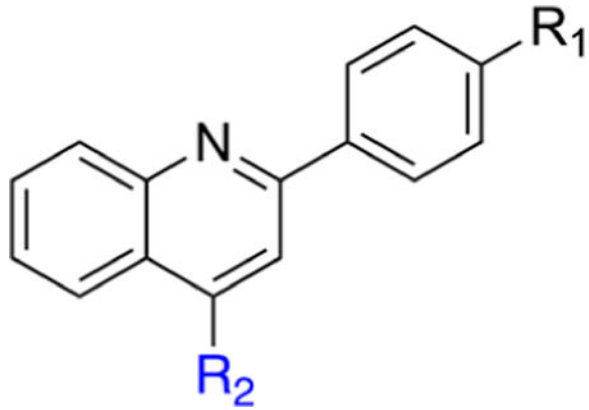

#	R_1	R_2	DHODH Assay IC_{50} (μM)	cLogP	LipE	MTT Assay HCT-116 IC_{50} (μM)	MTT Assay MIA PaCa-2 IC_{50} (μM)
27	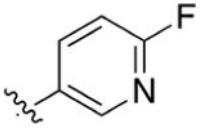	CO_2H	12.5 ± 1.1	4.40	0.50	16.8 ± 2.9	> 100
28	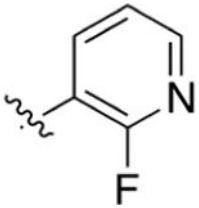	CO_2H	1.42 ± 0.37	4.40	1.45	11.2 ± 2.6	32.1 ± 24
29	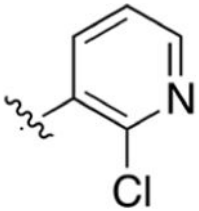	CO_2H	0.0327 ± 0.021	4.72	2.77	3.30 ± 0.75	7.13 ± 1.4

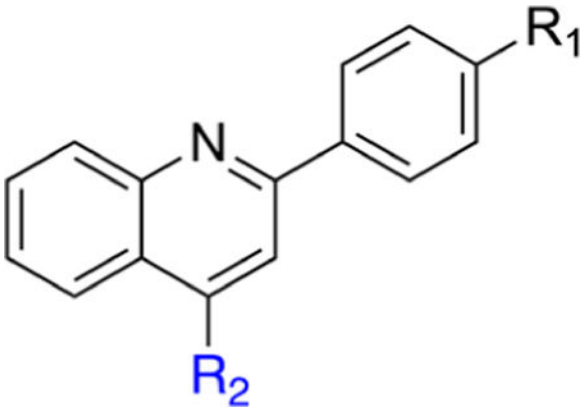

#	R_1	R_2	DHODH Assay IC_{50} (μM)	cLogP	LipE	MTT Assay HCT-116 IC_{50} (μM)	MIA PaCa-2 IC_{50} (μM)
30	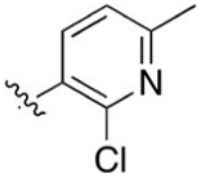	CO_2H	0.235 ± 0.11	5.22	1.41	5.13 ± 3.1	14.2 ± 7.3
31	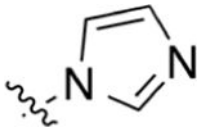	CO_2H	8.4 ± 3.2	3.52	1.56	> 100	> 100

[a]Data for cLogP values was predicted using ChemBioDraw Professional 16. Lipophilic ligand efficiency (LipE) calculated LipE = $-pIC_{50}$ (M) – cLogP.[33]

[b]NT, not tested.

Table 4.

Biological Activity of C3 Methyl-Substituted Quinolines[a]

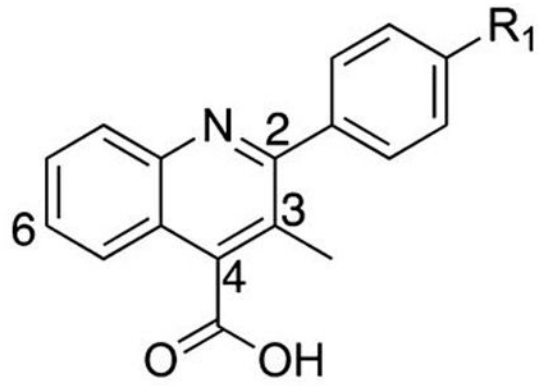

#	R_1	DHODH Assay IC_{50} (μM)	cLogP	LipE	MTT Assay HCT-116 IC_{50} (μM)	MTT Assay MIA PaCa-2 IC_{50} (μM)
32	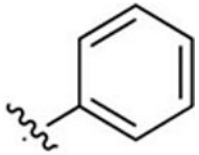	0.0754 ± 0.017	5.66	1.46	8.51 ± 2.0	5.29 ± 1.1
33	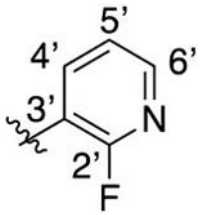	0.504 ± 0.25	4.30	2.00	21.3 ± 10	13.4 ± 2.6

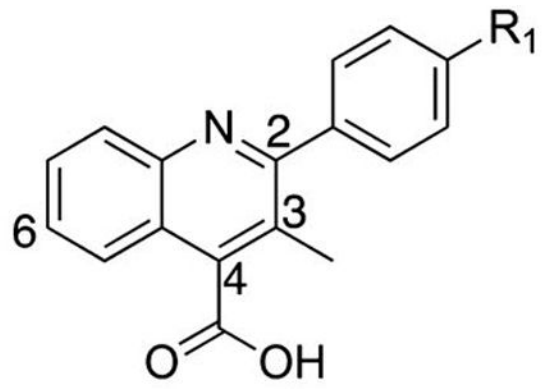

#	R_1	DHODH Assay IC_{50} (μM)	cLogP	LipE	MTT Assay HCT-116 IC_{50} (μM)	MTT Assay MIA PaCa-2 IC_{50} (μM)
34	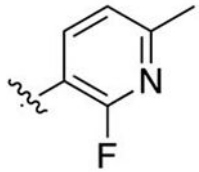	2.48 ± 0.40	4.80	0.81	23.9 ± 6.7	31.6 ± 6.8
35	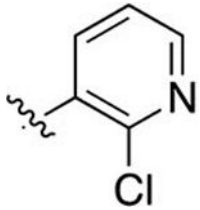	0.0543 ± 0.037	4.62	2.65	6.44 ± 0.67	8.64 ± 4.3
36	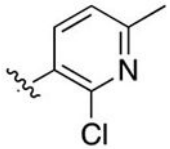	0.184 ± 0.015	5.12	1.62	15.5 ± 3.3	7.70 ± 2.3

[a]Data for cLogP values was predicted using ChemBioDraw Professional 16. Lipophilic ligand efficiency (LipE) calculated LipE = −pIC50 (M) − cLogP.[33]

Table 5.

Biological Activity of R_1/R_2 Substituted Quinolines[a]

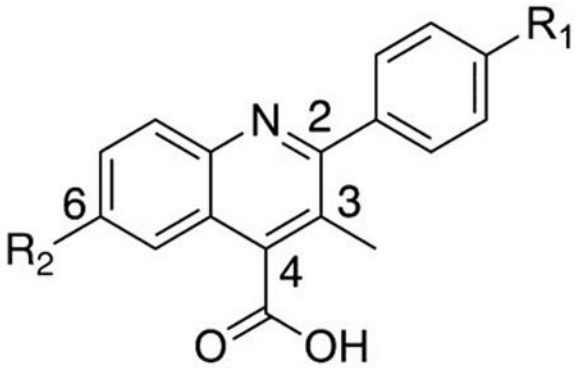

#	R_1	R_2	DHODH Assay IC_{50} (μM)	cLogP	LipE	MTT Assay HCT-116 IC_{50} (μM)	MIA PaCa-2 IC_{50} (μM)
37	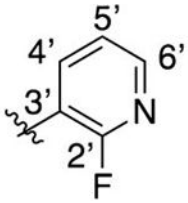	F	0.0794 ± 0.044	4.45	2.65	5.71 ± 1.1	23.6 ± 28
38	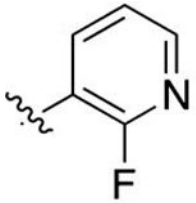	Cl	0.165 ± 0.035	5.02	1.76	5.43 ± 2.1	14.7 ± 6.9

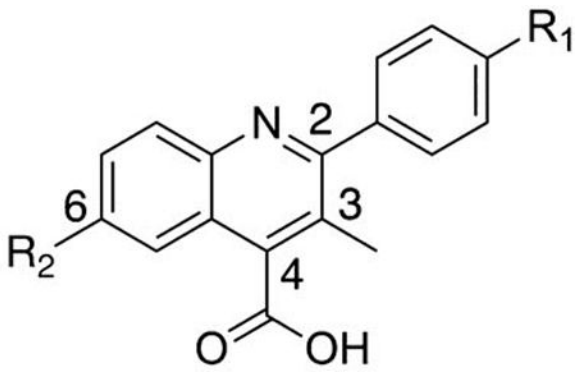

#	R_1	R_2	DHODH Assay IC_{50} (μM)	cLogP	LipE	MTT Assay HCT-116 IC_{50} (μM)	MIA PaCa-2 IC_{50} (μM)
39	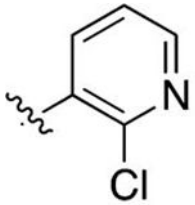	Me	0.0542 ± 0.012	5.12	2.15	11.1 ± 0.38	8.29 ± 3.1
40	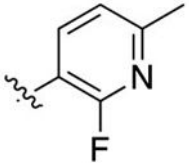	F	3.31 ± 0.17	4.95	0.53	33.7 ± 0.41	33.8 ± 13
41	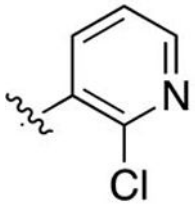	F	0.00971 ± 0.0014	4.76	3.25	3.02 ± 0.35	7.18 ± 2.3

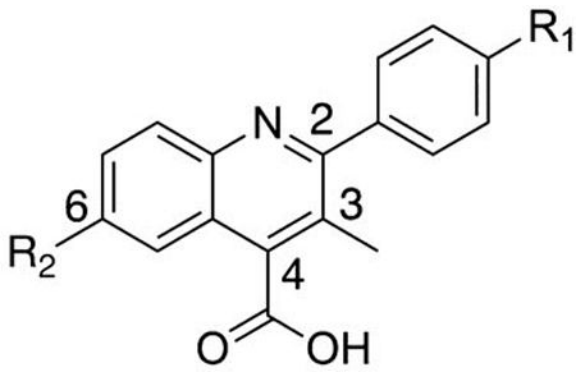

#	R_1	R_2	DHODH Assay IC_{50} (μM)	cLogP	LipE	MTT Assay HCT-116 IC_{50} (μM)	MIA PaCa-2 IC_{50} (μM)
42	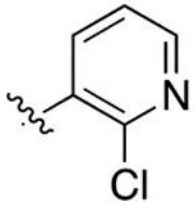	Cl	0.0360 ± 0.0058	5.34	2.10	4.36 ± 0.94	4.73 ± 2.8
43	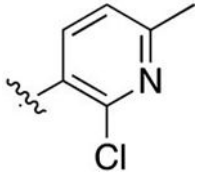	F	0.0262 ± 0.0018	5.27	2.31	1.98 ± 1.3	6.57 ± 5.0
44	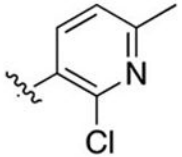	Cl	0.0744 ± 0.028	5.84	1.29	2.71 ± 1.3	7.56 ± 4.3

[a]Data for cLogP values was predicted using ChemBioDraw Professional 16. Lipophilic ligand efficiency (LipE) calculated LipE = $-pIC_{50}$ (M) – cLogP.[33]

Table 6.

Biological Activity of Naphthyridines[a]

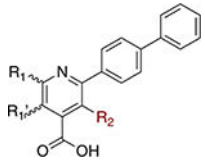

#	R_1	R_2	DHODH Assay IC_{50} (μM)	cLogP	LipE	MTT Assay HCT-116 IC_{50} (μM)	MTT Assay MIA PaCa-2 IC_{50} (μM)
32	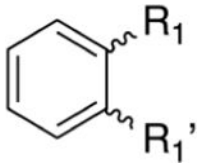	Me	0.0754 ± 0.017	5.66	1.46	8.51 ± 2.0	5.29 ± 1.1
45	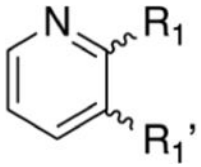	Me	1.22 ± 0.49	4.16	1.75	> 100	> 100
46	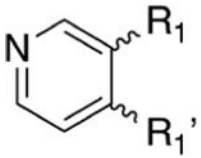	Me	0.0283 ± 0.0033	4.16	3.39	6.30 ± 7.0	4.50 ± 3.2
47	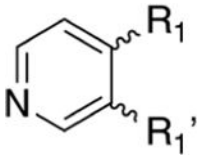	Me	2.79 ± 1.3	4.16	1.39	26.7 ± 11	28.1 ± 8.1

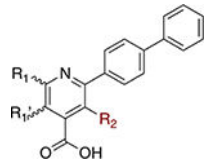

#	R_1	R_2	DHODH Assay IC_{50} (μM)	cLogP	LipE	MTT Assay HCT-116 IC_{50} (μM)	MIA PaCa-2 IC_{50} (μM)
48	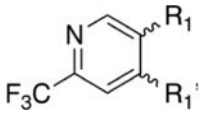	Me	0.0212 ± 0.0039	5.04	2.63	0.880 ± 0.13	2.18 ± 1.7

[a]Data for cLogP values was predicted using ChemBioDraw Professional 16. Lipophilic ligand efficiency (LipE) calculated LipE = $-pIC_{50}$ (M) – cLogP.[33]

Table 7.

Biological Activity of R_2 Pyridine-Substituted Naphthyridines[a]

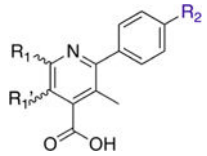

#	R_1	R_2	DHODH Assay IC_{50} (μM)	cLogP	LipE	MTT Assay HCT-116 IC_{50} (μM)	MIA PaCa-2 IC_{50} (μM)
49	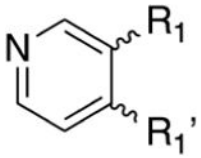	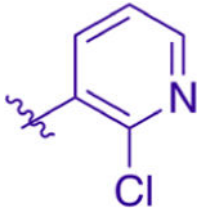	0.259 ± 0.0035	3.13	3.46	> 100	> 100
50	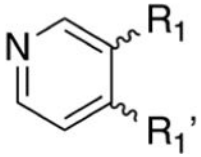	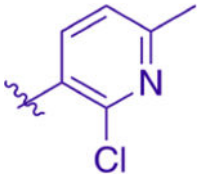	5.26 ± 2.2	3.63	1.65	> 100	> 100
51	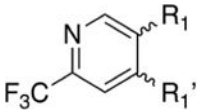	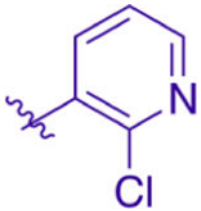	0.201 ± 0.071	4.01	2.69	25.7 ± 6.3	21.5 ± 7.0

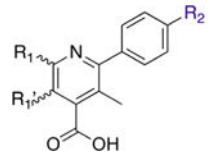

#	R_1	R_2	DHODH Assay IC_{50} (μM)	cLogP	LipE	MTT Assay HCT-116 IC_{50} (μM)	MIA PaCa-2 IC_{50} (μM)
52	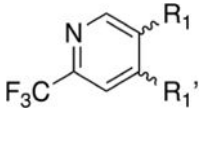	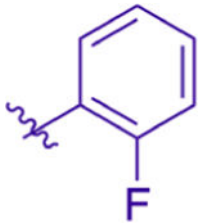	0.0118 ± 0.00090	5.19	2.74	0.333 ± 0.13	0.454 ± 0.14

[a]Data for cLogP values was predicted using ChemBioDraw Professional 16. lipophilic ligand efficiency (LipE) calculated LipE = $-pIC_{50}$ (M) – cLogP.[33]

Table 8.

Pharmacokinetic Parameters of Analogue 41[a]

Compd	route	dose (mg/m^2(	C_{max} (μg/mL)	C_0/C_{max}	T_{max} (h)	AUC (0–TLDC) (h·μg/mL)	AUD (0–INF) (h·μg/mL)	$t_{1/2}$ (h)	CL (L/h/m^2)	CL-F (L/h/m^2)	V_{ss} (L/m^2)	Vz_F (L/m^2)	F(%)
1 [b]	IV[58]	8	1.8		N/A	3.2		2.9	3.2	N/A	8.2	N/A	N/A
	IV[58]	16	2.7		N/A	3.8		3.1	4.9	N/A	11.6	N/A	N/A
	IV[59]	36			N/A	20.7		4.3		N/A	7.48	N/A	N/A
Compd	route	dose (mg/kg)	C_{max} (μg/mL)	C_0/C_{max} (ng/mL)	T_{max} (h)	AUC (0–TLDC) (h·ng/mL)	AUD (0–INF) (h·ng/mL)	$t_{1/2}$ (h)	CL (mL/h/kg)	CL-F (mL/h/kg)	V_{ss} (mL/kg)	Vz_F (mL/kg)	F(%)
41	IV	10		45381	N/A	32261	32306	2.73	309	N/A	496	N/A	N/A
	PO	20		5313	0.25	35896	36035	2.78	N/A	555	N/A	2226	56

[a]PK parameters were estimated using noncompartmental analysis with Phoenix/WINONLIN. C_0 = initial concentration, C_{max} = maximum observed concentration, T_{max} = time to reach C_{max}, AUC (0–TLDC) = area under the concentration–time curve from time zero to time of last detectable concentration, AUC (0–inf) = area under the concentration–time curve from time zero to infinite, CL = Systemic clearance, CL_F = apparent clearance, V_{ss} = volume of distribution at steady state, Vz_F = volume of distribution associated with the terminal elimination phrase, terminal elimination half-life ($t_{1/2}$) was calculated based on data points (3) in the terminal phase with correlation of coefficient >0,90, F = % bioavailability

[b]PK parameters for brequinar from the cited clinical trials.

Table 9.

Thermodynamic Solubility of Selected Analogues[a]

compd	μM	(μg/mL)	initial dose concentration (mg/mL)	pH after assay
1 (brequinar)	1085.2	407.4	6.2	7.4
	1048.6	393.6	6.4	7.4
3	43.9	14.5	2.9	7.4
	48.0	15.9	4.9	7.4
41	1000.1	392.8	5.8	7.4
	982.1	385.8	4.9	7.4
46	2628.4	894.6	6.7	7.4
	3096.3	1053.6	8.7	7.4

[a]Assay performed using CLND in phosphate buffer saline, pH 7.4. Each entry lists a single run. Analyte concentrations were determined via a standard calibration curve.